

Response to reviewers for the paper “Characterization of a real-time tracer for IEPOX-SOA from aerosol mass spectrometer measurements”

By W.W. Hu et al

We appreciate the reviewer’s comments and support for publication of this manuscript after minor revisions. Following the reviewer’s suggestions, we have carefully revised the manuscript. To facilitate the review process we have copied the reviewer comments in black text. Our responses are in regular blue font. We have responded to all the referee comments and made alterations to our paper (**in bold text**).

Anonymous Referee #1

General Comments

R1.0. In this manuscript, the authors analyze AMS data from multiple sources to determine whether m/z 82 and, more specifically the C_5H_6O fragment, are robust AMS tracers for SOA formed from isoprene epoxydiols (IEPOX). The main goals of the manuscript are to determine the range of $f_{C_5H_6O}$ in ambient IEPOX PMF factors, determine the background $f_{C_5H_6O}$ in different ambient environments, and determine whether SOA generated from monoterpenes (MT) and analyzed with the AMS have significant signal at the C_5H_6O fragment. The authors quantify the $f_{C_5H_6O}$ for areas influenced by biomass burning and urban pollution, areas with heavy MT emissions, and areas with strong isoprene emissions. They present a method for estimating the SOA mass formed from IEPOX chemistry from $f_{C_5H_6O}$ and compare this method to PMF results from the SOAS campaign. They argue that IEPOX SOA mass estimated from $f_{C_5H_6O}$ should be within a factor of 2 of that determined by a more rigorous PMF analysis.

This manuscript will primarily be of interest to AMS users and less so to general readers of ACP. Nevertheless, the AMS is probably widespread enough to justify publication in ACP rather than a more specialized journal (e.g., AMT). In general, the conclusions are well-supported and the analysis seems to be carefully done and robust. There are however, several things that the authors should do before publication to improve the clarity and readability of the manuscript. First, many of the key figures are essentially illegible because a large amount of data is placed in multi-panel figures that end up being too small to read. Figures 3 and 5 are particularly bad though several others would also benefit from being larger and from multiple datasets being differentiated from one another more clearly. Second, there are several places where the authors could be more clear/specific in their writing. For example, when they refer to IEPOX SOA, it often isn’t clear whether they are talking about the PMF factor or the general concept of SOA formed from IEPOX. As another example it isn’t clear how exactly all the average $f_{C_5H_6O}$ values were calculated. There are a relatively large number of typos and grammatical mistakes and, while it was generally clear what the authors meant, it would be good if the authors gave the manuscript a more careful read before final publication. After these corrections are made, the manuscript should be publishable in ACP.

A1.0: All of the items mentioned here are addressed in response to the more specific comments below, in particular R1.1-R1.7, R1.9, R1.13, R2.1, R2.4 and R2.9.

Major Specific Comments

R1.1. P 11227, lines 1-2 and Page 11244 , lines 19-21. Can you be more specific about how you arrive at your conclusion that the IEPOX SOA estimate from $f_{C_5H_6O}$ will be accurate to within a factor of 2? Have you used your estimation method on more than the SOAS datasets to estimate the accuracy? As you mention, the SOAS data probably represents a best case scenario.

A1.1: The justification on how we obtain the method accuracy to be ~2 may not have been stated clearly enough. We have addressed this topic in detail in 1.2 part of the supporting information of the revised manuscript:

“To estimate the accuracy of our IEPOX-SOA tracer-based estimation method, we used this method to estimate IEPOX-SOA from another two ambient datasets with the lowest and highest $f_{C_5H_6O}^{IEPOX-SOA}$ in PMF-resolved IEPOX-SOA (IEPOX-SOA_{PMF}) among all the studies in this paper. The lowest value is from a dataset in the pristine Amazon forest (AMAZE-08) where $f_{C_5H_6O}^{IEPOX-SOA} = 12\%$ (Chen et al., 2015) and the highest value from a dataset in a Borneo forest with $f_{C_5H_6O}^{IEPOX-SOA} = 38\%$ (Robinson et al., 2011). Since the $f_{C_5H_6O}^{IEPOX-SOA}$ values in these two datasets are the two farthest from the average $f_{C_5H_6O}^{IEPOX-SOA}$ ($22 \pm 7\%$), the estimation method results from these two datasets represent the worst case scenarios for all datasets published so far.

The estimation results from both datasets are shown in Fig. S13 and Fig. S14. Both of the background OA corrections for areas strongly influenced by urban+BB emissions and by monoterpene emissions are used.

Overall, all variants of the estimated IEPOX-SOA correlate well with PMF-resolved IEPOX-SOA (all $R \geq 0.93$). When average $f_{C_5H_6O}^{IEPOX-SOA} = 22\%$ is used, the slope between estimated IEPOX-SOA vs PMF-resolved IEPOX-SOA is between 0.43-1.5, i.e. within a factor of 2.2. When the actual $f_{C_5H_6O}^{IEPOX-SOA}$ in each dataset is used, the slope between estimated IEPOX-SOA vs PMF-resolved IEPOX-SOA is in a range of 0.7-1.2, i.e. within 30%.”

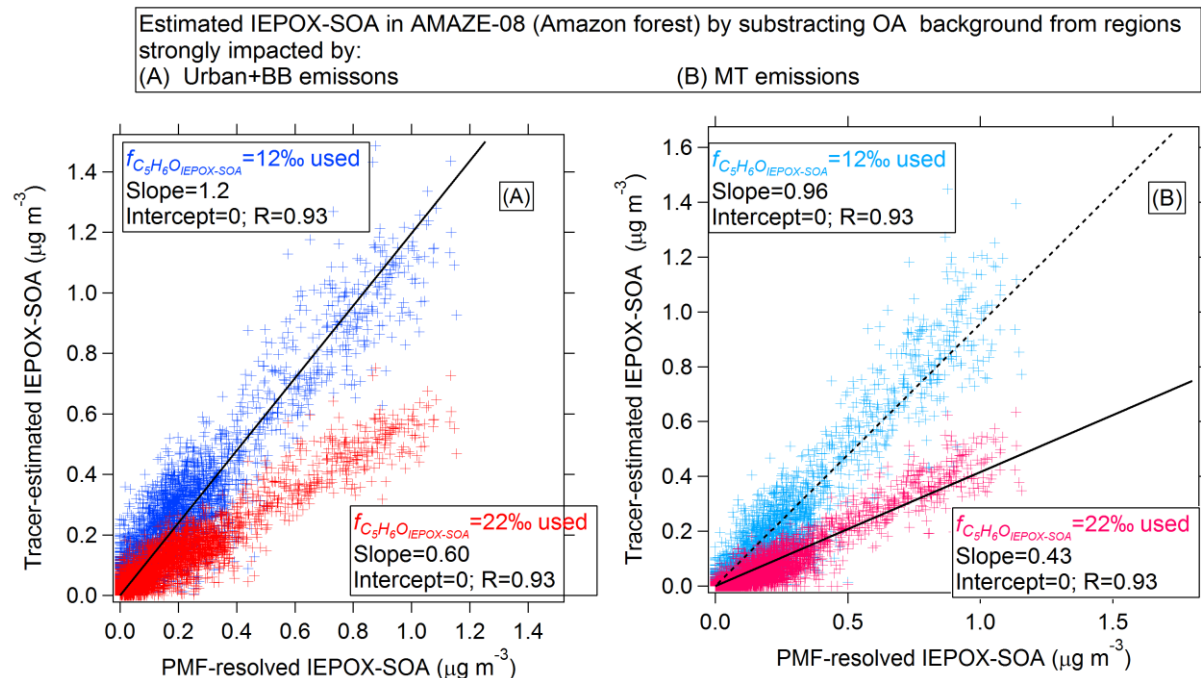


Figure S13. Scatter plot between tracer-estimated IEPOX-SOA and PMF-resolved IEPOX-SOA at a pristine Amazon forest site (AMAZE-08). The tracer-based IEPOX-SOA was estimated using OA background from regions strongly influenced by (A) urban and biomass-burning emissions and (B) monoterpene emissions. In each plot, we used two $f_{C_5H_6O}^{IEPOX-SOA}$, from the average IEPOX-SOA_{PMF} ($f_{C_5H_6O}^{IEPOX-SOA}=22\%$) and from the IEPOX-SOA_{PMF} in Amazon forest study ($f_{C_5H_6O}^{IEPOX-SOA}=12\%$).

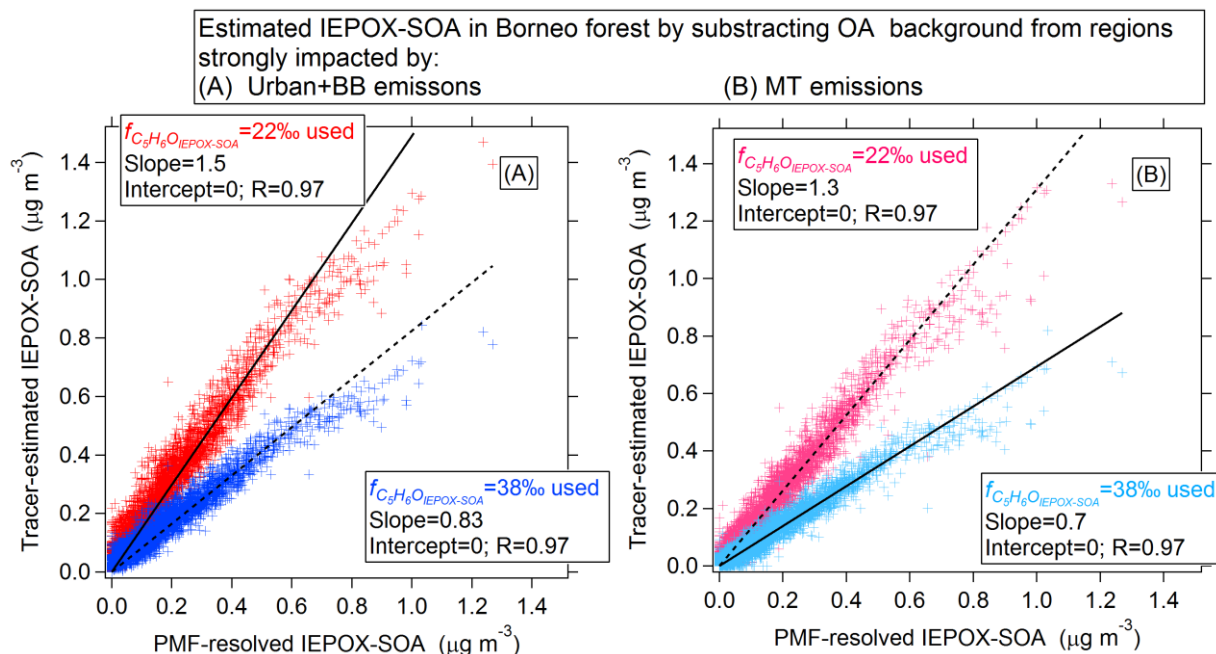


Figure S14 Scatter plot between estimated IEPOX-SOA and PMF-resolved IEPOX-SOA at a Borneo forest site. The tracer-based IEPOX-SOA was estimated using OA background from regions strongly influenced by (A) urban and biomass-burning emissions and (B) monoterpene emissions. In each plot, we used two $f_{C_5H_6O}^{IEPOX-SOA}$, from the average IEPOX-SOA_{PMF} ($f_{C_5H_6O}^{IEPOX-SOA}=22\%$) and from the IEPOX-SOA_{PMF} in Borneo forest study ($f_{C_5H_6O}^{IEPOX-SOA}=38\%$).

R1.2. Can you explain the bounds of when your $f_{C_5H_6O}$ estimation method can/can't or should/shouldn't be used? Is there a lower limit on $f_{C_5H_6O}$ (relative to the total organic particle mass) below which the estimation method is no longer accurate? In general it would be a benefit to the AMS community if you can explain the limits and bounds of your estimation method more clearly.

A1.2: Following the reviewer's suggestion, we have addressed this point in the supporting information.

In the main text, we have added a mention of this new information in the last part of section 3.9:

“Several scenarios based on different $f_{C_5H_6O}^{OA}$ values to use this tracer-based method are addressed in the supporting information. The justification from users on using this method is needed.”

In the supporting information part 1.1 we have added the following text:

“In theory, our method can easily produce an estimate of “IEPOX-SOA” from an AMS dataset, but the errors could be substantial in some cases. The guidelines below are meant to limit the errors when applying this method:

- 1) We first recommend making the scatter plot of $f_{CO_2}^{OA}$ and $f_{C_5H_6O}^{OA}$ and then compare it to Fig. 5 in this study to help evaluate the possible presence of IEPOX-SOA.**
- 2) For datasets where an important influence of MT-SOA is suspected: if all the $f_{C_5H_6O}^{OA}$ in total OA are $\sim 3.1\%$ or lower within measurement noise, the estimated IEPOX-SOA will show negative and positive values scattered around zero, indicating negligible IEPOX-SOA in the dataset. A similar conclusion can be reached for urban or BB-dominated locations when $f_{C_5H_6O}^{OA} \sim 1.7\%$ or lower for most data points.**
- 3) When the scatter plot between $f_{CO_2}^{OA}$ and $f_{C_5H_6O}^{OA}$ shows obvious enhanced $f_{C_5H_6O}^{OA}$ above the most-relevant background value, users can easily use the tracer-based method to estimate the IEPOX-SOA mass concentration. If the source of the background OA is not known, we suggest using both background corrections and reporting the range of results.**

- 4) Cases intermediate between No. 2 and 3 above, i.e. when $f_{C_5H_6O}^{OA}$ is only slightly above the relevant background level will have the largest relative uncertainty. In this case we recommend applying the method and evaluating the results carefully, as exemplified for the Rocky Mountain dataset in this paper (section 3.5). E.g. diurnal variations of $f_{C_5H_6O}^{OA}$ and SOA precursors (e.g., isoprene and monoterpene) and of estimated IEPOX-SOA provide useful indicators about whether the results are meaningful. For cases in which the fraction of IEPOX-SOA in total OA is relatively low (e.g., <5%) and the fraction of MT-SOA in total OA is high (e.g., >50%), the uncertainty of the IEPOX-SOA estimate will be very high. For this type of situation the full PMF method may be required.

Besides ease of use, another advantage of the tracer-based estimation method is that it can be used to quantify IEPOX-SOA based on brief periods of elevated concentrations, e.g. as often encountered in aircraft studies. In those cases it may be difficult for PMF to resolve an IEPOX-SOA factor, but no such limitation applies to this estimation method.”

R1.3. Abstract, lines 18-19 and several other places in paper (e.g., p 11243 lines 13-16). Several times in the manuscript, the authors compare $f_{C_5H_6O}$ of a bulk OA sample (for example, monoterpene SOA) to the $f_{C_5H_6O}$ found for the PMF factor attributed to IEPOX SOA. They authors do this to illustrate that $f_{C_5H_6O}$ is enhanced in IEPOX SOA and presumably to imply that the IEPOX $f_{C_5H_6O}$ signal is enhanced relative to other potential interferences (i.e., monoterpene SOA). However, it isn't really relevant to compare the $f_{C_5H_6O}$ of a PMF factor that is ~15% of the total OA to the $f_{C_5H_6O}$ for the entire OA sample. To me this is misleading.

A1.3: We thank the reviewer for pointing out this ambiguity, which appears to have been the largest source of confusion for the ACPD version. To avoid confusion we have changed this notation in the revised paper to always make explicit what we are referring to, as described in the added text below:

“We use a superscript to clarify the type of OA for which $f_{C_5H_6O}$ is being discussed: $f_{C_5H_6O}^{OA}$ refers to $f_{C_5H_6O}$ in total OA, $f_{C_5H_6O}^{IEPOX-SOA}$ to $f_{C_5H_6O}$ in IEPOX-SOA, $f_{C_5H_6O}^{MT-SOA}$ to the $f_{C_5H_6O}$ value in pure MT-SOA and $f_{C_5H_6O}^{OA-Bkg-UB}$ and $f_{C_5H_6O}^{OA-Bkg-MT}$ refer to background $f_{C_5H_6O}^{OA}$ from areas strongly influenced by urban+biomass-burning emissions and by monoterpene emissions, respectively. If we refer to $f_{C_5H_6O}$ in general, we will still use $f_{C_5H_6O}$.”

R1.4. From reading the manuscript, it seems the background $f_{C_5H_6O}$ is a minimum of 2 per mil and up to 4 per mil for areas of high MT emissions. The $f_{C_5H_6O}$ for all OA seems to be 5-6 per mil in many areas heavily influenced by isoprene emissions. So the $f_{C_5H_6O}$ “signal” from IEPOX SOA relative to the background $f_{C_5H_6O}$ “noise” isn't very elevated in most areas. Borneo (and perhaps the Amazon) seems to be an exception. Can the authors comment more on this issue?

A1.4: We have emphasized the differences of $f_{C_5H_6O}$ between IEPOX-SOA and MT-SOA in the abstract to be clearer:

“The average laboratory monoterpene SOA value ($5.5 \pm 2.0\%$) is 4 times lower than the average for IEPOX-SOA ($22 \pm 7\%$), which leaves some room to separate both contributions to OA.”

We have modified the main text and added a new Fig. S8 to more clearly illustrate this difference in the supporting information:

“We note that the average lab-generated MT-SOA value is still 4 times lower than the average for IEPOX-SOA_{PMF} and IEPOX-SOA_{lab} (Fig. S8), and thus there is some room to separate both contributions”

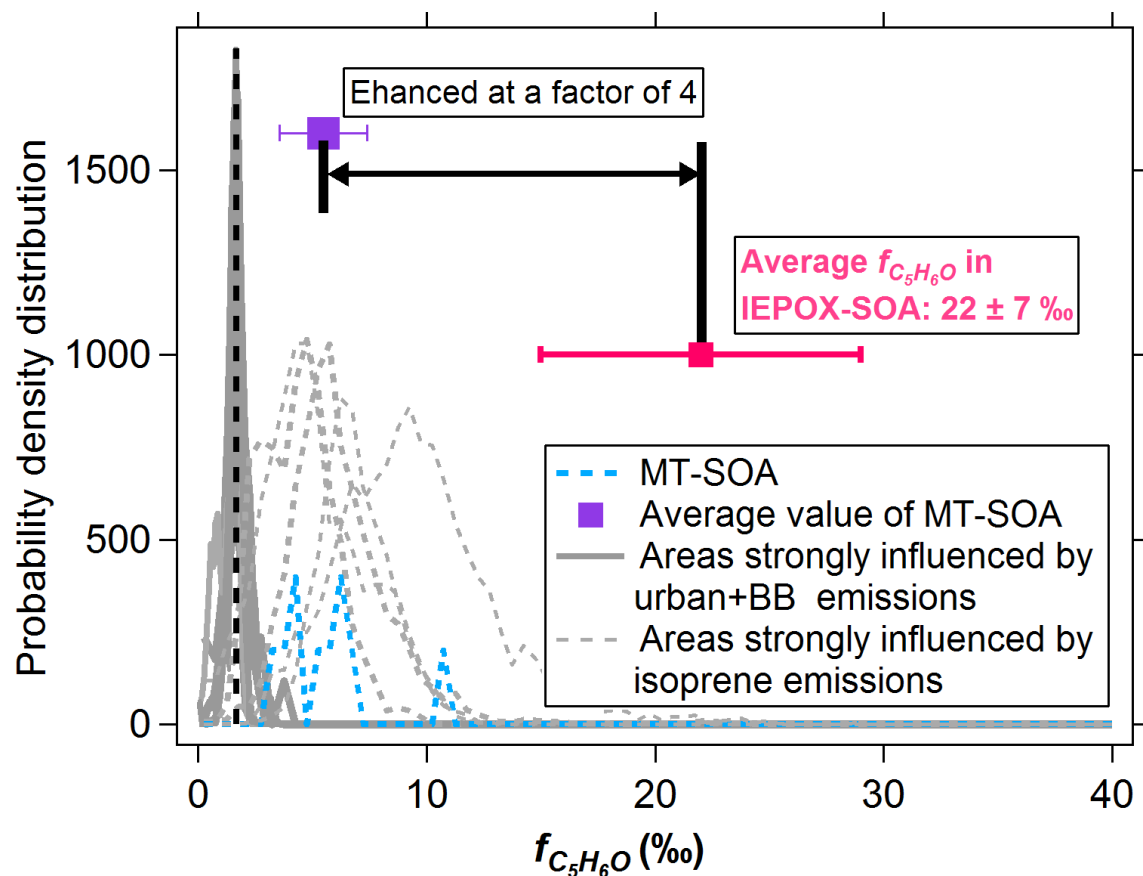


Figure S8 Comparison between $f_{C_5H_6O}^{MT-SOA}$ and $f_{C_5H_6O}^{IEPOX-SOA}$, $f_{C_5H_6O}^{OA}$ from areas strongly influenced by urban + biomass burning and isoprene emissions are also shown.

We also address the reason why smaller differences are observed in $f_{C_5H_6O}^{OA}$ between areas strongly influenced by isoprene emissions and by monoterpene emissions in the last part of section 3.5:

“Note that the difference between $f_{C_5H_6O}^{OA}$ in areas strongly influenced by monoterpene emissions ($3.1\pm 0.6\%$) and isoprene emissions ($6.5\pm 2.2\%$) is reduced, compared to a factor of 4 difference between pure MT-SOA ($5.5\pm 2.0\%$) and IEPOX-SOA ($22\pm 7\%$). This is likely due to the physical mixing of OA from different sources and in different proportions at each location.

R1.5. Abstract lines 15-20 and through paper. Please explain how you are weighting the average $f_{C_5H_6O}$ when combining data from many different studies, if at all. I can easily imagine that high frequency data from one study would completely overwhelm the average because of the larger number of points. As an example, aircraft data are recorded generally at 0.1 – 1 Hz, but ground data are typically averaged over significantly longer timescales. How do you treat this?

A1.5: We have added the following text to clarify this issue:

“When we report the average $f_{C_5H_6O}^{OA}$ in each campaign, as shown in the Table 1, we used the average from the time series of $f_{C_5H_6O}^{OA}$ at their raw time resolution (secs to mins). During this process, we exclude points whose OA mass concentrations are below twice the detection limit of OA in AMS (typically $2 \times 0.26 \mu\text{g m}^{-3} = 0.5 \mu\text{g m}^{-3}$). When averaging $f_{C_5H_6O}^{OA}$ values across datasets, we counted each dataset as one data point.”

R1.6. Related to this point, in the abstract, you list the average $f_{C_5H_6O}$ for MT influenced airmasses as 3.1 per mil. The Rocky Mountain data average is 3.7 per mil, the DC3 data influenced by MT emissions average 4.1 per mil and the boreal forest data average 2.5 per mil. From these values, it seems like the $f_{C_5H_6O}$ for MT background should be a little higher than 3.1. How do you calculate the 3.1 number given in the abstract?

A1.6: The 3.1‰ comes from the average value of 2.5‰ in boreal forest and 3.7‰ in Rocky Mountain dataset. We did not include 4.1‰ from DC3 dataset in this calculation, because 4.1‰ is only a single data point that we observed in an aircraft flight, and using that value could bias the average high. When we average all the enhanced $f_{C_5H_6O}^{OA}$ values (from 1.7‰-4.1‰) corresponding to the enhanced monoterpene concentrations for the DC3 flight in the Fig. 6, we obtain a $f_{C_5H_6O}^{OA}$ estimate of $3.0\pm 0.3\%$ from this period, which is similar to the average of 3.1‰ averaged from the Rocky mountain site and boreal forest site. We have modified the text in section 3.5 to clarify this point as:

“The average $f_{C_5H_6O}^{OA}$ in areas strongly influenced by monoterpene emissions is $3.1\pm 0.6\%$, obtained by averaging the values from the Rocky mountain forest (3.7‰), European boreal forest (2.5‰), and DC3 flight (3.0‰).”

R1.7 Through paper: There are a large number of unpublished studies cited in this manuscript. 11 cited referenced are unpublished; 6 are under review (i.e., discussion manuscripts) and 5 are “in preparation”. Some of the “in preparation” datasets, primarily from PMF analysis of field data, are used in the manuscript. To me this seems unusual because there has been no peer-

review of this data and insufficient details are provided in the manuscript to assess the data quality. I was unable to find ACP's policy on this, so I leave it to the editor to decide if this is an issue or not. The "in preparation" data are used heavily in the figures and it is difficult to say whether the authors would have come to the same conclusions or whether their conclusions would have been as robust, if this data were to be excluded.

A1.7: We understand the reviewer's concern about citing unpublished studies in our paper. Unfortunately when working on new and very active areas of research, this can sometimes be the case as the other relevant studies are mostly being conducted at the same time. Also importantly our paper should be considered the reference that presents the data for the unpublished studies, and the additional references are provided as a linkage to the literature for readers interested in additional detail on those studies. In addition, excluding the results for which a cited reference is unpublished does not change our conclusions.

In detail, in the ACPD version of our paper, 5 papers were under review but publicly accessible (in ACPD or AMTD) and 5 papers were in preparation. As of the submission of the revised version of our paper, the number of unpublished references has been reduced from 10 to 3. Five papers have been accepted for publication while our paper was under review and revision (an indication of the very active state of this area of research).

One paper is a citation to a referee comment on an ACPD paper that suggested the potential interference of MT-SOA in $f_{C_5H_6O}^{OA}$. We have kept this reference as it was the only mention of this issue that we could find in the literature, and since we only use this reference to suggest a problem that we proceed to explore in detail in our paper. This reference is:

"Anonymous_referee: Interactive comment on "Airborne observations of IEPOX-derived isoprene SOA in the Amazon during SAMBBA" by J. D. Allan et al., Atmos. Chem. Phys. Discuss., 14, C5277–C5279, 2014."

We also cited the overview paper for the SEAC4RS study, which is still in preparation.

"Toon, O. B.: Planning, implementation and scientific goals of the Studies of Emissions and Atmospheric Composition, Clouds and Climate Coupling by Regional Surveys (SEAC4RS) field mission, in prep., 2015".

However, since the SEAC4RS and DC3 datasets used here have been described in another paper, we change this citation to be:

"Liao, J., Froyd, K. D., Murphy, D. M., Keutsch, F. N., Yu, G., Wennberg, P. O., St. Clair, J. M., Crounse, J. D., Wisthaler, A., Mikoviny, T., Jimenez, J. L., Campuzano Jost, P., Day, D. A., Hu, W., Ryerson, T. B., Pollack, I. B., Peischl, J., Anderson, B. E., Ziemba, L. D., Blake, D. R., Meinardi, S., and Diskin, G.: Airborne measurements of organosulfates over the continental US, Journal of Geophysical Research: Atmospheres, 120, 2990-3005, 10.1002/2014jd022378, 2015."

As of the submission of this revised paper, only 1 paper is submitted and 2 papers are in preparation (listed below).

Submitted

Hu, W., Hu, M., Hu, W., Jimenez, J.-L., Yuan, B., Chen, W., Wang, M., Wu, Y., Wang, Z., Chen, C., Peng, J., Shao, M., and Zeng, L.: Chemical composition, sources and aging process of sub-micron aerosols in Beijing: contrast between summer and winter, submitted to JGR, 2015.

In preparation:

Carbone, S., De Brito, J. F., Andreae, M., Pöhlker, C., Chi, X., Saturno, J., Barbosa, H., and Artaxo, P.: Preliminary characterization of submicron secondary aerosol in the amazon forest– ATTO station, in preparation, 2015.

de Sá, S. S., Palm, B. B., Campuzano-Jost, P., Day, D. A., Hu, W., Newburn, M. K., Brito, J., Liu, Y., Isaacman-VanWertz, G., Yee, L. D., Goldstein, A. H., Artaxo, P., Souza, R., Manzi, A., Jimenez, J. L., Alexander, M. L., and Martin, S. T.: Mass spectral observations of fine aerosol particles and production of SOM at an anthropogenically influenced site during GoAmazon2014wet season, in preparation, 2015.

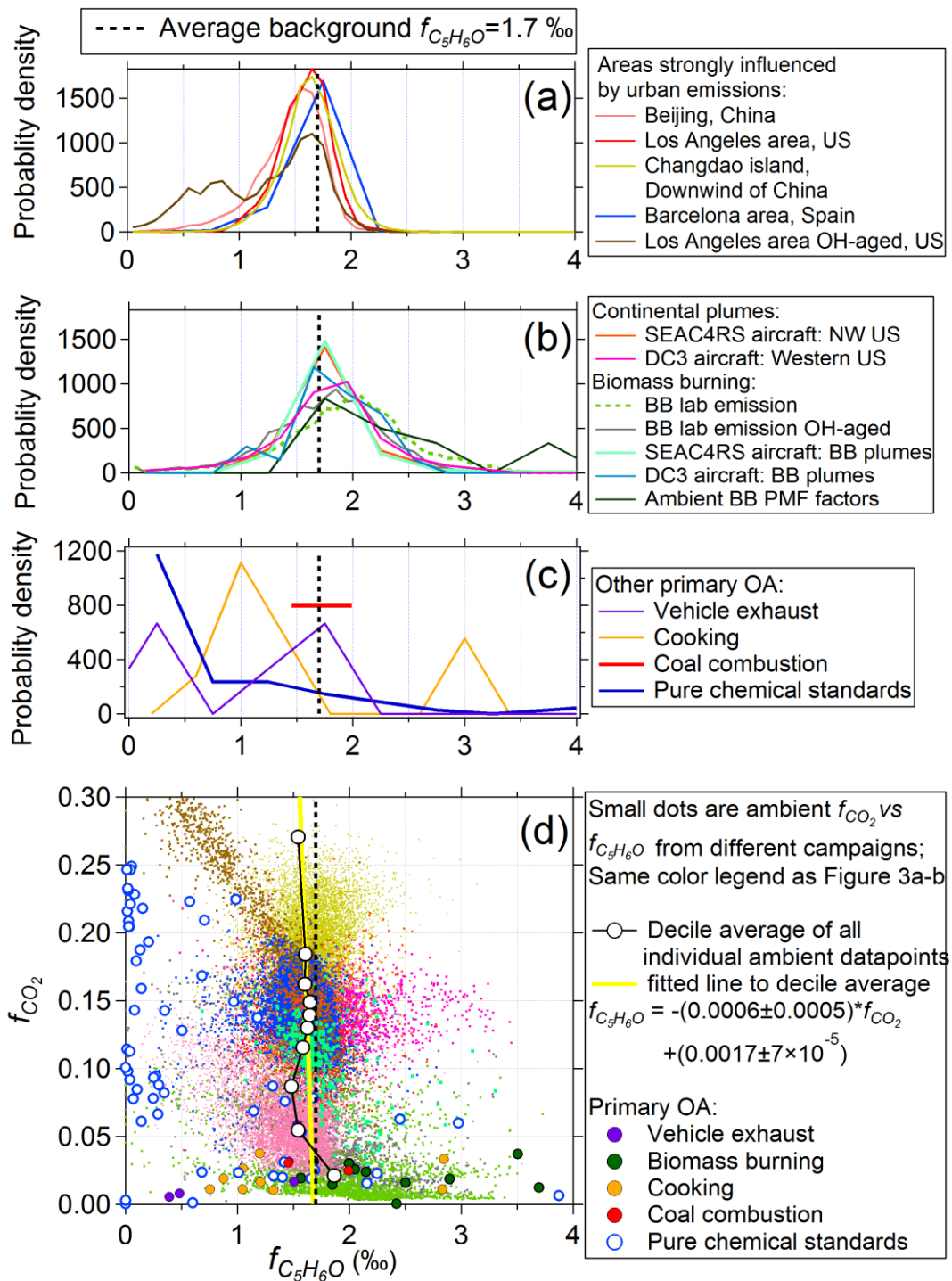
R1.8. Page 11233, line6-8. $f_{C_5H_6O}$ has a very specific meaning as does f_{82} . They are not the same. I find it highly objectionable that UMR f_{82} data are included in the $f_{C_5H_6O}$ average and labeled as $f_{C_5H_6O}$. Further, it isn't clear which datasets were analyzed for $f_{C_5H_6O}$ and which for f_{82} . Please either remove the f_{82} from the $f_{C_5H_6O}$ average or call the average f_{82} .

A1.8: We disagree with the reviewer on this point. We have updated the text to clarify this issue:

“The average $f_{C_5H_6O}^{IEPOX-SOA}$ value shown here also includes f_{82} data from four UMR IEPOX-SOA_{PMF} spectra. This is justified since $C_5H_6O^+$ accounts for over 95% of m/z 82 in IEPOX-SOA based on results from SOAS-CTR and other lab studies (Kuwata et al., 2015). Indeed the average does not change if the UMR studies are removed from the average.”

R1.9 Figure 3: This figure is generally illegible, with the legends particularly so. Please revise. What are the arrows pointing to on the right Y axes?

A1.9: Following the reviewer's suggestion, we have revised our Fig. 3 for clarity as shown below. The arrows have been removed for clarity.



R1.10. Figure 4. It looks like, if a PDF of $f_{C_5H_6O}$ for monoterpene SOA were placed on this figure, it would be very similar to the PDFs of the isoprene influenced field data. Can you also include the PDF for monoterpene SOA in the figure? Doesn't this argue that there is in fact a

very significant contribution of monoterpene SOA to $f_{C_5H_6O}$? It looks like the Borneo data PDF is significantly higher in $f_{C_5H_6O}$ than the others field data PDFs and the monoterpene lab SOA PDF.

This figure seems to suggest that the “interference” from monoterpene SOA could be worse than the authors argue. If the Borneo data are excluded from the average $f_{C_5H_6O}$, does it change significantly?

A1.10: We have updated the two figures below (Fig. 4 and Fig. S8, shown above in response A1.4) by adding the PDF of $f_{C_5H_6O}^{MT-SOA}$ (dashed blue line) from pure MT-SOA (10 data points). A detailed response to this comment can be found in the response to R 1.4.

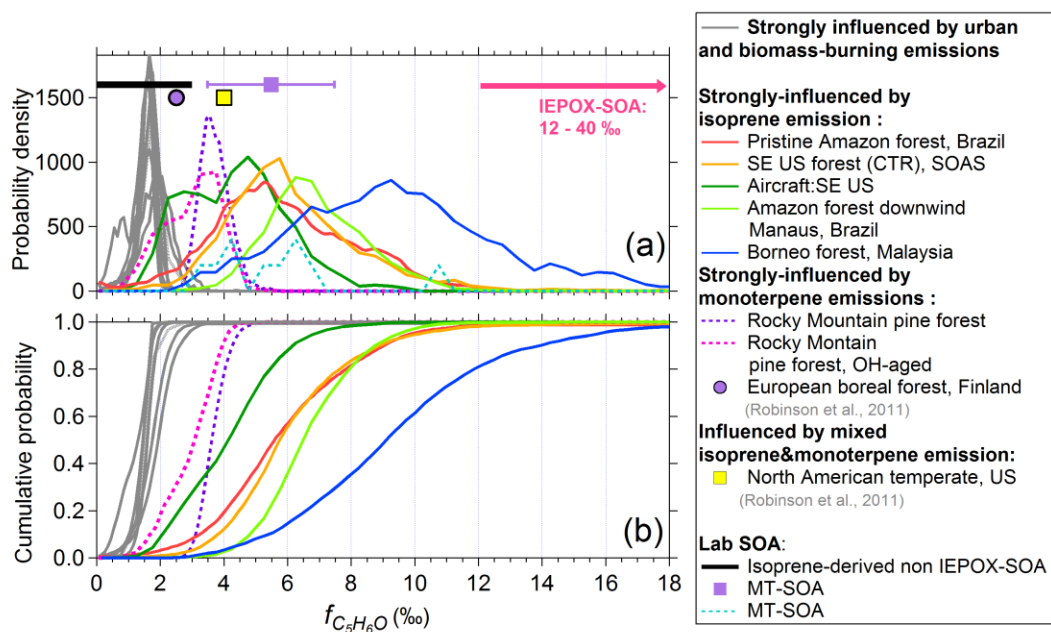


Figure 4. (a) Probability density and (b) cumulative probability distributions of $f_{C_5H_6O}^{OA}$ in studies strongly influenced by isoprene and/or monoterpene emissions. The ranges of $f_{C_5H_6O}$ from other non IEPOX-derived isoprene-SOA and MT-SOA are also shown. The background grey lines are from studies strongly influenced by urban and biomass-burning emissions and are the same data from Fig. 3a – b. The arrow in Fig. 4a indicates the range of $f_{C_5H_6O}^{IEPOX-SOA}$ between 12‰ (start of the arrow) to 40‰ which is beyond the range of x-axis scale.

R1.11. Figure 4: It is very difficult to distinguish the colors of many of the lines from one another because of the color choices and size of the figure. Please revise.

A1.11: The revised figure is shown in response to comment R1.10.

R1.12. It isn't clear what the arrow pointing to the right Y axis is meant to indicate.

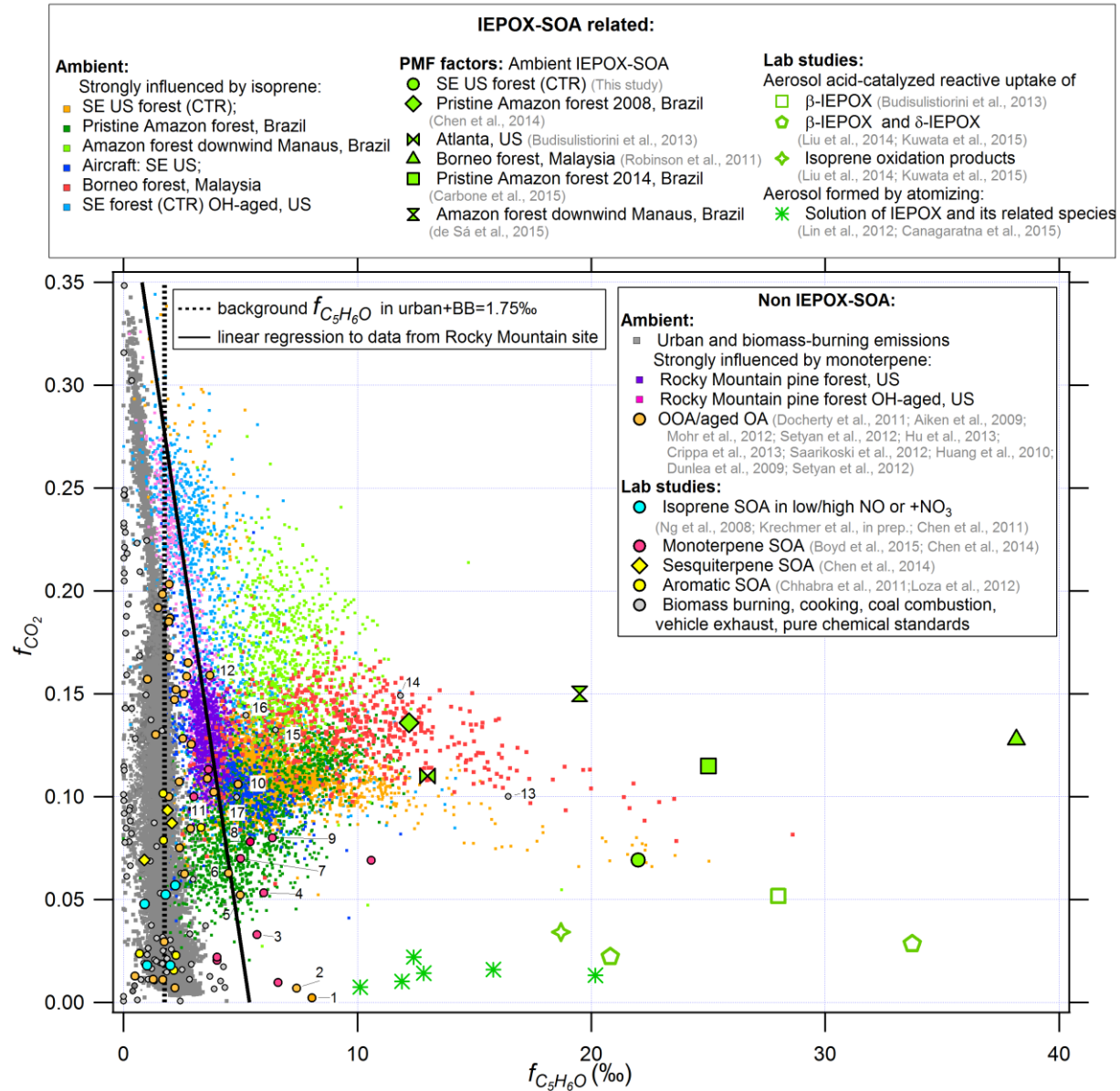
A1.12: We use this arrow to point out the highest $f_{C_5H_6O}^{IEPOX-SOA}$, which is beyond the range of the x-axis in Figure 4. We moved the arrow to the same height as MT-SOA and isoprene-derived

non IEPOX-SOA and added the corresponding explanation in the figure caption (as shown in the response to comment R1.10):

R1.13. Figure 5: The figure is generally illegible due to size and the amount of information on the figure. The symbols are indistinguishable from one another and the legend is impossible to read. I can't make out any of the numbered points aside from 1, 2, and 13. Please revise.

It isn't clear what the pink arrow in the middle of the figure is meant to indicate.

A1.13: Following the reviewer's suggestion, we significantly revised the figure as shown below:



Minor Comments and Technical Corrections

R1.14. Through paper: The authors often use the term average when the text seems to indicate they really mean mode (based on a vertical line drawn to the mode in most figures). Please clarify when/if you mean average and when/if you mean mode. This is relevant because few of the PDFs appear to be normally distributed.

A1.14: We have revised the text as needed to clarify what kind of value (average vs. mode) has used in the paper. Please see the details of the averaging methods used in the response to comment R1.5.

R1.15. Abstract and through paper. It would be helpful to define the per mil symbol the first time in is introduced.

A1.15: Following the reviewer's suggestion, we have defined the per mil in the abstract and main text when it show up in the first time.

In the abstract: **“A background of $\sim 1.7 \pm 0.1\%$ ($\%$ =parts per thousand) is observed”**

In the main text: **“ $f_{C_5H_6O}^{IEPOX-SOA}$ in IEPOX-SOA from SOAS and other field and laboratory studies (Table 1) ranges from 12% to 40% ($\%$ =parts per thousand)...”**

R1.16. Page 11226, line 4-5. What other low NO oxidation pathways would produce IEPOX-SOA? This is alluded to several times, but never defined. Do you mean IEPOX-SOA the PMF factor or do you mean SOA produced from IEPOX? It is confusing at times to discern whether the authors are talking about SOA formed from IEPOX (a mix of some known and some unknown organics produced by a specific process) or the PMF factor attributed to IEPOX SOA (an output of PMF). This is one clear case.

A1.16: We are referring to the recent finding in Jacobs et al. (2014): IEPOX can be formed in the oxidation of isoprene under high NO, via oxidation the 4-hydroxy-3-nitroxy isoprene (13%). Thus, we revised our sentence in the abstract to be:

“Total IEPOX-SOA, which may include SOA formed from other parallel isoprene oxidation pathways...”

We also added corresponding text in the introduction part to clarify:

“Note that some IEPOX can also be formed from isoprene in high NO region via oxidation of the product 4-hydroxy-3-nitroxy isoprene (Jacobs et al., 2014) , however this pathway is thought to be much smaller than the low-NO pathway.”

We agree with the reviewer's comment that the specific meaning of the term “IEPOX-SOA” in the paper text can be confusing. Thus, we have added the text below to clarify:

“We denote the IEPOX-SOA factor from PMF as “IEPOX-SOA_{PMF}” and IEPOX-SOA from lab studies as “IEPOX-SOA_{lab}”. If we use “IEPOX-SOA” in the paper, it refers to a broad concept of IEPOX-SOA.”

R1.17. Page 11226, line 9-11. Consider revising this sentence for clarity.

A1.17: We revised this sentence as:

“During the Southern Oxidant and Aerosol Study (SOAS) study, 78% of PMF-resolved IEPOX-SOA is accounted by the measured IEPOX-SOA molecular tracers (methyltetrols, C5-Triols and IEPOX-derived organosulfate), making it the highest level of molecular identification of an ambient SOA component to our knowledge”

R1.18. Page 11228, lines 22-25. Conversion of IEPOX to IEPOX-SOA requires gas-to-particle partitioning. I think you mean non-reactive partitioning here, but please clarify.

A1.18: Yes, the reviewer is correct. We mean non-reactive partitioning here. We revised the sentence to read:

“... because gas-phase IEPOX has high volatility, non-reactive gas-to-particle partitioning of IEPOX into OA is negligible under typical ambient concentrations in forest areas”

R1.19. Page 11230, lines 8-9. What is the rationale for including the polluted Amazon site in the “strongly influenced by isoprene” category as opposed to “strongly influenced by urban emissions” category? To me “polluted” in this context means influenced by Manaus emission. It would be good to clarify why the data were placed in one category rather than the other.

A1.19: We added the reason why we classify this site as strongly influenced by isoprene emissions:

“Two pristine forest site and one forest site partially impacted by urban plumes in the Amazon rain forest (Brazil). The latter site is classified in this category because (i) high isoprene concentrations (e.g. 3 ppb in average peaks in the afternoon) were observed during the study; (ii) the impact of biogenic SOA formed during 1000 km where the air travels over the pristine forest upwind of Manaus; (iii) PMF results indicate an important impact of IEPOX-SOA at this site (de Sá et al., 2015); and (iv) PTRMS results indicate a substantial concentration of the isoprene hydroperoxyde formed by low-NO chemistry.”

R1.20. Page 11230, lines 14-15. Many of campaigns actually haven't been described in the literature and the referenced are listed as “in preparation” (see related comment in major comments section).

A1.20: Please see the response to comment R1.7.

R1.21. Page 11232, lines 26-28. Revise this sentence for clarity.

A1.21: Revised.

Original sentence: “The temporal variation of ion $C_5H_6O^+$ correlates best ($R=0.96$) with that IEPOX-SOA among all OA ions (Table S1), suggesting that it may be the best tracer among all ions for IEPOX-SOA”.

Revised sentence: **“The temporal variation of ion $C_5H_6O^+$ correlates best ($R=0.96$) with IEPOX-SOA_{PMF} among all measured OA ions (Table S1). This result suggests that $C_5H_6O^+$ ion may be the best ion tracer for IEPOX-SOA among all OA ions. ”**

R1.22. Page 11235, line 14. Add “that” between conditions and are.

A1.22: Added.

R1.23. Page 11240, line 4. Revise “Amazon forest down Manaus campaigns”.

A1.23: We modified this text to read: “**Amazon forest downwind of Manaus**”

R1.24. Page 11240, line 12. Revise “have low $f_{C_5H_6O}$ are”

A1.24: We revised the original sentence to be:

“...points with both lower $f_{CO_2}^{OA}$ (<0.08) and low $f_{C_5H_6O}^{OA}$ ($< 8\%$) values are thought...”

R1.25. Figure5, page 112340, lines 14-19. I’m struggling to see how the points group into a triangle. The points don’t seem to group into any shape at all. Please clarify.

A1.25: This trend was perhaps obscured by the complexity of the figure. We have added Figure S10, shown below, to more clearly illustrate the applicability of the “triangle area.”

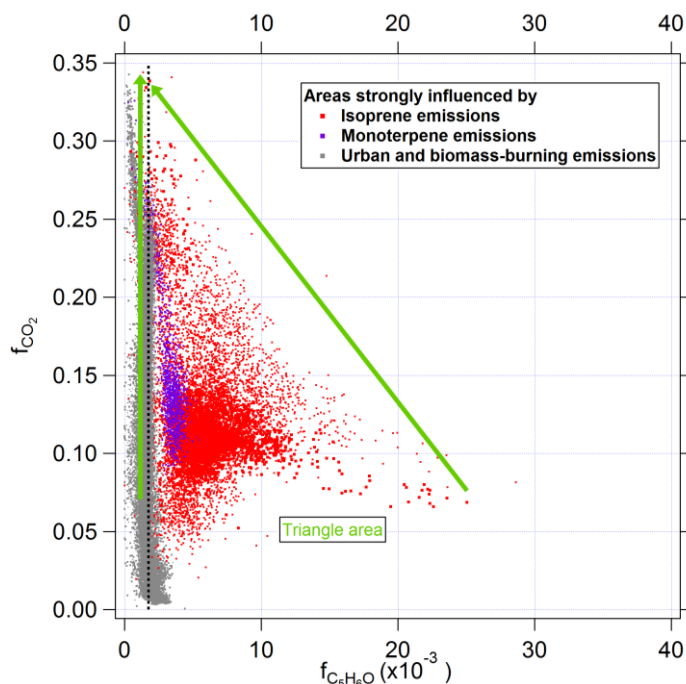


Figure S10. Scatter plot between $f_{CO_2}^{OA}$ and $f_{C_5H_6O}^{OA}$ for all the ambient OA dataset. Green arrows are added to guide the eye.

R1.26 Page 11240, line 16-18. Revise for clarity.

A1.26: Revised.

Original sentence: “This “triangle shape” indicates that in most of campaigns of this study shows the local OA with IEPOX-SOA contributions is influenced by the ambient oxidation processes or mixing with more aged aerosols.”

Revised sentence: “This “triangle shape” indicates that as the ambient OA oxidation increases, the IEPOX-SOA signature is reduced, potentially by the ambient oxidation processes or by physical mixing with airmasses containing more aged aerosols.”

R1.27 Page 11243, line 13, Revise “An alternative estimate as $f_{C_5H_6O}$ from area”

A 1.27: We revised the sentence to be:

“An alternative estimate for background $f_{C_5H_6O}^{OA}$ in areas with strong monoterpene emissions”

R1.28 Section 3.10 and Figure 8. In the preceding section (3.9), you present two alternative expressions for estimating $f_{C_5H_6O}$ background for MT influenced areas. Which expression was used in Figure 8?

A1.28: In the Fig. 8, we applied the $f_{C_5H_6O}$ at the Rocky Mountain site estimated by $f_{C_5H_6O} = (0.41 - f_{CO_2}) \times 0.013$ as background $f_{C_5H_6O}^{OA}$ for areas with strong MT-SOA contributions. We added one sentence in the main text to clarify:

“Finally, we have decided to use $f_{C_5H_6O}^{OA}$ estimated from the Rocky Mountain site as $f_{C_5H_6O}^{OA-Bkg-MT}$ in the following calculation.”

Anonymous Referee #2

General comments

This manuscript presents a relatively comprehensive study using a variety of field and lab results to investigate the strength and limitation of using AMS data to represent ambient SOA formed from IEPOX. This study shows a positive relationship between AMS IEPOX-SOA and GEOSChem modeled gas phase IEPOX at many locations globally w and w/o isoprene emission. This study also estimates the interference in C₅H₆O signal from monoterpene and other sources (e.g urban, biomass burning). The authors found that IEPOX-SOA mass loading derived from AMS data is comparable to the measured molecular tracers concentrations in SOAS. The authors also provide a new method to estimate IEPOX-SOA w/o PMF, which may be useful when PMF is not available. This study brings the aerosol community a better understanding of IEPOX SOA derived from AMS measurements, which have been used in many studies of SOA formed from IEPOX. In general, the authors interpret their data carefully. However, there are a few places not clear in the manuscript. I think this manuscript is suitable for publishing in ACP after the authors address my comments below.

Specific comments

R 2.1. The manuscript uses both PMF IEPOX-SOA factor and $f_{C_5H_6O^+}$ to evaluate if AMS data can well represent SOA from IEPOX. I think the PMF IEPOX-SOA factor is the one that most people in the AMS community use to represent IEPOX SOA mass loadings. The authors checked the background values of $f_{C_5H_6O^+}$ in many non-isoprene dominant environments. Could the authors be clear about how those interferences would be reflected in the IEPOX-SOA factor ($\mu\text{g}/\text{m}^3$) ?

A 2.1: The PMF-resolved IEPOX-SOA factor is indeed the one reported as IEPOX-SOA in most of ambient measurements (Slowik et al., 2010;Robinson et al., 2011;Budisulistiorini et al., 2013;Xu et al., 2014;Budisulistiorini et al., 2015;Chen et al., 2015). One study from Allan et al. (2014) used f_{82} as a tracer for IEPOX-SOA in flight measurements over the Amazon forest. The tracer method was not available until the publication of our paper, and thus it has not been used in past literature.

We believe that the reviewer is asking us to quantify the uncertainty of the IEPOX-SOA mass concentrations reported from PMF. This uncertainty will depend on each specific case. As a representative example, we estimate this uncertainty for the SOAS dataset using the bootstrap method, which provides a quantitative assessment of the uncertainty of the factors (Ulbrich et al., 2009). 100 bootstrapping runs are carried out. The results are shown in the figure below, which was also added to the supporting information (Fig. S1).

The uncertainty (standard deviation) for C₅H₆O⁺ in IEPOX-SOA is around 3%. The average uncertainty of the IEPOX-SOA mass concentration time series is ~9%.

A summary of this result was added into the paper: “An uncertainty of IEPOX-SOA_{PMF} mass concentration of ~9% was estimated from 100 bootstrapping runs in PMF analysis (Ulbrich et al., 2009) (Fig. S1). This uncertainty concerns only the PMF separation method. In practice the uncertainty in IEPOX-SOA_{PMF} concentration is dominated by the larger uncertainty on the AMS concentrations arising from the collection efficiency and relative ionization efficiency (Middlebrook et al., 2012).”

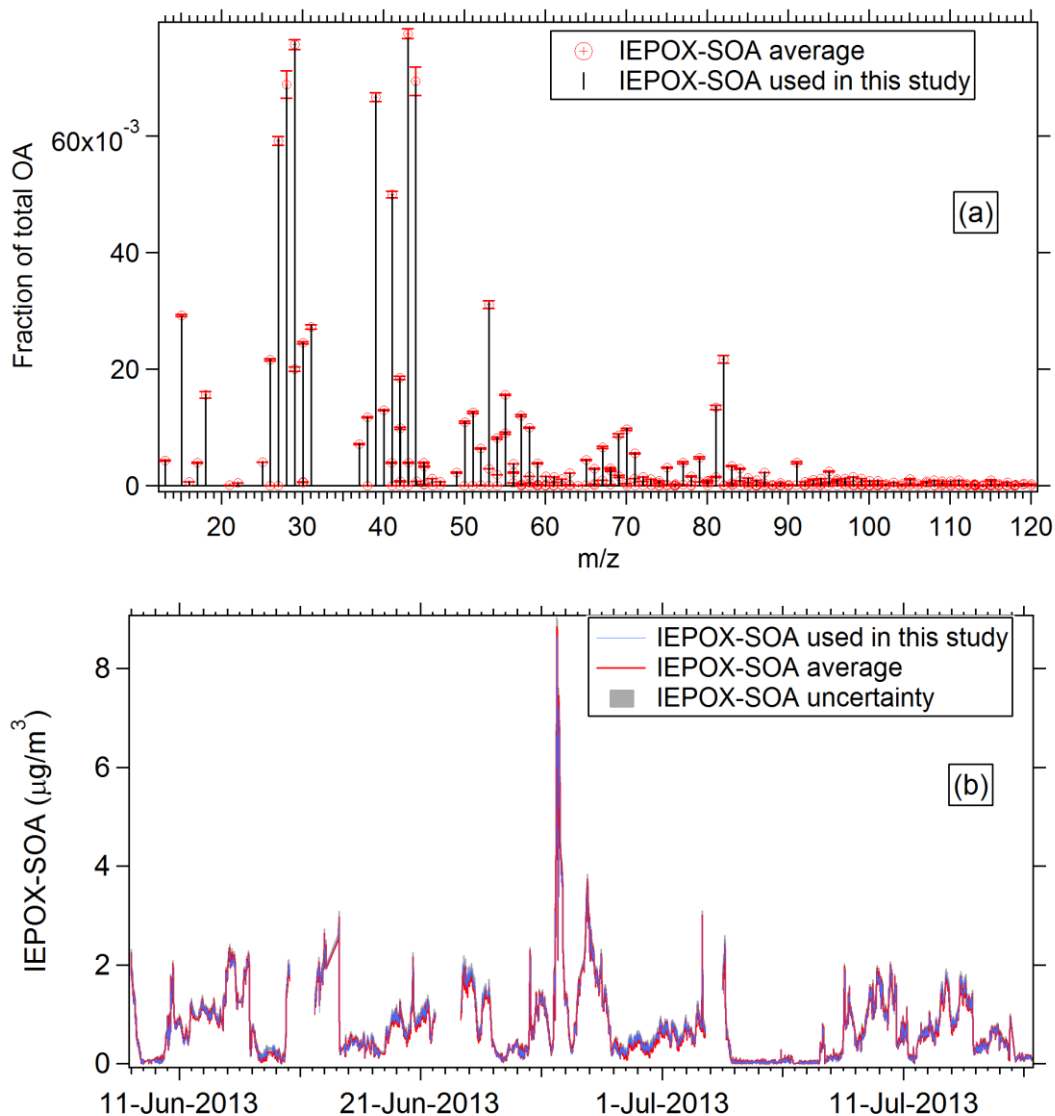


Figure S1. Results from bootstrapping analysis of the 4-factor solution of the SOAS dataset. Average IEPOX-SOA, with standard deviation, are shown for IEPOX-SOA (a) mass spectrum and (b) time series.

R 2.2. Also, it is often not clear when the $f_{C_5H_6O^+}$ values in the manuscript are $C_5H_6O^+/OA$ from IEPOX-SOA factor mass spectra only, from all data or from non-IEPOX-SOA factor data. I

think it is important to keep them consistent. I suggest using “ $f_{C_5H_6O+.all}$ ” or other symbol to represent from all data and using “ $f_{C_5H_6O+.IEPOX-SOA}$ ” or other different symbol to represent from IEPOX-SOA factor data only. I was misled at the beginning when I read the manuscript. For example, in the abstract, $f_{C_5H_6O}$ in IEPOX-SOA of (12–40 ‰) looks much higher than that influenced by monoterpene (3.1 ‰). These values are actually apples and oranges.

A2.2: Please see the response to comment R1.3

R2.3. Page 11226 line 24-25: Please state clearly if “the low $f_{C_5H_6O}$ (< 3 ‰) observed in non IEPOX-derived isoprene-SOA” is the result in the lab or in the ambient. Also I think the abstract should be clearer if this result is from part of this study or derived from previous published results.

A2.3: We revised our sentence to clarify this point as:

Original: “The low $f_{C_5H_6O}$ (< 3 ‰) observed in non IEPOX-derived isoprene-SOA indicates that this tracer ion is specifically enhanced from IEPOX-SOA, and is not a tracer for all SOA from isoprene”

Revised: **“The low $f_{C_5H_6O}$ (<3‰) reported in non IEPOX-derived isoprene-SOA from chamber studies indicates that this tracer ion is specifically enhanced from IEPOX-SOA, and is not a tracer for all SOA from isoprene”**

R2.4. Figure 2(b) What about the correlation between IEPOX-SOA and C5-alkene triols and IEPOX-derived organosulfates and dimers?

A2.4: We have added the relevant information to the main text (section 3.1) and also Fig. S2 to the supporting information:

“Other IEPOX-SOA tracers, such as C5-alkene triols, IEPOX-organosulfates, and dimers containing them, can also be measured by offline GC-EI/MS and LC/MS (Lin et al., 2014; Budisulistiorini et al., 2015), and they account for 28% and 24% in total IEPOX-SOA in SOAS (R=0.7), respectively (Fig. S2).”

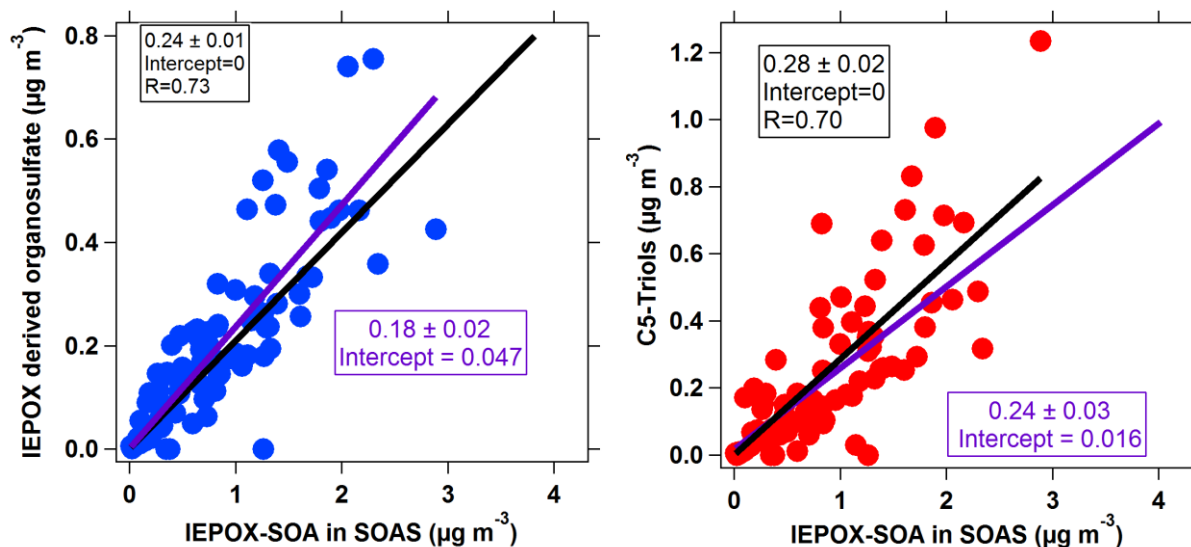


Figure S2. Scatter plots between IEPOX-derived organosulfate and C5-triols vs IEPOX-SOAPMF in the SOAS study. The IEPOX-derived organosulfate and C5-triols were measured in GC/MS and LC/MS analysis of filter extracts (Lin et al., 2014; Budisulistiorini et al., 2015).

R2.5. Page 11232:

“No IEPOX-SOA factor found in areas strongly influenced by urban emissions (e.g. Hayes et al., 2013)” does not give us information whether IEPOX pathway is suppressed by high NO unless you measured high isoprene levels there.

A2.5: We have modified this text to clarify this issue:

“No IEPOX-SOAPMF factor (i.e. below the PMF detection limit of ~5% of OA, Ulbrich et al., 2009) was found in areas strongly influenced by urban emissions where high NO concentrations suppress the IEPOX pathway, even in the presence of substantial isoprene concentrations (e.g. Hayes et al., 2013).”

R2.6. Page 11244: “Given the spread of values of f_{C5H6O} IEPOX-SOA (12–40 %) in different studies, if no additional local IEPOX-SOA spectrum is available for a given site, the estimation from this method should be within a factor of 2 of the actual concentration.”

Considering that the interference from monoterpene oxidation is important (e.g. f_{C5H6O} in rocky mountain comparable to SE aircraft data: Figure 4) and that estimation from monoterpene interference is derived from only one site (rocky mountain), I think more data are needed to testify the method and the above conclusion is a little bit too strong.

A2.6: Please see response to comment R1.1.

R2.7 Page 11245

Paragraph 2 “Low tracer values ($f_{C_5H_6O} < 3 \text{ ‰}$) are observed in non IEPOX-derived isoprene-SOA, indicating that the tracer ion is specifically enhanced from IEPOX-SOA, and is not a tracer for all SOA from isoprene.” Please also state if this is lab or ambient result because the paragraph starts with “ In ambient OA ...” and this sentence is somehow misleading when I read.

A2.7: This is effectively the same comment as R2.3, but here referring to the text in the conclusions, rather than the main text. Consistent with our response to R2.3, we have revised the next in the conclusions to read:

“Low tracer values ($f_{C_5H_6O} < 3 \text{ ‰}$) are observed in non IEPOX-derived isoprene-SOA from laboratory studies, indicating that the tracer ion is specifically enhanced from IEPOX-SOA, and is not a tracer for all SOA from isoprene”

R2.8 Figure 2 and Figure 7:

Could the authors give more information about how to get IEPOX-SOA in $\mu\text{g}/\text{m}^3$? The mass spectrum of IEPOX-SOA factor in Figure 2 (b) shows many other peaks besides 82 m/z. Is IEPOX-SOA in $\mu\text{g}/\text{m}^3$ a function of $f_{C_5H_6O}$ in IEPOX-SOA factor and the “weighing” of IEPOX-SOA factor compared to other OA factors? I think this is important to help non AMS people better understand AMS IEPOX-SOA data. The results in Figure 7 and the statement in abstract “During the SOAS study, 78% of IEPOX-SOA is accounted for the measured molecular tracers” rely heavily on this.

A2.8: We addressed this in section 3.1 with the text below, as well as with the description of the tracer-based estimation method in Section 3.9. The uncertainty of IEPOX-SOA_{PMF} is addressed in response to comment R2.1.

“The IEPOX-SOA_{PMF} mass concentration is the sum of mass concentrations of all the ions in the IEPOX-SOA_{PMF} mass spectra. The “mass concentration” of an ion is used to represent the mass of the species whose detection resulted in the observed ion current of that ion, based on the properties of electron ionization (Jimenez et al., 2003)”,

R2.9 In addition, could the authors provide the uncertainties (or error bars) of the data shown in Figure 7? The statement of “During the SOAS study, 78% of IEPOX-SOA is accounted for the measured molecular tracers, making it the highest level of molecular identification of an ambient SOA component to our knowledge.” in the abstract also points to the importance to know the uncertainty.

A2.9: The explanation was added in the main text:

“The uncertainty (standard deviation) of the fraction of IEPOX-SOA molecular tracers in IEPOX-SOA_{PMF} in SOAS study (42%) is estimated by combining the overall uncertainty from IEPOX-SOA molecular tracer measurement (24%), linear regression between tracer vs IEPOX-SOA_{PMF} (17%, see Fig. 2b and Fig. S2), IEPOX-SOA_{PMF} in PMF separation

method (9%) and the quantification of IEPOX-SOA_{PMF} based on AMS calibration (30%) (Middlebrook et al., 2012).”

The uncertainty bar was added to Fig. 7 as well.

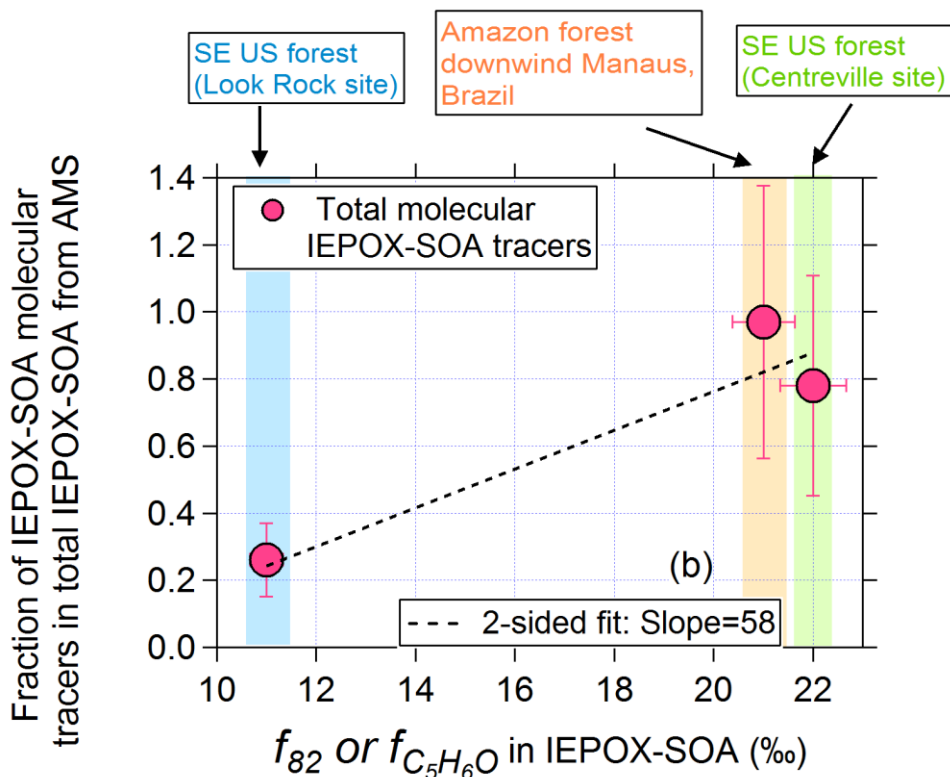


Figure 7. Scatter plot between total IEPOX-SOA molecular tracers (=Methyltetrol + C5-alkene triols +IEPOX-derived organosulfates and dimers) in IEPOX-SOA_{PMF} and $f_{82}^{IEPOX-SOA}$. Besides SOAS, the other two datasets in the graph are from Budisulistiorini et al. (2015) and de Sá et al.(2015). The relative uncertainty value estimated for the SOAS study is applied to the other two datasets.

Technical correction:

R2.10 Page 11226 Line 9: please define “SOAS”

A2.10: Corrected.

We revised the sentence to be: “**During the Southern Oxidant and Aerosol Study (SOAS) study...**”

R2.11 Figure 3: red curves in (a) are hard to distinguish. So are the green ones in (b). Please state clearly what the small dots are in (d).

A2.11: Following the reviewer’s suggestion, we revised our Figure 3. Please see the response to the comment R1.9.

R2.12 Figure 3 and 5: the legends are way too small and won't show up readable in print version.

A2.12: Please see the response to comments R1.9 and R1.13.

R2.13 Check the references to make sure they are recently updated.

A2.13: Thank for reviewer's reminder. We have checked through all the references and made sure they are all updated, and will check again on the ACP proofs after the paper is hopefully accepted. See also our response to comment R1.7.

References:

- Allan, J. D., Morgan, W. T., Darbyshire, E., Flynn, M. J., Williams, P. I., Oram, D. E., Artaxo, P., Brito, J., Lee, J. D., and Coe, H.: Airborne observations of IEPOX-derived isoprene SOA in the Amazon during SAMBBA, *Atmos. Chem. Phys.*, 14, 11393-11407, 10.5194/acp-14-11393-2014, 2014.
- Budisulistiorini, S. H., Canagaratna, M. R., Croteau, P. L., Marth, W. J., Baumann, K., Edgerton, E. S., Shaw, S. L., Knipping, E. M., Worsnop, D. R., Jayne, J. T., Gold, A., and Surratt, J. D.: Real-Time Continuous Characterization of Secondary Organic Aerosol Derived from Isoprene Epoxydiols in Downtown Atlanta, Georgia, Using the Aerodyne Aerosol Chemical Speciation Monitor, *Environ Sci Technol*, 47, 5686-5694, 10.1021/es400023n, 2013.
- Budisulistiorini, S. H., Li, X., Bairai, S. T., Renfro, J., Liu, Y., Liu, Y. J., McKinney, K. A., Martin, S. T., McNeill, V. F., Pye, H. O. T., Nenes, A., Neff, M. E., Stone, E. A., Mueller, S., Knote, C., Shaw, S. L., Zhang, Z., Gold, A., and Surratt, J. D.: Examining the effects of anthropogenic emissions on isoprene-derived secondary organic aerosol formation during the 2013 Southern Oxidant and Aerosol Study (SOAS) at the Look Rock, Tennessee, ground site, *Atmos. Chem. Phys. Discuss.*, 15, 7365-7417, 10.5194/acpd-15-7365-2015, 2015.
- Chen, Q., Farmer, D. K., Rizzo, L. V., Pauliquevis, T., Kuwata, M., Karl, T. G., Guenther, A., Allan, J. D., Coe, H., Andreae, M. O., Pöschl, U., Jimenez, J. L., Artaxo, P., and Martin, S. T.: Submicron particle mass concentrations and sources in the Amazonian wet season (AMAZE-08), *Atmos. Chem. Phys.*, 15, 3687-3701, 10.5194/acp-15-3687-2015, 2015.
- de Sá, S. S., Palm, B. B., Campuzano-Jost, P., Day, D. A., Hu, W., Newburn, M. K., Brito, J., Liu, Y., Isaacman-VanWertz, G., Yee, L. D., Goldstein, A. H., Artaxo, P., Souza, R., Manzi, A., Jimenez, J. L., Alexander, M. L., and Martin, S. T.: Mass spectral observations of fine aerosol particles and production of SOM at an anthropogenically influenced site during GoAmazon2014 wet season, *In prep.*, 2015.
- Jacobs, M. I., Burke, W. J., and Elrod, M. J.: Kinetics of the reactions of isoprene-derived hydroxynitrates: gas phase epoxide formation and solution phase hydrolysis, *Atmos. Chem. Phys.*, 14, 8933-8946, 10.5194/acp-14-8933-2014, 2014.
- Jimenez, J. L., Jayne, J. T., Shi, Q., Kolb, C. E., Worsnop, D. R., Yourshaw, I., Seinfeld, J. H., Flagan, R. C., Zhang, X. F., Smith, K. A., Morris, J. W., and Davidovits, P.: Ambient aerosol sampling using the Aerodyne Aerosol Mass Spectrometer, *J Geophys Res-Atmos*, 108, 8425, Doi 10.1029/2001jd001213, 2003.
- Kuwata, M., Liu, Y., McKinney, K., and Martin, S. T.: Physical state and acidity of inorganic sulfate can regulate the production of secondary organic material from isoprene photooxidation products, *Phys Chem Chem Phys*, 17, 5670-5678, 10.1039/c4cp04942j, 2015.
- Lin, Y.-H., Budisulistiorini, S. H., Chu, K., Siejack, R. A., Zhang, H., Riva, M., Zhang, Z., Gold, A., Kautzman, K. E., and Surratt, J. D.: Light-Absorbing Oligomer Formation in

- Secondary Organic Aerosol from Reactive Uptake of Isoprene Epoxydiols, *Environ Sci Technol*, 48, 12012-12021, 10.1021/es503142b, 2014.
- Middlebrook, A. M., Bahreini, R., Jimenez, J. L., and Canagaratna, M. R.: Evaluation of Composition-Dependent Collection Efficiencies for the Aerodyne Aerosol Mass Spectrometer using Field Data, *Aerosol Sci Tech*, 46, 258-271, 10.1080/02786826.2011.620041, 2012.
- Robinson, N. H., Hamilton, J. F., Allan, J. D., Langford, B., Oram, D. E., Chen, Q., Docherty, K., Farmer, D. K., Jimenez, J. L., Ward, M. W., Hewitt, C. N., Barley, M. H., Jenkin, M. E., Rickard, A. R., Martin, S. T., McFiggans, G., and Coe, H.: Evidence for a significant proportion of Secondary Organic Aerosol from isoprene above a maritime tropical forest, *Atmos. Chem. Phys.*, 11, 1039-1050, 10.5194/acp-11-1039-2011, 2011.
- Slowik, J. G., Stroud, C., Bottenheim, J. W., Brickell, P. C., Chang, R. Y. W., Liggiio, J., Makar, P. A., Martin, R. V., Moran, M. D., Shantz, N. C., Sjostedt, S. J., van Donkelaar, A., Vlasenko, A., Wiebe, H. A., Xia, A. G., Zhang, J., Leaitch, W. R., and Abbatt, J. P. D.: Characterization of a large biogenic secondary organic aerosol event from eastern Canadian forests, *Atmos. Chem. Phys.*, 10, 2825-2845, 10.5194/acp-10-2825-2010, 2010.
- Ulbrich, I. M., Canagaratna, M. R., Zhang, Q., Worsnop, D. R., and Jimenez, J. L.: Interpretation of organic components from Positive Matrix Factorization of aerosol mass spectrometric data, *Atmos Chem Phys*, 9, 2891-2918, 2009.
- Xu, L., Guo, H., Boyd, C. M., Klein, M., Bougiatioti, A., Cerully, K. M., Hite, J. R., Isaacman-VanWertz, G., Kreisberg, N. M., Knote, C., Olson, K., Koss, A., Goldstein, A. H., Hering, S. V., de Gouw, J., Baumann, K., Lee, S.-H., Nenes, A., Weber, R. J., and Ng, N. L.: Effects of anthropogenic emissions on aerosol formation from isoprene and monoterpenes in the southeastern United States, *Proceedings of the National Academy of Sciences*, 112, 37-42, 10.1073/pnas.1417609112, 2014.

1 **Characterization of a Real-Time Tracer for Isoprene Epoxydiols-Derived Secondary**
2 **Organic Aerosol (IEPOX-SOA) from Aerosol Mass Spectrometer Measurements**

3 Weiwei Hu^{1,2}, Pedro Campuzano-Jost^{1,2}, Brett B. Palm^{1,2}, Douglas A. Day^{1,2}, Amber M.
4 Ortega^{1,3}, Patrick L. Hayes^{1,2*}, Jordan E. Krechmer^{1,2}, Qi Chen^{4,5}, Mikinori Kuwata^{4,6}, Yingjun
5 Liu⁴, Suzane S. de Sá⁴, [Karina McKinney⁴](#), Scot T. Martin⁴, Min Hu⁶, Sri Hapsari
6 Budisulistiorini⁷, Matthieu Riva⁷, Jason D. Surratt⁷, Jason M. St. Clair^{8**,**}, Gabriel Isaacman-
7 Van Wertz⁹, Lindsay D. Yee⁹, Allen H. Goldstein^{9,10}, Samara Carbone¹¹, [Joel F. de Brito¹¹](#)
8 Paulo Artaxo¹¹, Joost de A. Gouw^{1,2,12}, Abigail Koss^{2,12}, Armin Wisthaler^{13,14}, Tomas
9 Mikoviny¹³, Thomas Karl¹⁵, Lisa Kaser^{16,14}, Werner Jud¹⁴, Armin Hansel¹⁴, Kenneth S.
10 Docherty¹⁷, [M. Elizabeth Alexander¹⁸](#), Niall H. Robinson^{19****}, Hugh. Coe¹⁹, James D. Allan^{19,20},
11 Manjula R. Canagaratna²¹, Fabien Paulot^{22,23}, and Jose L. Jimenez^{1,2}.

12 1 Cooperative Institute for Research in Environmental Sciences, University of Colorado,
13 Boulder, CO, USA
14 2 Department of Chemistry and Biochemistry, University of Colorado, Boulder, CO, USA
15 3 Department of Atmospheric and Oceanic Sciences, University of Colorado, Boulder, CO, USA
16 4 School of Engineering and Applied Sciences and Department of Earth and Planetary Sciences,
17 Harvard University, Cambridge, MA, USA
18 5 State Key Joint Laboratory of Environmental Simulation and Pollution Control, College of
19 Environmental Sciences and Engineering, Peking University, Beijing, China
20 6 Earth Observatory of Singapore, Nanyang Technological University, Singapore 7 Department
21 of Environmental Sciences and Engineering, Gillings School of Global Public Health, The
22 University of North Carolina at Chapel Hill, Chapel Hill, NC, USA
23 8 Division of Geological and Planetary Sciences, California Institute of Technology, Pasadena,
24 CA, USA
25 9 Department of Environmental Science, Policy, and Management, University of California,
26 Berkeley, CA, USA
27 10 Department of Civil and Environmental Engineering, University of California, Berkeley, CA,
28 USA
29 11 Department of Applied Physics, University of Sao Paulo, Sao Paulo, Brazil
30 12 NOAA Earth System Research Laboratory, Boulder, CO, USA
31 13 Department of Chemistry, University of Oslo, Oslo, Norway
32 14 Institute for Ion Physics and Applied Physics, University of Innsbruck, Innsbruck, Austria
33 15 [Institute of Atmospheric and Cryospheric Sciences, University of Innsbruck, Innsbruck, Austria](#)
34 16 Atmospheric Chemistry Division (ACD), National Center for Atmospheric Research,
35 Boulder, CO, USA
36 17 Alion Science and Technology, Research Triangle Park, NC, USA
37 [18 Environmental Molecular Sciences Laboratory, Pacific Northwest National Laboratory,](#)
38 [Richland, WA, USA](#)
39 19 School of Earth, Atmospheric and Environmental Sciences, University of Manchester, UK
40 20 National Centre for Atmospheric Science, University of Manchester, UK
41 21 Aerodyne Research, Inc., Billerica, MA, USA
42 22 NOAA Geophysical Fluid Dynamics Laboratory, Princeton, NJ, USA
43 23 Program in Atmospheric and Oceanic Sciences, Princeton University, Princeton, NJ, USA.

44 *Now at: Department of Chemistry, Université de Montréal, Montréal, QC, Canada
45 ** Now at: Atmospheric Chemistry and Dynamics Laboratory, NASA Goddard Space Flight
46 Center, Greenbelt, MD, USA
47 *** Now at: Joint Center for Earth Systems Technology, University of Maryland Baltimore
48 County, Baltimore, MD, USA.
49 **** Now at: Met Office, Exeter, UK
50

51 Abstract

52 Substantial amounts of secondary organic aerosol (SOA) can be formed from isoprene
53 epoxydiols (IEPOX), which are oxidation products of isoprene mainly under low-NO conditions.
54 Total IEPOX-SOA, which may include SOA formed from other parallel isoprene ~~low-NO~~
55 oxidation pathways, was quantified by applying Positive Matrix Factorization (PMF) to aerosol
56 mass spectrometer (AMS) measurements. The IEPOX-SOA fractions of OA in multiple field
57 studies across several continents are summarized here and show consistent patterns with the
58 concentration of gas-phase IEPOX simulated by the GEOS-Chem chemical transport model.
59 During the Southern Oxidant and Aerosol Study (SOAS) study, 78% of PMF-resolved IEPOX-
60 SOA is accounted by the measured IEPOX-SOA molecular tracers (methyltetrols, C5-Triols and
61 IEPOX-derived organosulfate and its dimers), making it the highest level of molecular
62 identification of an ambient SOA component to our knowledge. Enhanced signal at $C_5H_6O^+$ (m/z
63 82) is found in PMF-resolved IEPOX-SOA spectra. To investigate the suitability of this ion as a
64 tracer for IEPOX-SOA, we examine $f_{C_5H_6O}$ ($f_{C_5H_6O} = C_5H_6O^+/OA$) across multiple field, chamber
65 and source datasets. A background of $\sim 1.7 \pm 0.1\%$ (%=parts per thousand) is observed in studies
66 strongly influenced by urban, biomass-burning and other anthropogenic primary organic aerosol
67 (POA). Higher background values of $3.1 \pm 0.6\%$ are found in studies strongly influenced by
68 monoterpene emissions. The average laboratory monoterpene SOA value ($5.5 \pm 2.0\%$) is 4 times
69 lower than the average for IEPOX-SOA ($22 \pm 7\%$), which leaves some room to separate both
70 contributions to OA. Locations strongly influenced by isoprene emissions under low-NO levels
71 had higher $f_{C_5H_6O}$ ($\sim 6.5 \pm 2.2\%$ on average) than other sites, consistent with the expected IEPOX-
72 SOA formation in those studies. $f_{C_5H_6O}$ in IEPOX-SOA is always elevated ($12\text{--}40\%$) but varies
73 substantially between locations, which is shown to reflect large variations in its detailed
74 molecular composition. The low $f_{C_5H_6O}$ ($< 3\%$) reported in non IEPOX-derived isoprene-SOA
75 from chamber studies indicates that this tracer ion is specifically enhanced from IEPOX-SOA,
76 and is not a tracer for all SOA from isoprene. We introduce a graphical diagnostic to study the
77 presence and aging of IEPOX-SOA as a “triangle plot” of f_{CO_2} vs. $f_{C_5H_6O}$. Finally, we develop a
78 simplified method to estimate ambient IEPOX-SOA mass concentrations, which is shown to
79 perform well compared to the full PMF method. The uncertainty of the tracer method is up to a
80 factor of ~ 2 if the $f_{C_5H_6O}$ of the local IEPOX-SOA is not available. When only unit mass
81 resolution data is available, as with the aerosol chemical speciation monitor (ACSM), all
82 methods may perform less well because of increased interferences from other ions at m/z 82.
83 This study clarifies the strengths and limitations of the different AMS methods for detection of
84 IEPOX-SOA and will enable improved characterization of this OA component.

85 1. Introduction

86 Isoprene (2-methyl-1,3-butadiene, C₅H₈) emitted by vegetation is the most abundant non-
87 methane hydrocarbon emitted to the Earth's atmosphere (~440–600 TgC/year) (Guenther et al.,
88 2012). It is estimated to contribute substantially to the global secondary organic aerosol (SOA)
89 budget (Paulot et al., 2009b;Guenther et al., 2012). Higher SOA yields from isoprene are
90 observed under low-NO_x conditions (Surratt et al., 2010). Under low-NO conditions, i.e. when a
91 substantial fraction of the peroxy radicals do not react with NO, gas-phase isoprene epoxydiols
92 (IEPOX) are produced with high yield through a HO_x-mediated mechanism (Paulot et al.,
93 2009b). Note that some IEPOX can also be formed from isoprene in high NO region via
94 oxidation of the product 4-hydroxy-3-nitroxy isoprene (Jacobs et al., 2014) , however this
95 pathway is thought to be much smaller than the low-NO pathway. Subsequently, IEPOX can be
96 taken up by acidic aerosols (Gaston et al., 2014), where IEPOX-SOA can be formed through
97 acid-catalyzed oxirane ring-opening of IEPOX (Cole-Filipiak et al., 2010;Eddingsaas et al.,
98 2010;Lin et al., 2012;Nguyen et al., 2014), which is thought to be the main pathway to form
99 IEPOX-SOA (Surratt et al., 2010;Pye et al., 2013;Worton et al., 2013). Although the complete
100 molecular composition of IEPOX-SOA has not been elucidated, several molecular species that
101 are part of IEPOX-SOA have been identified through gas chromatography/mass spectrometry
102 (GC/MS), liquid chromatography/mass spectrometry (LC/MS) and particle analysis by laser
103 mass spectrometry (PALMS). They include 2-methyltetrols (and oligomers that contain them)
104 (Surratt et al., 2010;Lin et al., 2014), C₅-alkene triols (Wang et al., 2005), 3-
105 methyltetrahydrofuran-3,4-diols (Lin et al., 2012), and an IEPOX-organosulfate (Froyd et al.,
106 2010;Liao et al., 2014). These molecular species account for a variable fraction of the IEPOX-
107 SOA reported, e.g., 8% in a chamber study (Lin et al., 2012) or 26% in a field study at Look
108 Rock, TN (Budisulistiorini et al., 2015). An estimate of total IEPOX-SOA can also be derived

109 from an IEPOX-SOA molecular tracer(s) via multiplying the tracer concentration by the total
110 IEPOX-SOA to tracer ratio. However, that method is hindered by the limited information on
111 these molecular tracers and the reported variability of IEPOX-SOA to tracer ratios. IEPOX-SOA
112 may include SOA formed from other parallel isoprene low-NO oxidation pathways (Liu et al.,
113 2014; Krechmer et al. 2015). In addition, the IEPOX-SOA molecular tracers are typically
114 measured with slow time resolution (12/24 h).

115 Multiple field studies, supported by chamber studies, have shown that the total amount of
116 IEPOX-SOA can be obtained by factor analysis of organic spectra from an aerosol mass
117 spectrometer (AMS) or the aerosol chemical speciation monitor (ACSM) (Robinson et al.,
118 2011; Lin et al., 2012; Budisulistiorini et al., 2013; Nguyen et al., 2014). Robinson et al. (2011)
119 first reported an SOA factor with pronounced f_{82} ($= m/z$ 82/OA) in the mass spectra acquired
120 above a forest with high isoprene emissions in Borneo, and hypothesized that the elevated f_{82}
121 may have arisen from methylfuran (C_5H_6O), consistent with $C_5H_6O^+$ being the major ion at m/z
122 82 in isoprene-influenced areas. Lin et al. (2012) demonstrated that the 3-MeTHF-3,4-diols
123 associated with IEPOX-SOA result in enhanced f_{82} in AMS spectra, presumably through the
124 formation methylfuran-like structures during thermal desorption. Electron-impact ionization of
125 aerosols formed by atomizing a solution containing IEPOX ($C_5H_{10}O_3$) can also yield $C_5H_6O^+$
126 signals in an AMS via two dehydration reactions (Lin et al., 2012). However, because gas-phase
127 IEPOX has high volatility, non-reactive gas-to-particle partitioning of IEPOX into OA is
128 negligible under typical ambient concentrations in forest areas ($1-10 \mu g m^{-3}$) (Worton et al.,
129 2013).

130 IEPOX-SOA was estimated to account for 33% of ambient OA in summertime Atlanta from
131 PMF analysis of ACSM spectra. The source apportionment result was supported by the

132 pronounced f_{82} peak in the factor spectrum and good temporal correlation of the factor with
133 sulfate and 2-methyltetrols (Budisulistiorini et al., 2013). Sulfate is often strongly correlated with
134 the acidity of an aerosol, and might also play a direct role in the chemistry, e.g. via direct
135 reaction or nucleophilic effects (Surratt et al., 2007; Liao et al., 2014; Xu et al., 2014). While
136 discussing the results of a recent aircraft campaign from Brazil, Allan et al. (2014) also used f_{82}
137 as a tracer for IEPOX-SOA.

138 If f_{82} in AMS spectra (and/or $f_{C_5H_6O}$ in HR-AMS spectra) is dominated by IEPOX-SOA, f_{82}
139 would be a convenient, high-time-resolution, and potentially quantitative tracer for IEPOX-SOA.
140 Thus, it will be very useful for investigating the impacts of SOA formation from isoprene with
141 AMS/ACSM measurements, which have become increasingly common in recent years including
142 some continental-scale continuous networks (Fröhlich et al., 2015). However, no studies to date
143 have systematically examined whether enhanced f_{82} is unique to IEPOX chemistry or whether it
144 could also be enhanced in other sources. Nor has the range of f_{82} been determined for IEPOX-
145 SOA. Questions also have been raised about the uniqueness of this tracer and potential
146 contributions from monoterpene SOA (Anonymous_Referee, 2014).

147 In this study, the IEPOX-SOA results reported in various field campaigns are summarized
148 and compared to predicted gas-phase IEPOX concentrations from a global model to help confirm
149 the robustness of the AMS identification of this type of SOA. We then investigate the usefulness
150 and limitations of the IEPOX-SOA tracers $f_{C_5H_6O}$ ($= C_5H_6O^+/OA$) and f_{82} by combining AMS
151 data from multiple field and laboratory studies including a new dataset from the 2013 Southern
152 Oxidant and Aerosol Study (SOAS). We compare the tracer levels in different OA sources
153 (urban, biomass burning and biogenic), characterizing the background levels and interferences
154 on this tracer for both high-resolution (HR) and unit mass resolution (UMR) data. We also

155 provide a simplified method to rapidly estimate IEPOX-SOA from $f_{C_5H_6O}$ and f_{82} . While this
156 method is no substitute for a detailed IEPOX-SOA identification via PMF, it is a simple method
157 to estimate IEPOX-SOA concentrations (or its absence) in real-time from AMS or ACSM
158 measurements or under conditions in real-time, or where PMF analysis is not possible or is
159 difficult to perform.

160 **2 Experimental**

161 We classify the field datasets used in this study into three categories: (1) studies strongly
162 influenced by urban and biomass-burning emissions: Los Angeles area, US and Beijing, China
163 (urban); Changdao island, downwind of China and Barcelona area, Spain (urban downwind);
164 flight data from biomass-burning plumes and continental areas (NW and western, US) in
165 SEAC4RS and DC3 campaigns; and biomass burning lab emissions (FLAME-3 study). (2)

166 Studies strongly influenced by isoprene emissions, including a SE US forest site (SOAS
167 campaign); Two pristine forest site and one forest site partially impacted by urban plumes in the
168 Amazon rain forest (Brazil). The latter site is classified in this category because (i) high isoprene
169 concentrations (e.g. 3 ppb in average peaks in the afternoon) were observed during the study; (ii)
170 the impact of biogenic SOA formed during 1000 km where the air travels over the pristine forest
171 upwind of Manaus; (iii) PMF results indicate an important impact of IEPOX-SOA at this site (de
172 Sá et al., 2015); (iv) PTRMS results indicate a substantial concentration of the isoprene
173 hydroperoxyde formed by low-NO chemistry. Borneo rain forest in Malaysia; and flight data
174 from SE US flights from aircraft campaign (SEAC4RS); (3) Studies strongly influenced by
175 monoterpene emissions in a pine forest in the Rocky Mountains and a European boreal forest.
176 Locations and additional detailed information about these studies can be found in Fig. 1 and
177 Table 1.

178 With the exception of SOAS, all of the campaigns included in this analysis have been
 179 previously described elsewhere (Table 1). The SOAS campaign took place in a forested area of
 180 the SE US during June and July, 2013 (Fig. 1) and has several ground sites. The new dataset
 181 introduced below was acquired at the SEARCH supersite, Centreville (CTR), AL (32.95° N,
 182 87.13°W). Some results from a different SOAS site (Look Rock, TN) are also discussed later
 183 (Budisulistiorini et al., 2015). Relatively high average isoprene and monoterpene concentrations
 184 of 3.3 ± 2.4 ppb and 0.7 ± 0.4 ppb, respectively, were observed in SOAS-CTR by on-line GC/MS.
 185 Measurements of non-refractory aerosol components of submicron particles (PM_{10}) were made
 186 using an Aerodyne high-resolution time-of-flight aerosol mass spectrometer (HR-ToF-AMS,
 187 “AMS” hereafter) (DeCarlo et al., 2006). By applying positive matrix factorization (PMF) to the
 188 time series of organic mass spectra (Ulbrich et al., 2009), we separated contributions from
 189 IEPOX-SOA and other sources/components of OA. The AMS PMF results used here are very
 190 consistent with those from a separate HR-ToF-AMS operated by another group at the same site
 191 (Xu et al., 2014). The global gas-phase IEPOX concentrations in 2013 were modeled at as
 192 resolution of 2 x 2.5 degrees as described in Nguyen et al. (2015). The gas-phase chemistry of
 193 isoprene in GEOS-Chem is based on Paulot et al (2009a;2009b) as described by Mao et al.
 194 (2013).

195 In the following discussion, we denote the IEPOX-SOA factor from PMF as “IEPOX-
 196 SOA_{PMF}” and IEPOX-SOA from lab studies as “IEPOX-SOA_{lab}” for clarity. If we use “IEPOX-
 197 SOA” in the paper, it refers to a broad concept of IEPOX-SOA. We use a superscript to clarify
 198 the type of OA for which $f_{C_5H_6O}$ is being discussed: $f_{C_5H_6O}^{OA}$ refers to $f_{C_5H_6O}$ in total OA,
 199 $f_{C_5H_6O}^{IEPOX-SOA}$ to $f_{C_5H_6O}$ in IEPOX-SOA_{PMF} or IEPOX-SOA_{lab}, $f_{C_5H_6O}^{MT-SOA}$ to the $f_{C_5H_6O}$ value in pure
 200 MT-SOA and $f_{C_5H_6O}^{OA-Bkg-UB}$ and $f_{C_5H_6O}^{OA-Bkg-MT}$ refer to background $f_{C_5H_6O}^{OA}$ from areas strongly

201 influenced by urban+biomass-burning emissions and by monoterpene emissions, respectively. If
202 we refer to $f_{C_5H_6O}$ in general, we will still use $f_{C_5H_6O}$. When we report the average $f_{C_5H_6O}^{OA}$ in each
203 campaign, as shown in the Table 1, we used the average from the time series of $f_{C_5H_6O}^{OA}$ at their
204 raw time resolution (secs to mins). During this process, we exclude points whose OA mass
205 concentrations are below twice the detection limit of OA in AMS (typically $2 \times 0.26 \mu\text{g m}^{-3} = 0.5$
206 $\mu\text{g m}^{-3}$). When averaging $f_{C_5H_6O}^{OA}$ values across datasets, we counted each dataset as one data
207 point.

208 **3 Results and Discussion**

209 **3.1 IEPOX-SOA in a SE US forest during SOAS, 2013**

210 We use the SOAS-CTR field study (SE US-CTR) as an example for the determination of
211 IEPOX-SOA from AMS data via PMF analysis. The time series and mass spectrum of this
212 component are shown in Fig. 2. The IEPOX-SOA_{PMF} mass concentration is the sum of mass
213 concentrations of all the ions in the IEPOX-SOA_{PMF} mass spectra. The “mass concentration” of
214 an ion is used to represent the mass of the species whose detection resulted in the observed ion
215 current of that ion, based on the properties of electron ionization (Jimenez et al., 2003). An
216 uncertainty (standard deviation) of IEPOX-SOA_{PMF} mass concentration of ~9% was estimated
217 from 100 bootstrapping runs in PMF analysis (Ulbrich et al., 2009) (Fig. S1). This uncertainty
218 concerns only the PMF separation method. In practice the uncertainty in IEPOX-SOA_{PMF}
219 concentration is dominated by the larger uncertainty on the AMS concentrations arising from the
220 collection efficiency and relative ionization efficiency (Middlebrook et al., 2012).

221 A strong correlation is found between AMS IEPOX-SOA_{PMF} and 2-methyltetrols (R=0.79)
222 and sulfate (R = 0.75) as expected (Surratt et al., 2010; Lin et al., 2012; Nguyen et al., 2014; Xu et

223 al., 2014). The diurnal variation of IEPOX-SOA_{PMF} is also similar to gas-phase IEPOX and
224 isoprene measured in SOAS-CTR. 2-Methyltetrols, measured on-line by GC-EI/MS with the SV-
225 TAG instrument (Isaacman et al., 2014), comprise 26% of IEPOX-SOA_{PMF} in SOAS-CTR on
226 average, as shown in Fig. 2b. A similar ratio (29%) is found between 2-methyltetrols measured
227 by offline analysis of filter samples using GC-EI/MS and LC/MS (Lin et al., 2014) and IEPOX-
228 SOA_{PMF}. Other IEPOX-SOA tracers, such as C5-alkene triols, IEPOX-organosulfates, and
229 dimers containing them, can also be measured by offline GC-EI/MS and LC/MS (Lin et al.,
230 2014; Budisulistiorini et al., 2015), and they account for 28% and 24% in total IEPOX-SOA_{PMF}
231 in SOAS (R=0.7), respectively (Fig. S2). The total IEPOX-SOA tracers measured in SOAS
232 account for $\sim 78 \pm 42\%$ of the total IEPOX-SOA_{PMF} mass concentration. The uncertainty of the
233 fraction of IEPOX-SOA molecular tracers in IEPOX-SOA_{PMF} in SOAS study (42%) is estimated
234 by combining the overall uncertainty from IEPOX-SOA molecular tracer measurement (24%),
235 linear regression between tracer vs IEPOX-SOA_{PMF} (17%, see Fig. 2b and Fig. S2), IEPOX-
236 SOA_{PMF} in PMF separation method (9%) and the quantification of IEPOX-SOA_{PMF} based on
237 AMS calibration (30%) (Middlebrook et al., 2012). This is a remarkably high value compared to
238 the tracer to total SOA ratios for other SOA systems (e.g., SOA from monoterpenes or aromatic
239 hydrocarbons) (Lewandowski et al., 2013) ~~and it is the highest reported in the literature to our~~
240 ~~knowledge.~~ A total tracers to IEPOX-SOA_{PMF} ratio of 26% was reported for the Look Rock site
241 in SOAS (SOAS-LR) (Budisulistiorini et al., 2015). Thus, the measured total molecular tracer
242 fraction in total IEPOX-SOA appears to be quite variable (a factor of 3) even if the same or
243 similar techniques are used. Although the calibration methodology between different campaigns
244 may result in some uncertainties, this value likely changes significantly between different times

245 and locations, potentially due to changes in particle-phase reaction conditions such as sulfate and
246 water concentrations, acidity, and the identity and concentrations of oligomerization partners.

247 IEPOX-SOA_{PMF} accounts for 17% of the total OA mass concentration at SOAS-CTR. This is
248 shown in Fig. 1 along with the IEPOX-SOA_{PMF} fraction from several previous studies (Robinson
249 et al., 2011; Slowik et al., 2011; Budisulistiorini et al., 2013; Hayes et al., 2013; Hu et al.,
250 2013; Chen et al., 2014; Hu et al., 2015). Fig. 1 also shows the surface gas-phase IEPOX
251 concentrations for July, 2013 as simulated with GEOS-Chem. At all sites with at least ~30 ppt
252 predicted average IEPOX concentration, IEPOX-SOA_{PMF} is identified in AMS data. IEPOX-
253 SOA_{PMF} accounts for 6% – 36% of total OA in those studies, signifying the importance of
254 IEPOX-SOA for regional and global OA budgets. No IEPOX-SOA_{PMF} factor (i.e. below the
255 PMF detection limit of ~5% of OA, Ulbrich et al., 2009) was found in areas strongly influenced
256 by urban emissions where high NO concentrations suppress the IEPOX pathway, even in the
257 presence of substantial isoprene concentrations (e.g. Hayes et al., 2013). GEOS-Chem indeed
258 predicts negligible modeled gas-phase IEPOX concentrations in those areas, where isoprene
259 peroxy radicals are expected to react primarily with NO. Some IEPOX can also be formed via
260 high NO chemistry (Jacobs et al., 2014), however this pathway is thought to be much smaller
261 than the low-NO pathway, consistent with the lack of observation of IEPOX-SOA_{PMF} in the
262 polluted studies included here. The fraction of IEPOX-SOA_{PMF} positively correlates with
263 modeled gas-phase IEPOX, as shown in the inset of Fig. 1.

264 The mass spectrum of IEPOX-SOA during SOAS-CTR is similar to those from other studies
265 as seen in Fig. S3 – S4 (Robinson et al., 2011; Lin et al., 2012; Budisulistiorini et al., 2013; Chen
266 et al., 2014; Nguyen et al., 2014; Xu et al., 2014), and also exhibits a prominent C₅H₆O⁺ peak at
267 *m/z* 82. We investigated the correlation between the time series of IEPOX-SOA_{PMF} and each ion

268 in the OA spectra. The temporal variation of ion $C_5H_6O^+$ correlates best ($R=0.96$) with IEPOX-
269 SOA_{PMF} among all measured OA ions (Table S1). This result suggests that $C_5H_6O^+$ ion may be
270 the best ion tracer for IEPOX-SOA among all OA ions. $C_5H_5O^+$ (m/z 81), $C_4H_5^+$ (m/z 53),
271 $C_4H_6O^+$ (m/z 70) and $C_3H_7O_2^+$ (m/z 75) also correlate well with IEPOX-SOA_{PMF} in SOAS-CTR
272 and could be potential tracers for IEPOX-SOA_{PMF}. Scatter plots between these four ions and
273 $C_5H_6O^+$ at different campaigns indicate they either have higher background values or lower
274 signal-to-noise compared to $C_5H_6O^+$ (Fig. S5).

275 $f_{C_5H_6O}^{IEPOX-SOA}$ from SOAS and other field and laboratory studies (Table 1) ranges from 12% to
276 40‰ (‰=parts per thousand) and have an average value of $22\pm 7\%$. The average $f_{C_5H_6O}^{IEPOX-SOA}$
277 value shown here also includes f_{82} data from four UMR IEPOX-SOA_{PMF} spectra. This is justified
278 since $C_5H_6O^+$ accounts for over 95% of m/z 82 in IEPOX-SOA based on results from SOAS-
279 CTR and other lab studies (Kuwata et al., 2015). Indeed the average does not change if the UMR
280 studies are removed from the average. These values are substantially higher than those from
281 other types of OA or from locations with little impact from IEPOX-SOA, as discussed below.

282 3.2 $f_{C_5H_6O}$ in areas with strong influence from urban and biomass burning emissions

283 We next examine whether POA or SOA from field studies in areas strongly influenced by
284 urban and biomass-burning emissions and without substantial predicted gas-phase IEPOX
285 concentrations or IEPOX-SOA contributions can lead to enhanced $f_{C_5H_6O}^{OA}$. Figure 3a shows the
286 distribution of $f_{C_5H_6O}^{OA}$ in this category of studies peaks at $1.7\pm 0.1\%$ (range 0.02 – 3.5%). Data
287 from continental air masses sampled from aircraft over the western and northwest US (where
288 isoprene emissions are low) are shown in Fig. 3b and show a similar range as the polluted ground
289 sites.

290 Biomass burning emissions and plumes sampled over multiple studies show a similar range
291 to the pollution studies, with some slightly higher values. The peak of the distribution of $f_{C_5H_6O}^{OA}$
292 from fresh biomass-burning smoke across many different biomasses during the FLAME-3 study
293 is 2.0‰. During the SEAC4RS aircraft campaign, many biomass burning plumes were sampled,
294 where OA concentrations varied over a wide range (several tens to more than one thousand μg
295 m^{-3}). The average $f_{C_5H_6O}^{OA}$ across these biomass-burning plumes was 1.75‰ with low variability
296 ($\sim 20\%$), see Fig. [S6](#).

297 We also explore whether other anthropogenic primary OA (POA) emission sources could
298 elevate $f_{C_5H_6O}$ above the observed background levels of $\sim 1.7\%$. Figure 3c shows $f_{C_5H_6O}$ for POA
299 spectra from vehicle exhaust, cooking, coal combustion, and multiple pure chemical standards
300 (e.g., some alcohols; di- or poly acids) (Canagaratna et al., 2015). Almost all the values are
301 below 2‰, with exceptions for one type of cooking POA at 3‰, the polyol xylitol (4.2‰), and
302 some acids (5-Oxoazelaic acid = 4.8‰, Gamma ketopimelic acid = 5.2‰, ketopimelic acid =
303 6.5‰, 3-Hydroxy-3-Methylglutaric acid = 11.8‰, Adipic acid = 16.4‰). All the tracers
304 resulting in elevated $f_{C_5H_6O}$ contain multiple hydroxyl groups, and may result in furan-like
305 structures via facile dehydration reactions (Canagaratna et al., 2015). Xylitol has been proposed
306 as a tracer of toluene SOA (Hu et al., 2008). It has a similar structure to 2-methyltetrols, with 5 -
307 OH groups instead of 4. In the AMS, xylitol may form the methylfuran structure through
308 dehydration reactions like 2-methyltetrols. However, $f_{C_5H_6O}$ in other toluene SOA tracers in our
309 dataset show background levels of $f_{C_5H_6O}$ ($< 2\%$). Given the small fraction of xylitol in toluene
310 SOA (Hu et al., 2008), xylitol is unlikely to increase $f_{C_5H_6O}$ in anthropogenic SOA, consistent
311 with our results.

312 In summary, in the absence of strong impacts from biogenic SOA, the AMS high resolution
313 ion $C_5H_6O^+$ has a clear and stable background, spanning a small range (0.02 – 3.5‰) with an
314 average values around $1.7 \pm 0.1‰$ ($f_{C_5H_6O}^{OA-Bkg-UB}$), about an order of magnitude lower than the
315 average value ($22 \pm 7‰$) of $f_{C_5H_6O}^{IEPOX-SOA}$.

316 **3.3 Enhancements of $f_{C_5H_6O}$ in areas strongly influenced by isoprene emissions**

317 GEOS-Chem predicts much higher surface gas-phase IEPOX concentrations over the SE US
318 and Amazon rainforest than those in temperate urban areas (Fig. 1). This is expected from high
319 isoprene concentrations (e.g. 3.3 ppb in SOAS-CTR and 4 ppb in the Amazon) under low
320 average NO concentrations (~ 0.1 ppb) (Karl et al., 2009; Ebben et al., 2011). Probability
321 distributions of $f_{C_5H_6O}^{OA}$ during both campaigns are shown in Fig. 4a, and are very similar with
322 averages of 5 – 6‰ (range 2.5‰ – 11‰). The Amazon forest downwind of Manaus and a
323 Borneo tropical forest study show even higher averages of 7‰ and 10‰, respectively (Robinson
324 et al., 2011; de Sá et al., 2015). During the SEAC4RS aircraft campaign, the average $f_{C_5H_6O}^{OA}$
325 ($4.4 \pm 1.6‰$) from all SE US flights is also enhanced compared to levels observed in the
326 northwest and western US continental air masses ($1.7 \pm 0.3‰$) where isoprene emissions are
327 much smaller (Guenther et al., 2012). Thus, campaigns in locations strongly influenced by
328 isoprene emissions under lower NO conditions show systematically higher $f_{C_5H_6O}^{OA}$ values (with
329 an average peak of $6.5‰ \pm 2.2‰$) than background levels found in other locations (1.7‰). The
330 fact that $f_{C_5H_6O}^{OA}$ ($6.5 \pm 2.2‰$) in these studies is lower than the values in IEPOX-SOA ($22‰ \pm 7‰$)
331 is expected, since ambient datasets also include OA from other sources, and confirms that
332 IEPOX-SOA is not an overwhelmingly dominant OA source at most of those locations (See Fig.
333 S7).

3.4 Values of $f_{C_5H_6O}$ in laboratory studies of non IEPOX-derived isoprene SOA

We also investigate $f_{C_5H_6O}$ in laboratory SOA from isoprene in Fig. 4a. For SOA produced by chamber isoprene photooxidation under high NO_x conditions, low $f_{C_5H_6O}$ (<2‰) within the background level is observed (Kroll et al., 2006; Chen et al., 2011). SOA from oxidation of isoprene hydroxyhydroperoxide (ISOPOOH, a product of low-NO oxidation of isoprene) under low-NO conditions, when formed under conditions that are not favorable for the reactive uptake of IEPOX into aerosols also has low $f_{C_5H_6O}$ of 2‰ (Krechmer et al., 2015). Low values of $f_{C_5H_6O}$ (<3‰) are also observed in SOA from isoprene + NO_3 radical reactions without acid seeds (Ng et al., 2008). The low $f_{C_5H_6O}$ (<3‰) observed in non IEPOX-derived isoprene SOA indicate that $f_{C_5H_6O}$ is specifically enhanced from IEPOX-SOA, and is not a tracer for all SOA from isoprene.

3.5 Enhancements of $f_{C_5H_6O}$ in areas strongly influenced by monoterpene emissions

The BEACHON-RoMBAS campaign was carried out in a Rocky Mountain pine forest with high monoterpene emissions that account for 34% in daytime and 66 % at night of the total VOC mixing ratios (on average peaking at 0.15 ppb during day and 0.7 ppb at night) (Fry et al., 2013) but lower isoprene emissions (peaking at 0.35 ppb during daytime) (Kaser et al., 2013; Karl et al., 2014). One-third of the RO_2 radicals react via the low-NO route (i.e. via $RO_2 + HO_2$) at this site (Fry et al., 2013). The isoprene/monoterpene ratio at the Rocky Mountain site is 0.48, and is ~ 10 – 20 times lower than the value (4.7) in SOAS-CTR and (8.3) in Amazon studies (Chen et al., 2014), suggesting that $f_{C_5H_6O}^{OA}$ may be near background levels because of the very low potential contribution of IEPOX-SOA at the Rocky Mountain site. However, the average $f_{C_5H_6O}^{OA}$ at the Rocky Mountain site is $3.7 \pm 0.5\%$ (Fig. 4a), which although lower than the average $f_{C_5H_6O}^{OA}$

356 (6.5‰) found in the SE US-CTR, Amazon and Borneo forests, it is still twice the $f_{C_5H_6O}^{OA-Bkg-UB}$
357 values of 1.7‰ observed in pollution and smoke-dominated locations.

358 Three circumstances may lead to such an enhanced $f_{C_5H_6O}^{OA}$ at the Rocky Mountain site, which
359 we examine here. (1) A small amount of IEPOX-SOA may be formed from the limited isoprene
360 present at the Rocky Mountain site and surrounding region. However, the average isoprene
361 concentration in this pine forest area is only 0.2 ppb, which is around 16 times less than that (3.3
362 ppb) at the SE US site in SOAS. The conditions at the Rocky Mountain site were less favorable
363 for IEPOX-SOA formation due to a higher fraction (70% in daytime) of the RO₂ radicals
364 reacting with NO and less acidic aerosols (Fry et al., 2013;Levin et al., 2014). Thus we can
365 estimate an upper limit contribution of IEPOX-SOA to the $f_{C_5H_6O}^{OA}$ tracer at the Rocky Mountain
366 site assuming the same ratio of IEPOX-SOA to isoprene in both campaigns. In this case, we
367 would expect $f_{C_5H_6O}^{OA}$ at the Rocky Mountain site to be the background level (1.7‰) plus 1/16th of
368 the enhancement above the background observed in SOAS (5‰ – 1.7‰ = 3.3‰) multiplied by
369 the ratio of OA concentrations at both sites (4.8 μg m⁻³ in SE US site vs 1.8 μg m⁻³ in Rocky
370 Mountain site). This calculation results in an expected upper limit $f_{C_5H_6O}^{OA} \sim 2.25‰$ at the Rocky
371 Mountain site due to the IEPOX-SOA contribution. This estimate is much lower than the
372 observed average 3.7‰. Thus the elevated $f_{C_5H_6O}^{OA}$ in Rocky Mountain pine forest is very unlikely
373 to be due to IEPOX-SOA.

374 (2) The second explanation of high $f_{C_5H_6O}^{OA}$ observed at Rocky Mountain site is that SOA from
375 monoterpene oxidation (MT-SOA) may have a higher $f_{C_5H_6O}$ than background OA from other
376 sources. Several chamber studies show that MT-SOA, e.g., SOA from ozonolysis (Chhabra et al.,
377 2011;Chen et al., 2014) or photooxidation (Ng et al., 2007) of α-pinene, or NO₃ reaction with α-
378 pinene, or NO₃ reaction with α-pinene, β-pinene and Δ³-Carene (Fry et al., 2014;Boyd et al.,

379 2015) can result in higher $f_{C_5H_6O}$ (average $5.5 \pm 2.0\%$) than background levels of $\sim 1.7\%$ (Fig. 4a).
380 We note that the average lab-generated MT-SOA value ($f_{C_5H_6O}^{MT-SOA}$) is still 4 times lower than the
381 average $f_{C_5H_6O}^{IEPOX-SOA}$ for IEPOX-SOA_{PMF} and IEPOX-SOA_{lab} (Fig. S8), and thus there is some
382 room to separate both contributions. Oxidation of monoterpenes can lead to species with multiple
383 –OH groups, which may result in the production of methylfuran (or ions of similar structure)
384 upon AMS analysis. We do not observe enhanced $f_{C_5H_6O}$ in SOA from sesquiterpene oxidation
385 ($< 2\%$) (Chen et al., 2014). The values of $f_{C_5H_6O}^{MT-SOA}$ in chamber studies, together with the finding
386 of a substantial contribution of monoterpenes to SOA at this Rocky Mountain site (Fry et al.,
387 2013) suggest that MT-SOA may explain the values of $f_{C_5H_6O}^{OA}$ observed there.

388 Two other field studies support the conclusion that ambient MT-SOA may have slightly
389 enhanced $f_{C_5H_6O}$. Fig. 6 shows data from a DC3 aircraft flight in the areas around Missouri and
390 Illinois. Ambient $f_{C_5H_6O}^{OA}$ increases from background levels ($\sim 1.7\%$) to $\sim 4.1\%$ in a highly
391 correlated manner to monoterpene concentration increases (with an average of 3.0% during the
392 enhanced period). Meanwhile, isoprene and gas-phase IEPOX stay at low levels similar to the
393 rest of the flight, indicating that enhanced $f_{C_5H_6O}^{OA}$ in the periods with higher MT concentrations
394 should arise from MT-SOA and not IEPOX-SOA. Fig. 4a includes AMS measurements at a MT-
395 emission dominated European boreal forest (Hyytiälä in Finland) (Robinson et al., 2011).

396 Average $f_{C_5H_6O}^{OA}$ is $\sim 2.5\%$ at this site, which is again higher than the $f_{C_5H_6O}^{OA-Bkg-UB}$ value of 1.7% .
397 The slightly lower $f_{C_5H_6O}^{OA}$ in the Boreal forest vs. the Rocky Mountain site may be partially
398 explained by a small contribution from IEPOX-SOA at the latter (estimated above to increase
399 $f_{C_5H_6O}^{OA}$ up to 2.25% at the Rocky Mountain site), as well as by differences of the MT-SOA/OA

400 ratio at both sites (Corrigan et al., 2013) and the relative importance of different MT species and
401 oxidation pathways.

402 (3) The enhanced $f_{C_5H_6O}^{OA}$ at the Rocky Mountain site may have arisen from oxidation
403 products of 2-methyl-3-buten-2-ol (MBO, C₅H₁₀O) emitted from pine trees. MBO, with a
404 daytime average of 2 ppb accounts for ~50% of the total VOC mixing ratio during the day (Karl
405 et al., 2014). MBO has been shown to form aerosol with a 2 – 7 % yield in chamber studies,
406 which is thought to proceed via the uptake of epoxide intermediates (C₅H₁₀O₂, vs. IEPOX
407 C₅H₁₀O₃) under acidic aerosol conditions (Zhang et al., 2012;Mael et al., 2014;Zhang et al.,
408 2014). Some aerosol species formed by MBO-derived epoxides have similar structures (e.g.,
409 C₅H₁₂O₃) to the IEPOX oxidation products in SOA and thus they might contribute to $f_{C_5H_6O}^{OA}$. No
410 pure MBO-derived epoxides or their oxidation products in the aerosol phase have been measured
411 by AMS so far, to our knowledge.

412 To attempt to differentiate whether MT-SOA or MBO-SOA dominate the higher $f_{C_5H_6O}^{OA}$ at
413 the Rocky Mountain site, average diurnal variations of ambient $f_{C_5H_6O}^{OA}$, monoterpene and
414 isoprene+MBO are plotted in Fig. S9. $f_{C_5H_6O}^{OA}$ shows a diurnal pattern that increases at night and
415 peaks in the early morning, similar to the diurnal variation of monoterpenes. Monoterpenes
416 continue to be oxidized during nighttime at this site by NO₃ radical and O₃ with a lifetime of ~30
417 min (with 5 ppt of NO₃ and 30 ppb of O₃) (Fry et al., 2013). In contrast only a decrease and later
418 a plateau of $f_{C_5H_6O}^{OA}$ are observed during the period with high MBO concentration and higher
419 oxidation rate of MBO due to high OH radical in daytime (as MBO reacts slowly with O₃ and
420 NO₃) (Atkinson and Arey, 2003). While MBO-SOA may or may not have $f_{C_5H_6O}^{OA}$ above
421 background levels, the diurnal variations point to MT-SOA playing a dominant role in $f_{C_5H_6O}^{OA}$ at
422 this site.

423 The average $f_{C_5H_6O}^{OA}$ in areas strongly influenced by monoterpene emissions is $3.1\pm0.6\%$,
424 obtained by averaging the values from the Rocky mountain forest (3.7%), European boreal
425 forest (2.5%), and DC3 flight (3.0%). Note that the difference between $f_{C_5H_6O}^{OA}$ in areas strongly
426 influenced by monoterpene emissions ($3.1\pm0.6\%$) and isoprene emissions ($6.5\pm2.2\%$) is
427 reduced, compared to a factor of 4 differences between pure MT-SOA ($5.5\pm2.0\%$) and IEPOX-
428 SOA ($22\pm7\%$). This is likely due to the physical mixing of OA from different sources and in
429 different proportions at each location.

430 **3.6 $f_{C_5H_6O}$ vs OA oxidation level (f_{CO_2}) “triangle plot” – background studies**

431 In AMS spectra, the CO_2^+ ion is a marker of aging and oxidation processes (Alfarra et al.,
432 2004;Ng et al., 2011a). To evaluate whether oxidation plays a role on the observed $f_{C_5H_6O}$ for
433 different types of OA, in this section we use plots of f_{CO_2} (= CO_2^+/OA) vs. $f_{C_5H_6O}$ as a graphical
434 diagnostic of this process, similar to graphical diagnostics (“triangle plots”) used for other
435 purposes with AMS data (Cubison et al., 2011;Ng et al., 2011a). For studies strongly influenced
436 by urban and biomass-burning emissions in Fig. 3d we observe a wide range of $f_{CO_2}^{OA}$ values from
437 0.001 to 0.3 (= 30% or 300%). The wide range of $f_{CO_2}^{OA}$ is due to variable fractions of POA and
438 SOA (mixing effect) and a variable oxidation level of POA and SOA (oxidation effect) in the
439 different studies. In fact, to our knowledge, these studies encompass the values of $f_{CO_2}^{OA}$ observed
440 in all ambient AMS studies to date (Ng et al., 2011a). Several studies when urban and forest air,
441 or biomass burning smoke were aged by intense OH oxidation with an oxidation flow reactor
442 (OFR) (Kang et al., 2007;Li et al., 2013;Ortega et al., 2013) are also included. However, despite
443 the wide range of $f_{CO_2}^{OA}$, $f_{C_5H_6O}^{OA}$ changes little, staying in the range 0.02 – 3.5%, and with little
444 apparent dependence on $f_{CO_2}^{OA}$ for the ambient studies. A linear regression to quantiles from this

445 dataset results in an intercept of 1.7‰ and a very weak decrease with increasing $f_{CO_2}^{OA}$. A stronger
446 decrease is observed when aging urban air (Los Angeles) by intense OH exposure in flow
447 reactor, as shown in Fig. 3d.

448 Ambient $f_{CO_2}^{OA}$ at the Rocky Mountain forest site shows a moderate oxidation level (0.1 –
449 0.15), similar to the SE US-CTR (Fig. 5). $f_{C_5H_6O}^{OA}$ in the Rocky mountain site decreases linearly
450 when $f_{CO_2}^{OA}$ increases. During the Rocky Mountain study, the intense OH aging of ambient air in a
451 flow reactor shows a continuation of the trend observed for the ambient data, where $f_{C_5H_6O}^{OA}$
452 decreases as $f_{CO_2}^{OA}$ increases. A linear regression to the combined ambient and OFR datasets
453 ($f_{C_5H_6O}^{OA} = -0.013 \times f_{CO_2}^{OA} + 0.0054$) will be used below to estimate background $f_{C_5H_6O}^{OA}$ in areas with
454 strong monoterpene and low isoprene emissions.

455 $f_{C_5H_6O}$ in ambient SOA from other studies catalogued in the HR-AMS spectral database are
456 also shown in Fig. 5. Most urban oxygenated OA (OOA) are within $f_{C_5H_6O}^{OA-Bkg-UB}$ (average 1.7‰;
457 range: 0.02 – 3.5‰), which is consistent with the $f_{C_5H_6O}$ (<3‰) in lab aromatic SOA and other
458 urban OA in Fig. 5. However, some ambient SOA spectra do show higher $f_{C_5H_6O}$ (3 – 10‰) than
459 the $f_{C_5H_6O}^{OA-Bkg-UB}$ (0.02 – 3.5‰), which we will discuss in the next section.

460 3.7 $f_{C_5H_6O}$ vs. OA oxidation level (f_{CO_2}) – IEPOX-SOA influenced Studies

461 $f_{CO_2}^{OA}$ vs. $f_{C_5H_6O}^{OA}$ in studies impacted by IEPOX-SOA are shown in Fig. 5. Consistent with the
462 distributions discussed above, the bulk of points from these areas all show distinctively enhanced
463 $f_{C_5H_6O}^{OA}$ when compared to background $f_{C_5H_6O}^{OA}$ points of similarly moderate or higher oxidation
464 levels. The $f_{C_5H_6O}^{OA}$ measurements with lower $f_{CO_2}^{OA}$ values are more broadly distributed than the
465 $f_{C_5H_6O}^{OA}$ points with higher $f_{CO_2}^{OA}$ values in SE US-CTR, SEAC4RS, Borneo forest and [Amazon](#)

466 forest downwind of Manaus. However, increased $f_{C_5H_6O}^{OA}$ with higher $f_{CO_2}^{OA}$ was observed in the
467 Amazon. Both oxidation and mixing of air masses with different OA can influence these
468 observations. $f_{C_5H_6O}^{IEPOX-SOA}$ in IEPOX-SOA usually will decrease with oxidative aging. E.g.,
469 $f_{C_5H_6O}^{OA}$ from the SOAS oxidation flow reactor decreases continuously as OA becomes more
470 oxidized than ambient OA in SOAS-CTR ($f_{CO_2}^{OA}$ increases from 0.15 to 0.3). Air mass mixing
471 effects are more complex. Depending on the $f_{CO_2}^{OA}$ in the air masses mixed with, $f_{C_5H_6O}^{OA}$ in IEPOX-
472 SOA-rich air can show positive, neutral or negative trends with increasing $f_{CO_2}^{OA}$. E.g., in pristine
473 Amazon forest, points with both lower $f_{CO_2}^{OA}$ (<0.08) and $f_{C_5H_6O}^{OA}$ (< 8‰) values are thought to be
474 mainly caused by advection of POA from occasional local pollution.

475 The overall trend for the ambient measurements in studies strongly influenced by isoprene
476 emissions (Fig. 5) is that those points cluster in a triangle shape and $f_{C_5H_6O}^{OA}$ decreases as $f_{CO_2}^{OA}$
477 increases, as illustrated in Fig. S10. This “triangle shape” indicates that as the ambient OA
478 oxidation increases, the IEPOX-SOA signature is reduced, potentially by the ambient oxidation
479 processes or by physical mixing with air masses containing more aged aerosols.

480 Finally, points with higher $f_{C_5H_6O}$ in OOA/aged OA are labeled with numbers in Fig. 5. The
481 sources of those labeled points are summarized in Table S2. OA from those studies are all
482 partially influenced by biogenic emissions. For example, during measurements of ambient OA in
483 the Central Valley of California (number 2), high isoprene emissions and acidic particles were
484 observed (Dunlea et al., 2009), suggesting that potential IEPOX-SOA formed in this area may
485 explain the higher $f_{C_5H_6O}^{OA}$ there.

486 **3.8 Best estimate of $f_{C_5H_6O}$ in IEPOX-SOA**

487 IEPOX-SOA from different field campaigns and chamber studies lay towards the right and
488 on the bottom half of Fig. 5. IEPOX-SOA from chamber studies show systematically lower
489 $f_{CO_2}^{IEPOX-SOA}$ than ambient studies. This is likely explained by the lack of additional aging in the
490 laboratory studies, because all the lab IEPOX-SOA were measured directly after uptake gas-
491 phase IEPOX onto acidic aerosol without undergoing substantial additional oxidation.

492 A wide range (12 – 40‰) of $f_{C_5H_6O}^{IEPOX-SOA}$ is observed with an average of $22‰ \pm 7‰$ in
493 ambient and lab IEPOX-SOA. $f_{C_5H_6O}^{IEPOX-SOA}$ did not show a trend vs. $f_{CO_2}^{IEPOX-SOA}$. The IEPOX-
494 SOA molecular tracer 3-MeTHF-3,4-diols has been shown to enhance the $f_{C_5H_6O}$ in OA (Fig. 5)
495 (Lin et al., 2012; Canagaratna et al., 2015). Except 3-MeTHF-3,4-diols none of the other pure
496 IEPOX-derived polyols standards have been atomized and injected into the AMS system so far,
497 to our knowledge. We suspect other polyols such as 2-methyltetrols may also lead to such an
498 enhancement through dehydration reactions in the AMS vaporizer leading to methylfuran-type
499 structures. The diversity of $f_{C_5H_6O}^{IEPOX-SOA}$ in different studies is related with the variable content of
500 specific IEPOX-SOA molecular species that enhance $f_{C_5H_6O}^{IEPOX-SOA}$ differently. The fractions of
501 molecular IEPOX-SOA species in total IEPOX-SOA_{PMF} is plotted vs $f_{C_5H_6O}$ in IEPOX-SOA in
502 three different studies in Fig. 7, which show a strong correlation between each other. The strong
503 simultaneous variation of both quantities indicates that the diversity of $f_{C_5H_6O}^{IEPOX-SOA}$ is very likely
504 explained by the variability of the molecules comprising IEPOX-SOA among different studies.

505 During one day in SOAS (June 26th, 2013), IEPOX-SOA_{PMF} comprised 80 – 90% of total
506 OA (Fig. S11), possibly due to high sulfate concentrations favoring IEPOX-SOA formation.
507 $f_{C_5H_6O}^{OA}$ reached 25‰, which is similar to the 22‰ for the IEPOX-SOA_{PMF} from this study, and
508 consistent with a slightly lower value for the average vs. freshest ambient IEPOX-SOA. Among
509 the chamber studies, the study of reactive uptake of isoprene-oxidation products into an acidic

510 seed is most similar to the full chemistry in real ambient environments (Liu et al., 2014), and
 511 reports similar $f_{C_5H_6O}^{IEPOX-SOA}$ values (19%). Hence, we propose an average $f_{C_5H_6O}^{IEPOX-SOA}$ (22%)
 512 from both studies as the typical value of fresh IEPOX-SOA.

513 3.9 Proposed Method for Real-Time Estimation of IEPOX-SOA

514 So far, PMF of AMS spectra is the only demonstrated method for quantifying total IEPOX-
 515 SOA concentrations. However, the PMF method is labor-intensive and requires significant
 516 expertise, and may fail to resolve a certain factor when present in lower mass fractions (<5%). A
 517 simpler, real-time method to estimate IEPOX-SOA would be useful in many studies, including
 518 ground-based and aircraft campaigns.

519 We propose an estimation method for IEPOX-SOA based on the mass concentration of its
 520 tracer ion $C_5H_6O^+$. To do this, we express the mass concentration of $C_5H_6O^+$ as

$$521 \quad C_5H_6O_{total}^+ = C_5H_6O_{IEPOX-SOA,ambient}^+ + C_5H_6O_{background}^+. \quad (1)$$

522 Where, $C_5H_6O_{total}^+$ is measured total $C_5H_6O^+$ signal in AMS; $C_5H_6O_{IEPOX-SOA,ambient}$ and
 523 $C_5H_6O_{background}^+$ are the $C_5H_6O^+$ signals contributed by IEPOX-SOA in ambient OA and other
 524 background OA (non IEPOX-SOA).

525 Then, $C_5H_6O_{IEPOX-SOA,ambient}$ and $C_5H_6O_{background}^+$ can be calculated as:

$$526 \quad C_5H_6O_{IEPOX-SOA,ambient}^+ = IEPOX-SOA \times f_{C_5H_6O}^{IEPOX-OA}. \quad (2)$$

$$527 \quad C_5H_6O_{background}^+ = (OA_{mass} - IEPOX-SOA) \times f_{C_5H_6O}^{OA-Bkg}. \quad (3)$$

528 Where, $f_{C_5H_6O}^{IEPOX-OA}$ is the fractional contribution of $C_5H_6O^+$ to the total ion signal in the
 529 spectra of IEPOX-SOA from IEPOX-SOA_{lab} or IEPOX-SOA_{PMF} factors. $f_{C_5H_6O}^{OA-Bkg}$ is the
 530 background $f_{C_5H_6O}$ in other non-IEPOX-SOA, e.g., values from OA strongly influenced by urban
 531 and biomass-burning emissions ($f_{C_5H_6O}^{OA-Bkg-UB}$).

532 Then, by combining Eq. (1) – (3), we can express $C_5H_6O^+_{total}$ as:

533
$$C_5H_6O^+_{total} = IEPOX-SOA \times f_{C_5H_6O}^{IEPOX-OA} + (OA - IEPOX-SOA) \times f_{C_5H_6O}^{OA-Bkg} \quad (4)$$

534 Finally, IEPOX-SOA can be estimated as:

535
$$IEPOX-SOA = \frac{C_5H_6O^+_{total} - OA \times f_{C_5H_6O}^{OA-Bkg}}{f_{C_5H_6O}^{IEPOX-OA} - f_{C_5H_6O}^{OA-Bkg}} \quad (5)$$

536 In Eq. (5), $C_5H_6O^+_{total}$ and OA mass are measured directly by AMS. $f_{C_5H_6O}^{OA-Bkg}$ and
537 $f_{C_5H_6O}^{IEPOX-OA}$ are two parameters that must be determined by other means.

538 As discussed above, the background value in the absence of a substantial impact of MT-
539 SOA is ~1.7‰. In studies influenced by monoterpene emissions, the background value may be

540 elevated by MT-SOA. $f_{C_5H_6O}^{OA}$ at the Rocky Mountain site estimated by $f_{C_5H_6O}^{OA} = (0.41 -$

541 $f_{CO_2}^{OA}) \times 0.013$ (Fig. 5) can be used as $f_{C_5H_6O}^{OA-Bkg}$ for areas with strong MT-SOA contributions

542 $(f_{C_5H_6O}^{OA-Bkg-MT})$. There is some uncertainty in this value, due to possible contributions of a small

543 amount of IEPOX-SOA, MBO-SOA, and other OA sources at this site. An alternative estimate

544 for $f_{C_5H_6O}^{OA-Bkg-MT}$ would be $\sim 1.7‰ + 3 \times MT_{avg}$ (ppb), which is also approximately consistent with

545 our ambient data, but may have higher uncertainty. Further characterization of the background

546 $f_{C_5H_6O}$ in areas with MT-SOA impact is of interest for future studies. Finally, we have decided to

547 use $f_{C_5H_6O}^{OA}$ estimated from the Rocky Mountain site as $f_{C_5H_6O}^{OA-Bkg-MT}$ in the following calculation.

548 As discussed above, we use average $f_{C_5H_6O}^{IEPOX-OA} = 22‰$ in Eq. (3) as a representative value of

549 ambient IEPOX-SOA. Several scenarios based on different $f_{C_5H_6O}^{OA}$ values to use this tracer-based

550 method are addressed in the supporting information. The justification from users on using this

551 method is needed.

552 3.10 Application of the Real-Time Estimation Method of IEPOX-SOA

553 To test the proposed estimation method, we use SE US forest (SOAS) data as an example in
554 Fig. 8, applying both background estimates (urban & biomass burning, and monoterpene
555 emissions). Since there are high monoterpene concentrations (~1 ppb during the night) in SOAS,
556 we expect the MT-influenced background to be more accurate. The IEPOX-SOA estimated by
557 subtracting the MT-SOA background (IEPOX-SOA_{MT}) is indeed better correlated with IEPOX-
558 SOA_{PMF} (R=0.99) than that (R = 0.96) when the urban & biomass-burning background is applied
559 (IEPOX-SOA_{urb&bb}). The intercept of regression line between IEPOX-SOA_{MT} and IEPOX-
560 SOA_{PMF} is zero, indicating the background of IEPOX-SOA contributed by MT-SOA is clearly
561 deducted.

562 The regression slope between IEPOX-SOA_{MT} and IEPOX-SOA_{PMF} is 0.95, suggesting that
563 C₅H₆O⁺ in SE US CTR site (SOAS) may be slightly overcorrected by minimizing C₅H₆O⁺ from
564 monoterpene emissions. This underestimation may be associated with higher MT-SOA
565 contribution to C₅H₆O⁺ in Rocky Mountain pine forest site than SE US forest site, or interference
566 from IEPOX-SOA/MBO-SOA at the Rocky Mountain site. IEPOX-SOA_{urb&bb} is 1.26 times
567 higher than IEPOX-SOA_{PMF}. Thus, as expected IEPOX-SOA_{MT} and IEPOX-SOA_{urb&bb} provide
568 lower and upper limits of estimated IEPOX-SOA.

569 Among all the datasets introduced in this study, the SOAS-CTR dataset should be the best
570 case scenario since $f_{C_5H_6O}^{IEPOX-OA} = 22\%$ is coincidentally the same value in the spectrum of IEPOX-
571 SOA_{PMF} in SOAS-CTR and a large fraction (17%) of IEPOX-SOA existed in SOAS-CTR as
572 well. Given the spread of values of $f_{C_5H_6O}^{IEPOX-OA}$ (12 – 40%) in different studies, if no additional
573 local IEPOX-SOA spectrum is available for a given site, the estimation from this method should

574 be within a factor of ~2 of the actual concentration, as illustrated in Fig. S13-S14. Further
575 information concerning the estimation method using unit mass resolution m/z 82 (or f_{82}) can be
576 found in the Appendix.

577 4. Conclusions

578 To investigate if the ion $C_5H_6O^+$ (at m/z 82) in AMS spectra is a good tracer for IEPOX-SOA,
579 tens of field and lab studies are combined and compared, including the SOAS 2013 campaign in
580 the SE US. The results show that $f_{C_5H_6O}^{OA}$ is clearly elevated when IEPOX-SOA is present, and
581 thus has potential usefulness as a tracer of this aerosol type. The average $f_{C_5H_6O}^{IEPOX-OA}$ in chamber
582 and ambient studies is $22 \pm 7\%$ (range 12% – 40%). No dependence of $f_{C_5H_6O}^{IEPOX-OA}$ on oxidation
583 level ($f_{CO_2}^{IEPOX-SOA}$) was found. Background $f_{C_5H_6O}$ in OA strongly influenced by urban or
584 biomass-burning emissions or pure anthropogenic POAs averages $1.7 \pm 0.1\%$ (range 0.02 –
585 3.5%).

586 In ambient OA that is strongly influenced by isoprene emissions under lower NO, we observe
587 systematically higher $f_{C_5H_6O}^{OA}$ (with an average of $\sim 6.5 \pm 2.2\%$), consistent with presence of
588 IEPOX-SOA. Low tracer values ($f_{C_5H_6O} < 3\%$) are observed in non IEPOX-derived isoprene-
589 SOA from laboratory studies, indicating that the tracer ion is specifically enhanced from IEPOX-
590 SOA, and is not a tracer for all SOA from isoprene.

591 Higher background values of $f_{C_5H_6O}^{OA}$ ($3.1 \pm 0.6\%$ in average) were found in area strongly
592 impacted by monoterpene emissions. $f_{CO_2}^{MT-SOA}$ is $5.5 \pm 2.0\%$, which are substantially lower than
593 for IEPOX-SOA ($22 \pm 7\%$), and thus they leave some room to separate both contributions. A

594 $f_{C_5H_6O}^{OA-Bkg-MT}$ as a function of $f_{CO_2}^{OA}$ in monoterpene emissions is determined by linear regressing
595 the $f_{C_5H_6O}^{OA}$ and $f_{CO_2}^{OA}$ at a Rocky Mountain pine forest site.

596 A simplified method to estimate IEPOX-SOA based on measured ambient $C_5H_6O^+$, CO_2^+ and
597 OA in AMS is proposed. Good correlations ($R>0.96$) between estimated IEPOX-SOA and
598 IEPOX-SOA_{PMF} are obtained for SOAS, confirming the potential usefulness of this estimation
599 method. Given the observed variability in IEPOX-SOA composition, the method is expected to
600 be within a factor of ~ 2 of the true concentration if no additional information about the local
601 IEPOX-SOA is available for a given study. When only unit mass resolution data is available as
602 in ACSM data, all methods may perform less well because of increased interferences from other
603 ions at m/z 82.

604

605 ACKNOWLEDGMENT

606 This study was partially supported by NSF AGS-1243354 and AGS-1360834, NASA
607 NNX12AC03G, DOE (BER/ASR) DE-SC0011105, and NOAA NA13OAR4310063. B. Palm
608 and J. Krechmer are grateful for fellowships from EPA STAR (FP-91761701-0 and FP-
609 91770901-0) and CIRES. A. Ortega is grateful for a CU-Boulder Chancellor's and DOE SCGF
610 (ORAU/ORISE) fellowship. A. Wisthaler and T. Mikoviny were supported by the Austrian
611 Federal Ministry for Transport, Innovation and Technology (BMVIT) through the Austrian
612 Space Applications Programme (ASAP) of the Austrian Research Promotion Agency (FFG), and
613 the Visiting Scientist Program at the National Institute of Aerospace (NIA). G. Isaacman-
614 VanWertz is grateful for an NSF Fellowship (DGE-1106400). UC Berkeley was supported by
615 NSF AGS-1250569. We acknowledge the logistical support from the LBA Central Office at INPA
616 (Instituto Nacional de Pesquisas da Amazonia). P. Artaxo acknowledges support from FAPESP
617 grants 2013/05014-0 and 2014/05238-8 and CNPq support from grants 457843/2013-6 and
618 307160/2014-9. We acknowledge this work was funded by the U.S. Environmental Protection
619 Agency (EPA) through grant number 835404. The contents of this publication are solely the
620 responsibility of the authors and do not necessarily represent the official views of the U.S. EPA.
621 Further, the U.S. EPA does not endorse the purchase of any commercial products or services
622 mentioned in the publication. The U.S. EPA through its Office of Research and Development
623 collaborated in the research described here. It has been subjected to Agency review and approved
624 for publication, but may not necessarily reflect official Agency policy. The authors would also like
625 to thank the Electric Power Research Institute (EPRI) for their support. M. Riva and J. D. Surratt
626 wish to thank the Camille and Henry Dreyfus Postdoctoral Fellowship Program in
627 Environmental Chemistry for their financial support. We thank J. Crouse and P. Wennberg
628 from Caltech for gas-phase IEPOX data in SOAS-CTR and DC3, under support from NASA
629 NNX12AC06G. We thank Lu Xu and Nga Lee Ng from Georgia Tech for providing data from
630 their studies. We acknowledge funding from the UK Natural Environment Research Council through the
631 OP3 and SAMBBA projects (Grant refs. NE/D002117/1 and NE/J010073/1).

632 **APPENDIX**

633 In addition to the preceding high resolution $C_5H_6O^+$ data analysis, we also investigated unit mass
634 resolution (UMR) m/z 82 as a tracer of IEPOX-SOA. In addition to $C_5H_6O^+$ (m/z 82.0419), the
635 reduced ion $C_6H_{10}^+$ and oxygenated ion $C_4H_2O_2^+$ often contribute signal to UMR m/z 82. The
636 average background level of f_{82}^{OA} ($= m/z$ 82/OA) is from $4.3 \pm 0.9\%$ (0.01 to 10%) in studies
637 strongly influenced by urban, biomass-burning and other anthropogenic POA, as shown in Fig.

638 A1a – c. This value is higher than the high-resolution $f_{C_5H_6O}^{OA-Bkg-UB}$ (1.7%) in the same studies.

639 Background f_{82}^{OA} increases when OA is fresher (lower f_{44} , $f_{44}^{OA} = m/z$ 44/OA) as shown in Fig A1d,
640 and can be estimated as $f_{82}^{OA} = 5.5 \times 10^{-3} - 8.2 \times 10^{-3} \times f_{44}^{OA}$ in areas strongly impacted by urban and
641 biomass-burning emissions. The uncertainty of calculated f_{82} can be as high as 30% in the lower
642 fresh OA plumes by considering the uncertainties from quantile average and linear regression.

643 There are also some pure chemical species that exhibit high f_{82} values, as shown in Fig. A1c.

644 These species include docosanol, eicosanol and oleic acid. However, none of these pure chemical
645 species alone contributes substantially to ambient aerosol.

646 The probability density distributions of f_{82}^{OA} in studies strongly influenced by isoprene emissions
647 are shown in Fig. A2a. The peaks ($\sim 8.7 \pm 2.5\%$) are similar in SE US, pristine, polluted Amazon

648 forest, Borneo forest to high resolution $f_{C_5H_6O}^{OA}$ ($\sim 6.5 \pm 2.2\%$), indicating $C_5H_6O^+$ is the dominant
649 ion at UMR m/z 82 in these studies. Compared to the studies with strong urban and biomass-

650 burning emissions, clear enhancements of f_{82}^{OA} in studies strongly influenced by isoprene
651 emissions are still observed, but with less contrast than for in high resolution datasets (Fig. A2 –
652 A3).

653 Figure 2Aa also shows the probability density distributions of f_{82}^{OA} at Rocky Mountain and
654 European boreal forests (strongly influenced by monoterpene emissions). Those distributions

655 peak at ~5%, which are within the range (0.01 – 10%) of f_{82}^{OA} in aerosols strongly influenced by
 656 urban and biomass-burning emissions. In the lab studies, most of f_{82}^{MT-SOA} (average $6.7 \pm 2.2\%$;
 657 range 4 – 11%) observed in the spectra of MT-SOA are also comparable to background f_{82}^{OA}
 658 levels (average $4.3 \pm 0.9\%$; range 0.01–10%), and tend to be in the higher f_{82}^{OA} region from urban
 659 and biomass-burning emissions. A linear regression line of f_{44}^{OA} vs f_{82}^{OA} for the Rocky Mountain
 660 site ($f_{82}^{OA} = 7.7 \times 10^{-3} - 0.019 \times f_{44}^{OA}$) is used to estimate the background f_{82}^{OA} from areas strongly
 661 influenced by monoterpene emissions.

662 In summary, elevated f_{82}^{OA} in studies with high isoprene-emissions is observed. Pronounced
 663 $f_{82}^{IEPOX-SOA}$ should be a key feature of IEPOX-SOA spectra. Thus IEPOX-SOA can be estimated
 664 as Eq. (6) here:

$$665 \quad \text{IEPOX-SOA} = \frac{m_{82}^{\text{total}} - m_{82}^{\text{background}}}{f_{82}^{\text{IEPOX-SOA}} - f_{82}^{\text{OA-Bkg}}} = \frac{m_{82}^{\text{total}} - \text{OA}_{\text{mass}} \times f_{82}^{\text{OA-Bkg}}}{f_{82}^{\text{IEPOX-SOA}} - f_{82}^{\text{OA-Bkg}}}, \quad (6)$$

666 where $f_{82}^{\text{IEPOX-SOA}}$ is 22% as obtained average (Fig. A3). In Eq. (4), $f_{82}^{\text{OA-Bkg}}$ can be calculated
 667 as a function of f_{44}^{OA} in studies strongly influenced by urban and biomass-burning emissions
 668 ($f_{82}^{OA} = 5.5 \times 10^{-3} - 8.2 \times 10^{-3} \times f_{44}^{OA}$) or monoterpene emissions ($f_{82}^{OA} = 7.7 \times 10^{-3} - 0.019 \times f_{44}^{OA}$), as
 669 discussed earlier. m_{82}^{total} and OA_{mass} are the measured ambient m/z 82 and OA mass
 670 concentrations by AMS. Because f_{82} in MT-SOA and OA from urban and biomass-burning
 671 emissions cannot be separated, only one background value of $f_{82}^{\text{OA-Bkg}}$ will be used in the UMR
 672 method.

673 To test this UMR empirical method, we apply Eq. (6) to SOAS-CTR dataset, see Fig. A4. The
 674 estimated IEPOX-SOA in SOAS-CTR from both background corrections (urban+biomass
 675 burning vs monoterpene) both correlates well with $\text{IEPOX-SOA}_{\text{PMF}}$ with $R=0.97$ and $R=0.98$,

676 respectively. The regression slopes between estimated fresh IEPOX-SOA vs IEPOX-SOA_{PMF} are
677 1.11 and 0.94, which are within 15% of 1:1 line. The deviation of estimated IEPOX-SOA from
678 UMR by subtracting the background of MT-SOA influences is similar to that from HR in the
679 SOAS dataset, indicating the UMR-based IEPOX-SOA estimation may perform as well as HR in
680 areas with high IEPOX-SOA fractions. For areas with small IEPOX-SOA fractions, more
681 uncertainties may exist in UMR calculation, e.g., there are wider variations of f_{82}^{OA-Bkg} from
682 urban and biomass-burning emissions with oxidation level, whereas a smaller and less variable
683 $f_{C_5H_6O}^{OA-Bkg}$ is found in HR. Overall, m/z 82 in unit mass resolution data is also useful to estimate
684 IEPOX-SOA. The different methods to estimate IEPOX-SOA may perform less well because of
685 increased interferences from other ions at m/z 82, however at locations with very high fractions
686 of IEPOX-SOA such as SOAS-CTR, the UMR-based method performs well.

687

688 **References**

- 689 Aiken, A. C., Salcedo, D., Cubison, M. J., Huffman, J. A., DeCarlo, P. F., Ulbrich, I. M., Docherty, K. S.,
690 Sueper, D., Kimmel, J. R., Worsnop, D. R., Trimborn, A., Northway, M., Stone, E. A., Schauer,
691 J. J., Volkamer, R. M., Fortner, E., de Foy, B., Wang, J., Laskin, A., Shutthanandan, V., Zheng,
692 J., Zhang, R., Gaffney, J., Marley, N. A., Paredes-Miranda, G., Arnott, W. P., Molina, L. T., Sosa,
693 G., and Jimenez, J. L.: Mexico City aerosol analysis during MILAGRO using high resolution
694 aerosol mass spectrometry at the urban supersite (T0) - Part 1: Fine particle composition and
695 organic source apportionment, *Atmos Chem Phys*, 9, 6633-6653, 2009.
- 696 Alfarra, M.: Insights Into Atmospheric Organic Aerosols Using An Aerosol Mass Spectrometer, Doctor,
697 Institute of Science and Technology, University of Manchester, Manchester, 2004.
- 698 Alfarra, M. R., Coe, H., Allan, J. D., Bower, K. N., Boudries, H., Canagaratna, M. R., Jimenez, J. L.,
699 Jayne, J. T., Garforth, A. A., Li, S. M., and Worsnop, D. R.: Characterization of urban and rural
700 organic particulate in the lower Fraser valley using two aerodyne aerosol mass spectrometers,
701 *Atmos Environ*, 38, 5745-5758, DOI 10.1016/j.atmosenv.2004.01.054, 2004.
- 702 Allan, J. D., Morgan, W. T., Darbyshire, E., Flynn, M. J., Williams, P. I., Oram, D. E., Artaxo, P., Brito,
703 J., Lee, J. D., and Coe, H.: Airborne observations of IEPOX-derived isoprene SOA in the
704 Amazon during SAMBBA, *Atmos. Chem. Phys.*, 14, 11393-11407, 10.5194/acp-14-11393-2014,
705 2014.
- 706 Anonymous_Referee: Interactive comment on “Airborne observations of IEPOX-derived isoprene SOA
707 in the Amazon during SAMBBA” by J. D. Allan et al., *Atmos. Chem. Phys. Discuss*, 14., C5277–
708 C5279, 2014.
- 709 Atkinson, R., and Arey, J.: Atmospheric Degradation of Volatile Organic Compounds, *Chem Rev*, 103,
710 4605–4638, 10.1002/chin.200410285, 2003.
- 711 Bahreini, R., Keywood, M. D., Ng, N. L., Varutbangkul, V., Gao, S., Flagan, R. C., Seinfeld, J. H.,
712 Worsnop, D. R., and Jimenez, J. L.: Measurements of secondary organic aerosol from oxidation
713 of cycloalkenes, terpenes, and m-xylene using an Aerodyne aerosol mass spectrometer, *Environ*
714 *Sci Technol*, 39, 5674-5688, Doi 10.1021/Es048061a, 2005.
- 715 Barth, M. C., Cantrell, C. A., Brune, W. H., Rutledge, S. A., Crawford, J. H., Huntrieser, H., Carey, L. D.,
716 MacGorman, D., Weisman, M., Pickering, K. E., Bruning, E., Anderson, B., Apel, E.,
717 Biggerstaff, M., Campos, T., Campuzano-Jost, P., Cohen, R., Crouse, J., Day, D. A., Diskin, G.,
718 Flocke, F., Fried, A., Garland, C., Heikes, B., Honomichl, S., Hornbrook, R., Huey, L. G.,
719 Jimenez, J. L., Lang, T., Lichtenstern, M., Mikoviny, T., Nault, B., O'Sullivan, D., Pan, L. L.,
720 Peischl, J., Pollack, I., Richter, D., Riemer, D., Ryerson, T., Schlager, H., Clair, J. S., Walega, J.,
721 Weibring, P., Weinheimer, A., Wennberg, P., Wisthaler, A., Wooldridge, P. J., and Ziegler, C.:
722 The Deep Convective Clouds and Chemistry (DC3) Field Campaign, *B. Am. Meteorol. Soc.*,
723 published online first, doi:10.1175/bams-d-13-00290.1, 2014.
- 724 [Boyd, C. M., Sanchez, J., Xu, L., Eugene, A. J., Nah, T., Tuet, W. Y., Guzman, M. I., and Ng, N. L.:
725 Secondary organic aerosol formation from the \$\beta\$ -pinene+NO₃ system: effect of humidity and
726 peroxy radical fate, *Atmos. Chem. Phys.*, 15, 7497-7522, 10.5194/acp-15-7497-2015, 2015.](#)
- 727 Budisulistiorini, S. H., Canagaratna, M. R., Croteau, P. L., Marth, W. J., Baumann, K., Edgerton, E. S.,
728 Shaw, S. L., Knipping, E. M., Worsnop, D. R., Jayne, J. T., Gold, A., and Surratt, J. D.: Real-
729 Time Continuous Characterization of Secondary Organic Aerosol Derived from Isoprene
730 Epoxydiols in Downtown Atlanta, Georgia, Using the Aerodyne Aerosol Chemical Speciation
731 Monitor, *Environ Sci Technol*, 47, 5686-5694, 10.1021/es400023n, 2013.
- 732 [Budisulistiorini, S. H., Li, X., Bairai, S. T., Renfro, J., Liu, Y., Liu, Y. J., McKinney, K. A., Martin, S. T.,
733 McNeill, V. F., Pye, H. O. T., Nenes, A., Neff, M. E., Stone, E. A., Mueller, S., Knote, C., Shaw,
734 S. L., Zhang, Z., Gold, A., and Surratt, J. D.: Examining the effects of anthropogenic emissions
735 on isoprene-derived secondary organic aerosol formation during the 2013 Southern Oxidant and
736 Aerosol Study \(SOAS\) at the Look Rock, Tennessee ground site, *Atmos. Chem. Phys.*, 15, 8871-
737 8888, 10.5194/acp-15-8871-2015, 2015.](#)

738 Canagaratna, M. R., Jayne, J. T., Ghertner, D. A., Herndon, S., Shi, Q., Jimenez, J. L., Silva, P. J.,
739 Williams, P., Lanni, T., Drewnick, F., Demerjian, K. L., Kolb, C. E., and Worsnop, D. R.: Chase
740 studies of particulate emissions from in-use New York City vehicles, *Aerosol Sci Tech*, 38, 555-
741 573, Doi 10.1080/02786820490465504, 2004.

742 Canagaratna, M. R., Jimenez, J. L., Kroll, J. H., Chen, Q., Kessler, S. H., Massoli, P., Hildebrandt Ruiz,
743 L., Fortner, E., Williams, L. R., Wilson, K. R., Surratt, J. D., Donahue, N. M., Jayne, J. T., and
744 Worsnop, D. R.: Elemental ratio measurements of organic compounds using aerosol mass
745 spectrometry: characterization, improved calibration, and implications, *Atmos. Chem. Phys.*, 15,
746 253-272, 10.5194/acp-15-253-2015, 2015.

747 Carbone, S., De Brito, J. F., Andreae, M., Pöhlker, C., Chi, X., Saturno, J., Barbosa, H., and Artaxo, P.:
748 Preliminary characterization of submicron secondary aerosol in the amazon forest – ATTO
749 station, In prep., 2015.

750 Chang, R. Y. W., Leck, C., Graus, M., Müller, M., Paatero, J., Burkhardt, J. F., Stohl, A., Orr, L. H.,
751 Hayden, K., Li, S. M., Hansel, A., Tjernström, M., Leaitch, W. R., and Abbatt, J. P. D.: Aerosol
752 composition and sources in the central Arctic Ocean during ASCOS, *Atmos. Chem. Phys.*, 11,
753 10619-10636, 10.5194/acp-11-10619-2011, 2011.

754 Chen, Q., Liu, Y., Donahue, N. M., Shilling, J. E., and Martin, S. T.: Particle-Phase Chemistry of
755 Secondary Organic Material: Modeled Compared to Measured O:C and H:C Elemental Ratios
756 Provide Constraints, *Environ Sci Technol*, 45, 4763-4770, 10.1021/es104398s, 2011.

757 Chen, Q., Farmer, D. K., Rizzo, L. V., Pauliquevis, T., Kuwata, M., Karl, T. G., Guenther, A., Allan, J.
758 D., Coe, H., Andreae, M. O., Pöschl, U., Jimenez, J. L., Artaxo, P., and Martin, S. T.: Fine-mode
759 organic mass concentrations and sources in the Amazonian wet season (AMAZE-08), *Atmos.*
760 *Chem. Phys. Discuss.*, 14, 16151-16186, 10.5194/acpd-14-16151-2014, 2014.

761 Chhabra, P. S., Ng, N. L., Canagaratna, M. R., Corrigan, A. L., Russell, L. M., Worsnop, D. R., Flagan,
762 R. C., and Seinfeld, J. H.: Elemental composition and oxidation of chamber organic aerosol,
763 *Atmos. Chem. Phys.*, 11, 8827-8845, 10.5194/acp-11-8827-2011, 2011.

764 Coggon, M. M., Sorooshian, A., Wang, Z., Metcalf, A. R., Frossard, A. A., Lin, J. J., Craven, J. S.,
765 Nenes, A., Jonsson, H. H., Russell, L. M., Flagan, R. C., and Seinfeld, J. H.: Ship impacts on the
766 marine atmosphere: insights into the contribution of shipping emissions to the properties of
767 marine aerosol and clouds, *Atmos. Chem. Phys.*, 12, 8439–8458, doi:10.5194/acp-12-8439-2012,
768 2012.

769 Cole-Filipiak, N. C., O'Connor, A. E., and Elrod, M. J.: Kinetics of the Hydrolysis of Atmospherically
770 Relevant Isoprene-Derived Hydroxy Epoxides, *Environ Sci Technol*, 44, 6718-6723,
771 10.1021/es1019228, 2010.

772 Corrigan, A. L., Russell, L. M., Takahama, S., Äijälä, M., Ehn, M., Junninen, H., Rinne, J., Petäjä, T.,
773 Kulmala, M., Vogel, A. L., Hoffmann, T., Ebben, C. J., Geiger, F. M., Chhabra, P., Seinfeld, J.
774 H., Worsnop, D. R., Song, W., Auld, J., and Williams, J.: Biogenic and biomass burning organic
775 aerosol in a boreal forest at Hyytiälä, Finland, during HUMPPA-COPEC 2010, *Atmos. Chem.*
776 *Phys.*, 13, 12233-12256, 10.5194/acp-13-12233-2013, 2013.

777 Crippa, M., El Haddad, I., Slowik, J. G., DeCarlo, P. F., Mohr, C., Heringa, M. F., Chirico, R., Marchand,
778 N., Sciare, J., Baltensperger, U., and Prévôt, A. S. H.: Identification of marine and continental
779 aerosol sources in Paris using high resolution aerosol mass spectrometry, *J. Geophys. Res.*-
780 *Atmos.*, 118, 1950–1963, doi:10.1002/jgrd.50151, 2013.

781 Cubison, M. J., Ortega, A. M., Hayes, P. L., Farmer, D. K., Day, D., Lechner, M. J., Brune, W. H., Apel,
782 E., Diskin, G. S., Fisher, J. A., Fuelberg, H. E., Hecobian, A., Knapp, D. J., Mikoviny, T.,
783 Riemer, D., Sachse, G. W., Sessions, W., Weber, R. J., Weinheimer, A. J., Wisthaler, A., and
784 Jimenez, J. L.: Effects of aging on organic aerosol from open biomass burning smoke in aircraft
785 and laboratory studies, *Atmos. Chem. Phys.*, 11, 12049-12064, 10.5194/acp-11-12049-2011,
786 2011.

787 de Sá, S. S., Palm, B. B., Campuzano-Jost, P., Day, D. A., Hu, W., Newburn, M. K., Brito, J., Liu, Y.,
788 Isaacman-VanWertz, G., Yee, L. D., Goldstein, A. H., Artaxo, P., Souza, R., Manzi, A., Jimenez,
789 J. L., Alexander, M. L., and Martin, S. T., In prep., 2015.

790 DeCarlo, P. F., Kimmel, J. R., Trimborn, A., Northway, M. J., Jayne, J. T., Aiken, A. C., Gonin, M.,
791 Fuhrer, K., Horvath, T., Docherty, K. S., Worsnop, D. R., and Jimenez, J. L.: Field-deployable,
792 high-resolution, time-of-flight aerosol mass spectrometer, *Anal Chem*, 78, 8281-8289, Doi
793 10.1021/Ac061249n, 2006.

794 Docherty, K. S., Aiken, A. C., Huffman, J. A., Ulbrich, I. M., DeCarlo, P. F., Sueper, D., Worsnop, D. R.,
795 Snyder, D. C., Peltier, R. E., Weber, R. J., Grover, B. D., Eatough, D. J., Williams, B. J.,
796 Goldstein, A. H., Ziemann, P. J., and Jimenez, J. L.: The 2005 Study of Organic Aerosols at
797 Riverside (SOAR-1): instrumental intercomparisons and fine particle composition, *Atmos. Chem.*
798 *Phys.*, 11, 12387-12420, 10.5194/acp-11-12387-2011, 2011.

799 Dunlea, E. J., DeCarlo, P. F., Aiken, A. C., Kimmel, J. R., Peltier, R. E., Weber, R. J., Tomlinson, J.,
800 Collins, D. R., Shinozuka, Y., McNaughton, C. S., Howell, S. G., Clarke, A. D., Emmons, L. K.,
801 Apel, E. C., Pfister, G. G., van Donkelaar, A., Martin, R. V., Millet, D. B., Heald, C. L., and
802 Jimenez, J. L.: Evolution of Asian aerosols during transpacific transport in INTEX-B, *Atmos*
803 *Chem Phys*, 9, 7257-7287, 2009.

804 Dzepina, K., Arey, J., Marr, L. C., Worsnop, D. R., Salcedo, D., Zhang, Q., Onasch, T. B., Molina, L. T.,
805 Molina, M. J., and Jimenez, J. L.: Detection of particle-phase polycyclic aromatic hydrocarbons
806 in Mexico City using an aerosol mass spectrometer, *Int J Mass Spectrom*, 263, 152-170, DOI
807 10.1016/j.ijms.2007.01.010, 2007.

808 Ebben, C. J., Martinez, I. S., Shrestha, M., Buchbinder, A. M., Corrigan, A. L., Guenther, A., Karl, T.,
809 Petäjä, T., Song, W. W., Zorn, S. R., Artaxo, P., Kulmala, M., Martin, S. T., Russell, L. M.,
810 Williams, J., and Geiger, F. M.: Contrasting organic aerosol particles from boreal and tropical
811 forests during HUMPPA-COPEC-2010 and AMAZE-08 using coherent vibrational spectroscopy,
812 *Atmos. Chem. Phys.*, 11, 10317-10329, 10.5194/acp-11-10317-2011, 2011.

813 Eddingsaas, N. C., VanderVelde, D. G., and Wennberg, P. O.: Kinetics and Products of the Acid-
814 Catalyzed Ring-Opening of Atmospherically Relevant Butyl Epoxy Alcohols, *The Journal of*
815 *Physical Chemistry A*, 114, 8106-8113, 10.1021/jp103907c, 2010.

816 [Fröhlich, R., Crenn, V., Setyan, A., Belis, C. A., Canonaco, F., Favez, O., Riffault, V., Slowik, J. G., Aas,](#)
817 [W., Aijälä, M., Alastuey, A., Artiñano, B., Bonnaire, N., Bozzetti, C., Bressi, M., Carbone, C.,](#)
818 [Coz, E., Croteau, P. L., Cubison, M. J., Esser-Gietl, J. K., Green, D. C., Gros, V., Heikkinen, L.,](#)
819 [Herrmann, H., Jayne, J. T., Lunder, C. R., Minguillón, M. C., Močnik, G., O'Dowd, C. D.,](#)
820 [Ovadnevaite, J., Petralia, E., Poulain, L., Priestman, M., Ripoll, A., Sarda-Estève, R.,](#)
821 [Wiedensohler, A., Baltensperger, U., Sciare, J., and Prévôt, A. S. H.: ACTRIS ACSM](#)
822 [intercomparison – Part 2: Intercomparison of ME-2 organic source apportionment results from 15](#)
823 [individual, co-located aerosol mass spectrometers, *Atmos. Meas. Tech.*, 8, 2555-2576,](#)
824 [10.5194/amt-8-2555-2015, 2015.](#)

825 Froyd, K. D., Murphy, S. M., Murphy, D. M., de Gouw, J. A., Eddingsaas, N. C., and Wennberg, P. O.:
826 Contribution of isoprene-derived organosulfates to free tropospheric aerosol mass, *P. Natl. Acad.*
827 *Sci. USA*, 107, 21360–21365, doi:10.1073/pnas.1012561107, 2010.

828 Fry, J. L., Draper, D. C., Zarzana, K. J., Campuzano-Jost, P., Day, D. A., Jimenez, J. L., Brown, S. S.,
829 Cohen, R. C., Kaser, L., Hansel, A., Cappellin, L., Karl, T., Hodzic Roux, A., Turnipseed, A.,
830 Cantrell, C., Lefer, B. L., and Grossberg, N.: Observations of gas- and aerosol-phase organic
831 nitrates at BEACHON-RoMBAS 2011, *Atmos. Chem. Phys.*, 13, 8585-8605, 10.5194/acp-13-
832 8585-2013, 2013.

833 Fry, J. L., Draper, D. C., Barsanti, K. C., Smith, J. N., Ortega, J., Winkler, P. M., Lawler, M. J., Brown, S.
834 S., Edwards, P. M., Cohen, R. C., and Lee, L.: Secondary Organic Aerosol Formation and
835 Organic Nitrate Yield from NO₃ Oxidation of Biogenic Hydrocarbons, *Environ. Sci. Technol*, 48,
836 11944–11953, doi:10.1021/es502204x, 2014.

837 Gaston, C. J., Riedel, T. P., Zhang, Z., Gold, A., Surratt, J. D., and Thornton, J. A.: Reactive Uptake of an
838 Isoprene-Derived Epoxydiol to Submicron Aerosol Particles, *Environ. Sci. Technol.*, 48, 11178–
839 11186, doi:10.1021/es5034266, 2014.

840 Guenther, A. B., Jiang, X., Heald, C. L., Sakulyanontvittaya, T., Duhl, T., Emmons, L. K., and Wang, X.:
841 The Model of Emissions of Gases and Aerosols from Nature version 2.1 (MEGAN2.1): an
842 extended and updated framework for modeling biogenic emissions, *Geosci. Model Dev.*, 5, 1471–
843 1492, 10.5194/gmd-5-1471-2012, 2012.

844 Hayes, P. L., Ortega, A. M., Cubison, M. J., Froyd, K. D., Zhao, Y., Cliff, S. S., Hu, W. W., Toohey, D.
845 W., Flynn, J. H., Lefer, B. L., Grossberg, N., Alvarez, S., Rappenglück, B., Taylor, J. W., Allan,
846 J. D., Holloway, J. S., Gilman, J. B., Kuster, W. C., de Gouw, J. A., Massoli, P., Zhang, X., Liu,
847 J., Weber, R. J., Corrigan, A. L., Russell, L. M., Isaacman, G., Worton, D. R., Kreisberg, N. M.,
848 Goldstein, A. H., Thalman, R., Waxman, E. M., Volkamer, R., Lin, Y. H., Surratt, J. D.,
849 Kleindienst, T. E., Offenberg, J. H., Dusanter, S., Griffith, S., Stevens, P. S., Brioude, J.,
850 Angevine, W. M., and Jimenez, J. L.: Organic aerosol composition and sources in Pasadena,
851 California, during the 2010 CalNex campaign, *Journal of Geophysical Research: Atmospheres*,
852 118, 9233–9257, 10.1002/jgrd.50530, 2013.

853 He, L. Y., Lin, Y., Huang, X. F., Guo, S., Xue, L., Su, Q., Hu, M., Luan, S. J., and Zhang, Y. H.:
854 Characterization of high-resolution aerosol mass spectra of primary organic aerosol emissions
855 from Chinese cooking and biomass burning, *Atmos. Chem. Phys.*, 10, 11535–11543,
856 10.5194/acp-10-11535-2010, 2010.

857 Hersey, S. P., Craven, J. S., Schilling, K. A., Metcalf, A. R., Sorooshian, A., Chan, M. N., Flagan, R. C.,
858 and Seinfeld, J. H.: The Pasadena Aerosol Characterization Observatory (PACO): chemical and
859 physical analysis of the Western Los Angeles basin aerosol, *Atmos. Chem. Phys.*, 11, 7417–7443,
860 10.5194/acp-11-7417-2011, 2011.

861 Hu, D., Bian, Q., Li, T. W. Y., Lau, A. K. H., and Yu, J. Z.: Contributions of isoprene, monoterpenes, β -
862 caryophyllene, and toluene to secondary organic aerosols in Hong Kong during the summer of
863 2006, *Journal of Geophysical Research: Atmospheres*, 113, D22206, 10.1029/2008jd010437,
864 2008.

865 Hu, W., Hu, M., Hu, W., Jimenez, J.-L., Yuan, B., Chen, W., Wang, M., Wu, Y., Wang, Z., Chen, C.,
866 Peng, J., Shao, M., and Zeng, L.: Chemical composition, sources and aging process of sub-micron
867 aerosols in Beijing: contrast between summer and winter, submitted, 2015.

868 Hu, W. W., Hu, M., Yuan, B., Jimenez, J. L., Tang, Q., Peng, J. F., Hu, W., Shao, M., Wang, M., Zeng,
869 L. M., Wu, Y. S., Gong, Z. H., Huang, X. F., and He, L. Y.: Insights on organic aerosol aging and
870 the influence of coal combustion at a regional receptor site of central eastern China, *Atmos.*
871 *Chem. Phys.*, 13, 10095–10112, 10.5194/acp-13-10095-2013, 2013.

872 Huang, X. F., He, L. Y., Hu, M., Canagaratna, M. R., Sun, Y., Zhang, Q., Zhu, T., Xue, L., Zeng, L. W.,
873 Liu, X. G., Zhang, Y. H., Jayne, J. T., Ng, N. L., and Worsnop, D. R.: Highly time-resolved
874 chemical characterization of atmospheric submicron particles during 2008 Beijing Olympic
875 Games using an Aerodyne High-Resolution Aerosol Mass Spectrometer, *Atmos Chem Phys*, 10,
876 8933–8945, DOI 10.5194/acp-10-8933-2010, 2010.

877 Isaacman, G., Kreisberg, N. M., Yee, L. D., Worton, D. R., Chan, A. W. H., Moss, J. A., Hering, S. V.,
878 and Goldstein, A. H.: Online derivatization for hourly measurements of gas- and particle-phase
879 semi-volatile oxygenated organic compounds by thermal desorption aerosol gas chromatography
880 (SV-TAG), *Atmos. Meas. Tech.*, 7, 4417–4429, 10.5194/amt-7-4417-2014, 2014.

881 Jacobs, M. I., Burke, W. J., and Elrod, M. J.: Kinetics of the reactions of isoprene-derived
882 hydroxynitrates: gas phase epoxide formation and solution phase hydrolysis, *Atmos. Chem.*
883 *Phys.*, 14, 8933–8946, 10.5194/acp-14-8933-2014, 2014.

884 Jimenez-Group: Aerosol Mass Spectrometer Web Mass Spectral Database, High-Resolution
885 AMS Spectra, available at: <http://cires.colorado.edu/jimenez-group/HRAMSsd/> (last access:
886 15 December 2014); unit mass resolution spectra, available at: [http://cires.colorado.edu/](http://cires.colorado.edu/jimenez-group/AMSsd/)
887 [jimenez-group/AMSsd/](http://cires.colorado.edu/jimenez-group/AMSsd/) (last access: 15 December 2014), University of Colorado, Boulder,

888 2015.

889 Jimenez, J. L., Jayne, J. T., Shi, Q., Kolb, C. E., Worsnop, D. R., Yourshaw, I., Seinfeld, J. H., Flagan, R.
890 C., Zhang, X. F., Smith, K. A., Morris, J. W., and Davidovits, P.: Ambient aerosol sampling
891 using the Aerodyne Aerosol Mass Spectrometer, *J. Geophys. Res.-Atmos.*, 108, 8425,
892 doi:10.1029/2001jd001213, 2003.

893 Kang, E., Root, M. J., Toohey, D. W., and Brune, W. H.: Introducing the concept of Potential Aerosol
894 Mass (PAM), *Atmos. Chem. Phys.*, 7, 5727-5744, 10.5194/acp-7-5727-2007, 2007.

895 Karl, T., Guenther, A., Turnipseed, A., Tyndall, G., Artaxo, P., and Martin, S.: Rapid formation of
896 isoprene photo-oxidation products observed in Amazonia, *Atmos. Chem. Phys.*, 9, 7753-7767,
897 10.5194/acp-9-7753-2009, 2009.

898 Karl, T., Kaser, L., and Turnipseed, A.: Eddy covariance measurements of isoprene and 232-MBO based
899 on NO⁺ time-of-flight mass spectrometry, *Int J Mass Spectrom*, 365–366, 15-19, 2014.

900 Kaser, L., Karl, T., Schnitzhofer, R., Graus, M., Herdinger-Blatt, I. S., DiGangi, J. P., Sive, B.,
901 Turnipseed, A., Hornbrook, R. S., Zheng, W., Flocke, F. M., Guenther, A., Keutsch, F. N., Apel,
902 E., and Hansel, A.: Comparison of different real time VOC measurement techniques in a
903 ponderosa pine forest, *Atmos. Chem. Phys.*, 13, 2893-2906, 10.5194/acp-13-2893-2013, 2013.

904 Katrib, Y., Martin, S. T., Hung, H.-M., Rudich, Y., Zhang, H., Slowik, J. G., Davidovits, P., Jayne, J. T.,
905 and Worsnop, D. R.: Products and Mechanisms of Ozone Reactions with Oleic Acid for Aerosol
906 Particles Having Core–Shell Morphologies, *The Journal of Physical Chemistry A*, 108, 6686-
907 6695, 10.1021/jp049759d, 2004.

908 Krechmer, J. E., Coggon, M. M., Massoli, P., Nguyen, T. B., Crounse, J. D., Hu, W., Day, D. A., Tyndall,
909 G. S., Henze, D. K., Rivera-Rios, J. C., Nowak, J. B., Kimmel, J. R., Mauldin, R. L., Stark, H.,
910 Jayne, J. T., Sipilä, M., Junninen, H., St. Clair, J. M., Zhang, X., Feiner, P. A., Zhang, L., Miller,
911 D. O., Brune, W. H., Keutsch, F. N., Wennberg, P. O., Seinfeld, J. H., Worsnop, D. R., Jimenez,
912 J. L., and Canagaratna, M. R.: Formation of Low Volatility Organic Compounds and Secondary
913 Organic Aerosol from Isoprene Hydroxyhydroperoxide Low-NO Oxidation, *Environ Sci*
914 *Technol*, 10.1021/acs.est.5b02031, 2015.

915 Kroll, J. H., Ng, N. L., Murphy, S. M., Flagan, R. C., and Seinfeld, J. H.: Secondary organic aerosol
916 formation from isoprene photooxidation, *Environ Sci Technol*, 40, 1869-1877, Doi
917 10.1021/Es0524301, 2006.

918 Kuwata, M., Liu, Y., McKinney, K., and Martin, S. T.: Physical state and acidity of inorganic sulfate can
919 regulate the production of secondary organic material from isoprene photooxidation products,
920 *Phys Chem Chem Phys*, 17, 5670-5678, 10.1039/c4cp04942j, 2015.

921 Lanz, V. A., Alfarra, M. R., Baltensperger, U., Buchmann, B., Hueglin, C., and Prevot, A. S. H.: Source
922 apportionment of submicron organic aerosols at an urban site by factor analytical modelling of
923 aerosol mass spectra, *Atmos Chem Phys*, 7, 1503-1522, 2007.

924 Levin, E. J. T., Prenni, A. J., Palm, B. B., Day, D. A., Campuzano-Jost, P., Winkler, P. M., Kreidenweis,
925 S. M., DeMott, P. J., Jimenez, J. L., and Smith, J. N.: Size-resolved aerosol composition and its
926 link to hygroscopicity at a forested site in Colorado, *Atmos. Chem. Phys.*, 14, 2657-2667,
927 10.5194/acp-14-2657-2014, 2014.

928 Lewandowski, M., Piletic, I. R., Kleindienst, T. E., Offenber, J. H., Beaver, M. R., Jaoui, M., Docherty,
929 K. S., and Edney, E. O.: Secondary organic aerosol characterisation at field sites across the
930 United States during the spring–summer period, *International Journal of Environmental*
931 *Analytical Chemistry*, 93, 1084-1103, 10.1080/03067319.2013.803545, 2013.

932 Li, R., Palm, B. B., Borbon, A., Graus, M., Warneke, C., Ortega, A. M., Day, D. A., Brune, W. H.,
933 Jimenez, J. L., and de Gouw, J. A.: Laboratory Studies on Secondary Organic Aerosol Formation
934 from Crude Oil Vapors, *Environ Sci Technol*, 47, 12566-12574, 10.1021/es402265y, 2013.

935 Li, Y. J., Yeung, J. W. T., Leung, T. P. I., Lau, A. P. S., and Chan, C. K.: Characterization of Organic
936 Particles from Incense Burning Using an Aerodyne High-Resolution Time-of-Flight Aerosol
937 Mass Spectrometer, *Aerosol Sci Tech*, 46, 654-665, 10.1080/02786826.2011.653017, 2011.

938 Liao, J., Froyd, K. D., Murphy, D. M., Keutsch, F. N., Yu, G., Wennberg, P. O., Clair, J. S., Crouse, J.
939 D., Wisthaler, A., Mikoviny, T., Ryerson, T. B., Pollack, I. B., Peischl, J. L., Collett, J., Jimenez,
940 J. L., Campuzano-Jost, P., Day, D. A., Hu, W. W., Anderson, B. E., Ziemba, L. D., Blake, D. R.,
941 Meinardi, S., and Diskin, G.: Airborne organosulfates measurements over the continental US, *J*
942 *Geophys Res-Atmos*, 120, 2990-3005, 2014.

943 Liggio, J., Li, S. M., and McLaren, R.: Reactive uptake of glyoxal by particulate matter, *J Geophys Res-*
944 *Atmos*, 110, D10304, doi:10.1029/2004jd005113, 2005.

945 Lin, Y.-H., Zhang, Z., Docherty, K. S., Zhang, H., Budisulistiorini, S. H., Rubitschun, C. L., Shaw, S. L.,
946 Knipping, E. M., Edgerton, E. S., Kleindienst, T. E., Gold, A., and Surratt, J. D.: Isoprene
947 Epoxydiols as Precursors to Secondary Organic Aerosol Formation: Acid-Catalyzed Reactive
948 Uptake Studies with Authentic Compounds, *Environ Sci Technol*, 46, 250-258,
949 10.1021/es202554c, 2012.

950 Lin, Y.-H., Budisulistiorini, S. H., Chu, K., Siejack, R. A., Zhang, H., Riva, M., Zhang, Z., Gold, A.,
951 Kautzman, K. E., and Surratt, J. D.: Light-Absorbing Oligomer Formation in Secondary Organic
952 Aerosol from Reactive Uptake of Isoprene Epoxydiols, *Environ Sci Technol*, 48, 12012-12021,
953 10.1021/es503142b, 2014.

954 Liu, Y., Kuwata, M., Strick, B. F., Thomson, R. J., Geiger, F. M., McKinney, K., and Martin, S. T.:
955 Uptake of Epoxydiol Isomers Accounts for Half of the Particle-Phase Material Produced from
956 Isoprene Photooxidation via the HO₂ pathway, *Environ Sci Technol*, 49, 250-258,
957 10.1021/es5034298, 2014.

958 Loza, C. L., Chhabra, P. S., Yee, L. D., Craven, J. S., Flagan, R. C., and Seinfeld, J. H.: Chemical aging
959 of m-xylene secondary organic aerosol: laboratory chamber study, *Atmos. Chem. Phys.*, 12, 151-
960 167, 10.5194/acp-12-151-2012, 2012.

961 Mael, L. E., Jacobs, M. I., and Elrod, M. J.: Organosulfate and Nitrate Formation and Reactivity from
962 Epoxides Derived from 2-Methyl-3-buten-2-ol, *The Journal of Physical Chemistry A*,
963 10.1021/jp510033s, 2014.

964 Mao, J., Paulot, F., Jacob, D. J., Cohen, R. C., Crouse, J. D., Wennberg, P. O., Keller, C. A., Hudman,
965 R. C., Barkley, M. P., and Horowitz, L. W.: Ozone and organic nitrates over the eastern United
966 States: Sensitivity to isoprene chemistry, *Journal of Geophysical Research: Atmospheres*, 118,
967 2013JD020231, 10.1002/jgrd.50817, 2013.

968 Minguillón, M. C., Perron, N., Querol, X., Szidat, S., Fahrni, S. M., Alastuey, A., Jimenez, J. L., Mohr,
969 C., Ortega, A. M., Day, D. A., Lanz, V. A., Wacker, L., Reche, C., Cusack, M., Amato, F., Kiss,
970 G., Hoffer, A., Decesari, S., Moretti, F., Hillamo, R., Teinilä, K., Seco, R., Peñuelas, J., Metzger,
971 A., Schallhart, S., Müller, M., Hansel, A., Burkhardt, J. F., Baltensperger, U., and Prévôt, A. S. H.:
972 Fossil versus contemporary sources of fine elemental and organic carbonaceous particulate matter
973 during the DAURE campaign in Northeast Spain, *Atmos. Chem. Phys.*, 11, 12067-12084,
974 10.5194/acp-11-12067-2011, 2011.

975 Mohr, C., Huffman, J. A., Cubison, M. J., Aiken, A. C., Docherty, K. S., Kimmel, J. R., Ulbricht, I. M.,
976 Hannigan, M., and Jimenez, J. L.: Characterization of Primary Organic Aerosol Emissions from
977 Meat Cooking, Trash Burning, and Motor Vehicles with High-Resolution Aerosol Mass
978 Spectrometry and Comparison with Ambient and Chamber Observations, *Environ Sci Technol*,
979 43, 2443-2449, Doi 10.1021/Es8011518, 2009.

980 Mohr, C., DeCarlo, P. F., Heringa, M. F., Chirico, R., Slowik, J. G., Richter, R., Reche, C., Alastuey, A.,
981 Querol, X., Seco, R., Peñuelas, J., Jiménez, J. L., Crippa, M., Zimmermann, R., Baltensperger,
982 U., and Prévôt, A. S. H.: Identification and quantification of organic aerosol from cooking and
983 other sources in Barcelona using aerosol mass spectrometer data, *Atmos. Chem. Phys.*, 12, 1649-
984 1665, 10.5194/acp-12-1649-2012, 2012.

985 Ng, N. L., Chhabra, P. S., Chan, A. W. H., Surratt, J. D., Kroll, J. H., Kwan, A. J., McCabe, D. C.,
986 Wennberg, P. O., Sorooshian, A., Murphy, S. M., Dalleska, N. F., Flagan, R. C., and Seinfeld, J.

987 H.: Effect of NO_x level on secondary organic aerosol (SOA) formation from the photooxidation
 988 of terpenes, *Atmos Chem Phys*, 7, 5159-5174, 2007.
 989 Ng, N. L., Kwan, A. J., Surratt, J. D., Chan, A. W. H., Chhabra, P. S., Sorooshian, A., Pye, H. O. T.,
 990 Crounse, J. D., Wennberg, P. O., Flagan, R. C., and Seinfeld, J. H.: Secondary organic aerosol
 991 (SOA) formation from reaction of isoprene with nitrate radicals (NO₃), *Atmos. Chem. Phys.*, 8,
 992 4117-4140, 10.5194/acp-8-4117-2008, 2008.
 993 Ng, N. L., Canagaratna, M. R., Jimenez, J. L., Chhabra, P. S., Seinfeld, J. H., and Worsnop, D. R.:
 994 Changes in organic aerosol composition with aging inferred from aerosol mass spectra, *Atmos.*
 995 *Chem. Phys.*, 11, 6465-6474, 10.5194/acp-11-6465-2011, 2011a.
 996 Ng, N. L., Canagaratna, M. R., Jimenez, J. L., Zhang, Q., Ulbrich, I. M., and Worsnop, D. R.: Real-Time
 997 Methods for Estimating Organic Component Mass Concentrations from Aerosol Mass
 998 Spectrometer Data, *Environ Sci Technol*, 45, 910-916, 10.1021/es102951k, 2011b.
 999 Nguyen, T. B., Coggon, M. M., Bates, K. H., Zhang, X., Schwantes, R. H., Schilling, K. A., Loza, C. L.,
 1000 Flagan, R. C., Wennberg, P. O., and Seinfeld, J. H.: Organic aerosol formation from the reactive
 1001 uptake of isoprene epoxydiols (IEPOX) onto non-acidified inorganic seeds, *Atmos. Chem. Phys.*,
 1002 14, 3497-3510, 10.5194/acp-14-3497-2014, 2014.
 1003 Nguyen, T. B., Crounse, J. D., Teng, A. P., St. Clair, J. M., Paulot, F., Wolfe, G. M., and Wennberg, P.
 1004 O.: Rapid deposition of oxidized biogenic compounds to a temperate forest, *Proceedings of the*
 1005 *National Academy of Sciences*, 112, E392-E401, 10.1073/pnas.1418702112, 2015.
 1006 Ortega, A. M., Day, D. A., Cubison, M. J., Brune, W. H., Bon, D., de Gouw, J. A., and Jimenez, J. L.:
 1007 Secondary organic aerosol formation and primary organic aerosol oxidation from biomass-
 1008 burning smoke in a flow reactor during FLAME-3, *Atmos. Chem. Phys.*, 13, 11551-11571,
 1009 10.5194/acp-13-11551-2013, 2013.
 1010 Ortega, J., Turnipseed, A., Guenther, A. B., Karl, T. G., Day, D. A., Gochis, D., Huffman, J. A., Prenni,
 1011 A. J., Levin, E. J. T., Kreidenweis, S. M., DeMott, P. J., Tobo, Y., Patton, E. G., Hodzic, A., Cui,
 1012 Y. Y., Harley, P. C., Hornbrook, R. S., Apel, E. C., Monson, R. K., Eller, A. S. D., Greenberg, J.
 1013 P., Barth, M. C., Campuzano-Jost, P., Palm, B. B., Jimenez, J. L., Aiken, A. C., Dubey, M. K.,
 1014 Geron, C., Offenberg, J., Ryan, M. G., Fornwalt, P. J., Pryor, S. C., Keutsch, F. N., DiGangi, J.
 1015 P., Chan, A. W. H., Goldstein, A. H., Wolfe, G. M., Kim, S., Kaser, L., Schnitzhofer, R., Hansel,
 1016 A., Cantrell, C. A., Mauldin, R. L., and Smith, J. N.: Overview of the Manitou Experimental
 1017 Forest Observatory: site description and selected science results from 2008 to 2013, *Atmos.*
 1018 *Chem. Phys.*, 14, 6345-6367, 10.5194/acp-14-6345-2014, 2014.
 1019 Paulot, F., Crounse, J. D., Kjaergaard, H. G., Kroll, J. H., Seinfeld, J. H., and Wennberg, P. O.: Isoprene
 1020 photooxidation: new insights into the production of acids and organic nitrates, *Atmos. Chem.*
 1021 *Phys.*, 9, 1479-1501, 10.5194/acp-9-1479-2009, 2009a.
 1022 Paulot, F., Crounse, J. D., Kjaergaard, H. G., Kürten, A., St. Clair, J. M., Seinfeld, J. H., and Wennberg,
 1023 P. O.: Unexpected Epoxide Formation in the Gas-Phase Photooxidation of Isoprene, *Science*,
 1024 325, 730-733, 10.1126/science.1172910, 2009b.
 1025 Phinney, L., Leaitch, W. R., Lohmann, U., Boudries, H., Worsnop, D. R., Jayne, J. T., Toom-Sauntry, D.,
 1026 Wadleigh, M., Sharma, S., and Shantz, N.: Characterization of the aerosol over the sub-arctic
 1027 north east Pacific Ocean, *Deep-Sea Res Pt II*, 53, 2410-2433, DOI 10.1016/j.dsr2.2006.05.044,
 1028 2006.
 1029 Pye, H. O. T., Pinder, R. W., Piletic, I. R., Xie, Y., Capps, S. L., Lin, Y.-H., Surratt, J. D., Zhang, Z.,
 1030 Gold, A., Luecken, D. J., Hutzell, W. T., Jaoui, M., Offenberg, J. H., Kleindienst, T. E.,
 1031 Lewandowski, M., and Edney, E. O.: Epoxide Pathways Improve Model Predictions of Isoprene
 1032 Markers and Reveal Key Role of Acidity in Aerosol Formation, *Environ Sci Technol*, 47, 11056-
 1033 11064, 10.1021/es402106h, 2013.
 1034 Robinson, N. H., Hamilton, J. F., Allan, J. D., Langford, B., Oram, D. E., Chen, Q., Docherty, K., Farmer,
 1035 D. K., Jimenez, J. L., Ward, M. W., Hewitt, C. N., Barley, M. H., Jenkin, M. E., Rickard, A. R.,
 1036 Martin, S. T., McFiggans, G., and Coe, H.: Evidence for a significant proportion of Secondary

1037 Organic Aerosol from isoprene above a maritime tropical forest, *Atmos. Chem. Phys.*, 11, 1039-
1038 1050, 10.5194/acp-11-1039-2011, 2011.

1039 Saarikoski, S., Carbone, S., Decesari, S., Giulianelli, L., Angelini, F., Canagaratna, M., Ng, N. L.,
1040 Trimborn, A., Facchini, M. C., Fuzzi, S., Hillamo, R., and Worsnop, D.: Chemical
1041 characterization of springtime submicrometer aerosol in Po Valley, Italy, *Atmos. Chem. Phys.*,
1042 12, 8401–8421, doi:10.5194/acp-12-8401-2012, 2012.

1043 Sage, A. M., Weitkamp, E. A., Robinson, A. L., and Donahue, N. M.: Evolving mass spectra of the
1044 oxidized component of organic aerosol: results from aerosol mass spectrometer analyses of aged
1045 diesel emissions, *Atmos. Chem. Phys.*, 8, 1139-1152, 10.5194/acp-8-1139-2008, 2008.

1046 Schneider, J., Weimer, S., Drewnick, F., Borrmann, S., Helas, G., Gwaze, P., Schmid, O., Andreae, M.
1047 O., and Kirchner, U.: Mass spectrometric analysis and aerodynamic properties of various types of
1048 combustion-related aerosol particles, *Int J Mass Spectrom*, 258, 37-49, DOI
1049 10.1016/j.ijms.2006.07.008, 2006.

1050 Schneider, J., Freutel, F., Zorn, S. R., Chen, Q., Farmer, D. K., Jimenez, J. L., Martin, S. T.,
1051 Artaxo, P., Wiedensohler, A., and Borrmann, S.: Mass-spectrometric identification of pri15
1052 mary biological particle markers and application to pristine submicron aerosol measurements
1053 in Amazonia, *Atmos. Chem. Phys.*, 11, 11415–11429, doi:10.5194/acp-11-11415-
1054 2011, 2011.

1055 Setyan, A., Zhang, Q., Merkel, M., Knighton, W. B., Sun, Y., Song, C., Shilling, J. E., Onasch, T. B.,
1056 Herndon, S. C., Worsnop, D. R., Fast, J. D., Zaveri, R. A., Berg, L. K., Wiedensohler, A.,
1057 Flowers, B. A., Dubey, M. K., and Subramanian, R.: Characterization of submicron particles
1058 influenced by mixed biogenic and anthropogenic emissions using high-resolution aerosol mass
1059 spectrometry: results from CARES, *Atmos. Chem. Phys.*, 12, 8131-8156, 10.5194/acp-12-8131-
1060 2012, 2012.

1061 Slowik, J. G., Brook, J., Chang, R. Y. W., Evans, G. J., Hayden, K., Jeong, C. H., Li, S. M., Liggio, J.,
1062 Liu, P. S. K., McGuire, M., Mihele, C., Sjostedt, S., Vlasenko, A., and Abbatt, J. P. D.:
1063 Photochemical processing of organic aerosol at nearby continental sites: contrast between urban
1064 plumes and regional aerosol, *Atmos. Chem. Phys.*, 11, 2991-3006, 10.5194/acp-11-2991-2011,
1065 2011.

1066 Surratt, J. D., Kroll, J. H., Kleindienst, T. E., Edney, E. O., Claeys, M., Sorooshian, A., Ng, N. L.,
1067 Offenberg, J. H., Lewandowski, M., Jaoui, M., Flagan, R. C., and Seinfeld, J. H.: Evidence for
1068 organosulfates in secondary organic aerosol, *Environ Sci Technol*, 41, 517-527, Doi
1069 10.1021/Es062081q, 2007.

1070 Surratt, J. D., Chan, A. W. H., Eddingsaas, N. C., Chan, M., Loza, C. L., Kwan, A. J., Hersey, S. P.,
1071 Flagan, R. C., Wennberg, P. O., and Seinfeld, J. H.: Reactive intermediates revealed in secondary
1072 organic aerosol formation from isoprene, *Proceedings of the National Academy of Sciences*, 107,
1073 6640-6645, 10.1073/pnas.0911114107, 2010.

1074 Takegawa, N., Miyakawa, T., Kawamura, K., and Kondo, Y.: Contribution of selected dicarboxylic and
1075 omega-oxocarboxylic acids in ambient aerosol to the m/z 44 signal of an aerodyne aerosol mass
1076 spectrometer, *Aerosol Sci Tech*, 41, 418-437, Doi 10.1080/02786820701203215, 2007.

1077 Ulbrich, I. M., Canagaratna, M. R., Zhang, Q., Worsnop, D. R., and Jimenez, J. L.: Interpretation of
1078 organic components from Positive Matrix Factorization of aerosol mass spectrometric data,
1079 *Atmos Chem Phys*, 9, 2891-2918, 2009.

1080 Wang, W., Kourtchev, I., Graham, B., Cafmeyer, J., Maenhaut, W., and Claeys, M.: Characterization of
1081 oxygenated derivatives of isoprene related to 2-methyltetrols in Amazonian aerosols using
1082 trimethylsilylation and gas chromatography/ion trap mass spectrometry, *Rapid Commun Mass
1083 Sp*, 19, 1343-1351, 10.1002/rcm.1940, 2005.

1084 Weimer, S., Alfarra, M. R., Schreiber, D., Mohr, M., Prévôt, A. S. H., and Baltensperger, U.: Organic
1085 aerosol mass spectral signatures from wood-burning emissions: Influence of burning conditions
1086 and wood type, *J. Geophys. Res.*, 113, D10304, doi:10.1029/2007jd009309, 2008.

1087 Worton, D. R., Surratt, J. D., LaFranchi, B. W., Chan, A. W. H., Zhao, Y., Weber, R. J., Park, J.-H.,
1088 Gilman, J. B., de Gouw, J., Park, C., Schade, G., Beaver, M., Clair, J. M. S., Crounse, J.,
1089 Wennberg, P., Wolfe, G. M., Harrold, S., Thornton, J. A., Farmer, D. K., Docherty, K. S.,
1090 Cubison, M. J., Jimenez, J.-L., Frossard, A. A., Russell, L. M., Kristensen, K., Glasius, M., Mao,
1091 J., Ren, X., Brune, W., Browne, E. C., Pusede, S. E., Cohen, R. C., Seinfeld, J. H., and Goldstein,
1092 A. H.: Observational Insights into Aerosol Formation from Isoprene, *Environ Sci Technol*, 47,
1093 11403-11413, 10.1021/es4011064, 2013.

1094 Xu, L., Guo, H., Boyd, C. M., Klein, M., Bougiatioti, A., Cerully, K. M., Hite, J. R., Isaacman-VanWertz,
1095 G., Kreisberg, N. M., Knote, C., Olson, K., Koss, A., Goldstein, A. H., Hering, S. V., de Gouw,
1096 J., Baumann, K., Lee, S.-H., Nenes, A., Weber, R. J., and Ng, N. L.: Effects of anthropogenic
1097 emissions on aerosol formation from isoprene and monoterpenes in the southeastern United
1098 States, *Proceedings of the National Academy of Sciences*, 112, 37-42, 10.1073/pnas.1417609112,
1099 2014.

1100 Xu, L., Suresh, S., Guo, H., Weber, R. J., and Ng, N. L.: Aerosol characterization over the southeastern
1101 United States using high-resolution aerosol mass spectrometry: spatial and seasonal variation of
1102 aerosol composition and sources with a focus on organic nitrates, *Atmos. Chem. Phys.*, 15, 7307-
1103 7336, 10.5194/acp-15-7307-2015, 2015.

1104 Zhang, H., Worton, D. R., Lewandowski, M., Ortega, J., Rubitschun, C. L., Park, J.-H., Kristensen, K.,
1105 Campuzano-Jost, P., Day, D. A., Jimenez, J. L., Jaoui, M., Offenberg, J. H., Kleindienst, T. E.,
1106 Gilman, J., Kuster, W. C., de Gouw, J., Park, C., Schade, G. W., Frossard, A. A., Russell, L.,
1107 Kaser, L., Jud, W., Hansel, A., Cappellin, L., Karl, T., Glasius, M., Guenther, A., Goldstein, A.
1108 H., Seinfeld, J. H., Gold, A., Kamens, R. M., and Surratt, J. D.: Organosulfates as Tracers for
1109 Secondary Organic Aerosol (SOA) Formation from 2-Methyl-3-Buten-2-ol (MBO) in the
1110 Atmosphere, *Environ Sci Technol*, 46, 9437-9446, 10.1021/es301648z, 2012.

1111 Zhang, H., Zhang, Z., Cui, T., Lin, Y.-H., Bhathela, N. A., Ortega, J., Worton, D. R., Goldstein, A. H.,
1112 Guenther, A., Jimenez, J. L., Gold, A., and Surratt, J. D.: Secondary Organic Aerosol Formation
1113 via 2-Methyl-3-buten-2-ol Photooxidation: Evidence of Acid-Catalyzed Reactive Uptake of
1114 Epoxides, *Environmental Science & Technology Letters*, 1, 242-247, 10.1021/ez500055f, 2014.

1115
1116
1117

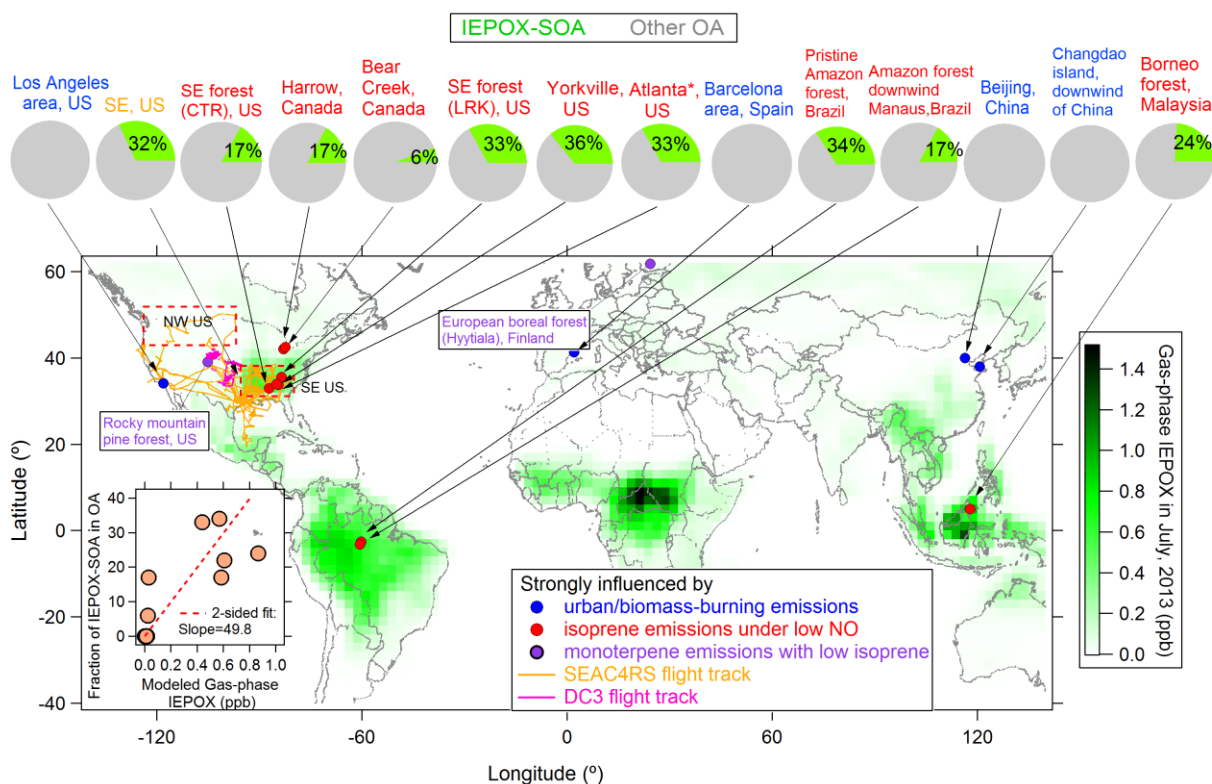
1118 **Table 1.** Datasets used in this study^a. Ranges or average plus standard deviation of $f_{C_5H_6O}$ (high resolution) and f_{82} (unit mass
1119 resolution) in different studies are also included.

Name of datasets	Time Period	Site locations and descriptions	Campaign name	Ranges or average±std.de v. $f_{C_5H_6O}$ (‰)	Ranges or average±std.de v. f_{82} (‰)	References
Studies strongly-influenced by isoprene emissions under lower NO						
SE US forest-CTR site	Jun-Jul, 2013	Centreville, AL,	SOAS	6.2±2.4	7.6±2.2	(1)
Pristine Amazon forest 2008, Brazil	Feb-Mar, 2008	Pristine rain forest site, TT34,	AMAZE-08	5.0±2.3	7.9±1.7	(2)
Amazon forest downwind Manaus, Brazil	Feb-Mar, 2014	T3 site, near Manacapuru	GoAmazon2014/5	6.9±1.6	7.1±1.0	(3)
Pristine Amazon forest 2014, Brazil	Aug-Dec, 2014	T0 site, ~150 km northeast of Manaus	GoAmazon2014/5	N/A	5.6±1.7	(4)
SE US	Aug-Sep, 2013	Aircraft measurement:	SEAC4RS	4.3±1.6	N/A	(5)
Borneo forest, Malaysia	Jun-Jul, 2008	Rain forest GAW station, Sabah, Malaysia	OP3	10±0.3	12.4±0.4	(6)
Atlanta, US	Aug-Sep, 2011	<u>Urban JST site, Atlanta, Georgia, US</u>	<u>N/A</u>	N/A	<u>3.7±1.9</u>	(7)
<u>Atlanta (JST), US</u>	<u>May, 2012</u>	<u>Urban JST site, Atlanta, Georgia, US</u>	<u>N/A</u>	<u>3.3±0.9</u>	<u>N/A</u>	<u>(8)</u>
<u>Atlanta (GT), US</u>	<u>Aug, 2012</u>	<u>Urban Georgia Tech site, Georgia, US</u>	<u>N/A</u>	<u>5.4±1.9</u>	<u>N/A</u>	<u>(8)</u>
<u>Yorkville, US</u>	<u>July, 2012</u>	<u>Rural sites, 80km northwest of JST site, Georgia, US</u>	<u>N/A</u>	<u>7.7±2.2</u>	<u>N/A</u>	<u>(8)</u>
Harrow, Canada	Jun-Jul, 2007	Harrow site, rural sites surrounded by farmland, Canada	BAQSMET	N/A	N/A	(9)
Bear Creek, Canada	Jun-Jul, 2007	Bear Creek site, wetlands area surrounded by farmland, Canada	BAQSMET	N/A	N/A	(9)
Studies strongly-influenced by monoterpene emissions						

Rocky mountain pine forest, CO, USA	Jul-Aug, 2011	Manitou Experimental Forest Observatory, CO,	BEACHON-RoMBAS	3.7±0.5	5.1±0.5	(10)
European Boreal forest, Finland	2008-2009	Hyytiala site in Pine forest, Finland	EUCAARI campaign	2.5±0.1 ^b	4.8±0.1 ^b	(11)
Studies mixed-influenced by isoprene and monoterpene emissions						
North American temperate, US	Aug-Sep, 2007	Blodgett Forest Ameriflux Site, CA, US	BEARPEX	4.0±<0.1 ^b	4.0±<0.1 ^b	(11)
Studies strongly-influenced by urban emissions						
Los Angeles area, CA, USA	May-Jun, 2010	Pasadena, US	CalNex	1.6±0.2	3.6±0.5	(12)
Beijing, China	Nov-Dec, 2010	Peking University, in NW of Beijing city, China	N/A	1.5±0.3	4.6±0.7	(13)
Changdao island, Downwind of China	Mar-Apr, 2011	Changdao island, China	CAPTAIN	1.6±0.2	3.8±0.5	(14)
Barcelona area, Spain	Feb-Mar, 2009	Montseny, Spain	DAURE	1.6±0.2	4.8±0.9	(15)
Studies of biomass-burning smokes						
BB Chamber study	Sep-Oct, 2009	Missoula, MO, USA	FLAME-3	1.9±0.6	5.9±1.4	(16)
Biomass burning plumes	Aug-Sep, 2013	All over US, aircraft measurement	SEAC4RS	1.8±0.5	N/A	(6)
Biomass burning plumes	May-Jun, 2011	All over US, aircraft measurement	DC-3	1.8±0.4	N/A	(17)
Continental plumes						
NW US	Aug-Sep, 2013	Aircraft measurement	SEAC4RS	1.7±0.3	N/A	(16)
Western US	May-Jun, 2011	Aircraft measurement	DC-3	1.9±0.6	N/A	(17)
OA from specific sources						
IEPOX-SOA from ambient PMF factors and chamber studies.				22±7	22±7	(18)
Isoprene derived non-IEPOX SOA (reaction with OH under conditions of high NO or low NO without seed not favorable for the reactive-uptake of IEPOX, reaction with NO ₃ without seed)				<3	<3	(19)

Monoterpene-derived SOA	5.5±2.0	6.7±2.0	(20)
Other SOA (not from isoprene and monoterpene)	2.2±0.9	6.1±2.1	(21)
Cooking	1.5±0.8	8.2±1.1	(22)
Coal combustion	1.4-2.0	N/A	(23)
Vehicle emission	1.1±0.6	5.1±1.1	(24)
Biomass burning	2.3±0.7	4.3±1.5	(25)
Pure chemical species	0.7±1.0	4.0±5.5	(26)

1120 a- HR-ToF-AMS was used for all the campaigns except the Atlanta, US and Pristine Amazon forest 2014, Brazil using ACSM.
1121 b- Standard error
1122 (1) This study; (2) (Chen et al., 2014); (3) (de Sá et al., 2015); (4) (Carbone et al., 2015); (5)(Liao et al., 2014) ; (6) (Robinson et
1123 al., 2011); (7) (Budisulistiorini et al., 2013); (8) (Xu et al., 2014; Xu et al., 2015) (89) (Slowik et al., 2011); (910) (Ortega et al.,
1124 2014); (101) (Robinson et al., 2011); (1112) (Hayes et al., 2013); (1213) (Hu et al., 2015); (1313) (Hu et al., 2013); (1415)
1125 (Minguillón et al., 2011); (1516) (Ortega et al., 2013); (1617) (Barth et al., 2014); (1718) (Chhabra et al., 2011; Robinson et al.,
1126 2011; Budisulistiorini et al., 2013; Chen et al., 2014; Liu et al., 2014; Kuwata et al., 2015); (1819) (Kroll et al., 2006; Ng et al.,
1127 2008; Krechmer et al., 2015); (1920) (Bahreini et al., 2005; Chen et al., 2014; Boyd et al., 2015); (2021) (Bahreini et al., 2005; Liggio
1128 et al., 2005; Chhabra et al., 2011; Loza et al., 2012); (2122) (Lanz et al., 2007; Mohr et al., 2009; He et al., 2010; Huang et al.,
1129 2010; Mohr et al., 2012; Crippa et al., 2013; Hu et al., 2015); (2223) (Hu et al., 2013; Hu et al., 2015); (2324) (Canagaratna et al.,
1130 2004; Lanz et al., 2007; Sage et al., 2008; Aiken et al., 2009; Mohr et al., 2009; Chang et al., 2011; Docherty et al., 2011; Hersey et al.,
1131 2011; Ng et al., 2011b; Coggon et al., 2012; Mohr et al., 2012; Saarikoski et al., 2012; Setyan et al., 2012; Crippa et al., 2013); (2425)
1132 (Schneider et al., 2006; Weimer et al., 2008; Aiken et al., 2009; He et al., 2010; Ng et al., 2011b; Schneider et al., 2011; Mohr et al.,
1133 2012; Saarikoski et al., 2012; Crippa et al., 2013; Hu et al., 2013; Hu et al., 2015); (2526) (Alfarra, 2004; Katrib et al., 2004; Phinney et
1134 al., 2006; Dzepina et al., 2007; Takegawa et al., 2007; Aiken et al., 2009; Li et al., 2011; Schneider et al., 2011)
1135

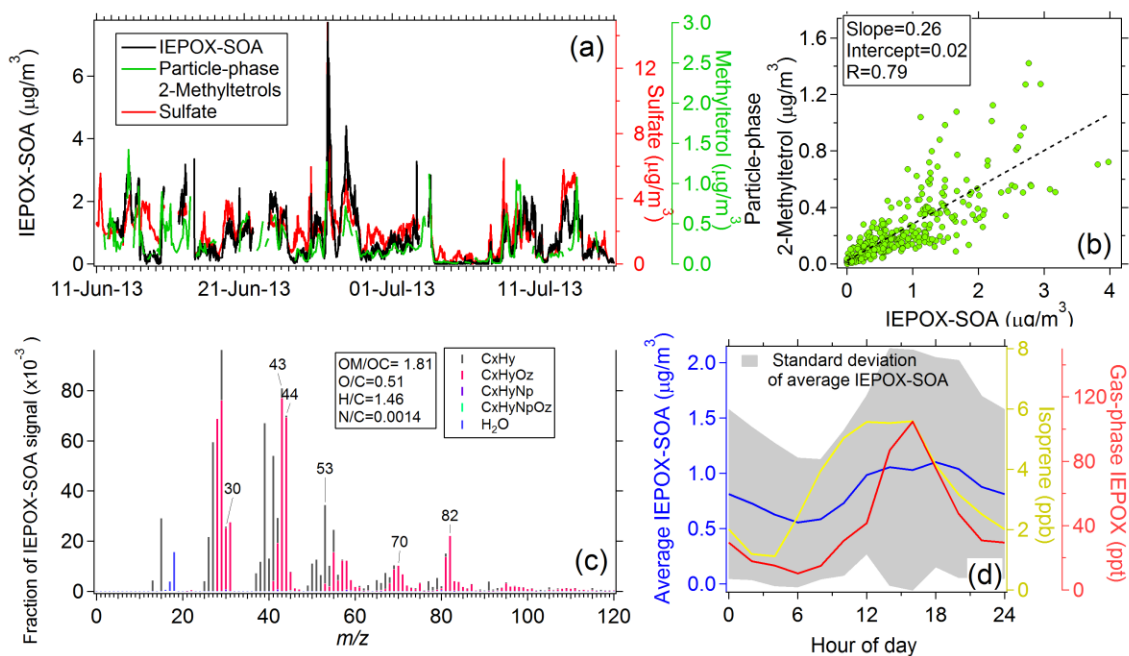


1137

1138 **Figure 1.** Locations of field campaigns used in this study. The IEPOX-SOA fractions of OA in
 1139 different studies are shown in the pie charts on the top of graph. Site names are color-coded with
 1140 site types. Detailed information these studies can be found in Table 1. Note that the Atlanta pie
 1141 chart was averaged by three urban datasets in Budisulistiorini et al. (2013) and Xu et al. (2015).
 1142 The green background is color coded with modeled global gas-phase IEPOX concentrations for
 1143 July, 2013 from the GEOS-Chem model. The insert shows as scatter plot of observed average
 1144 fraction of IEPOX-SOA in OA vs. GEOS-Chem modeled gas-phase IEPOX in various field
 1145 campaigns.

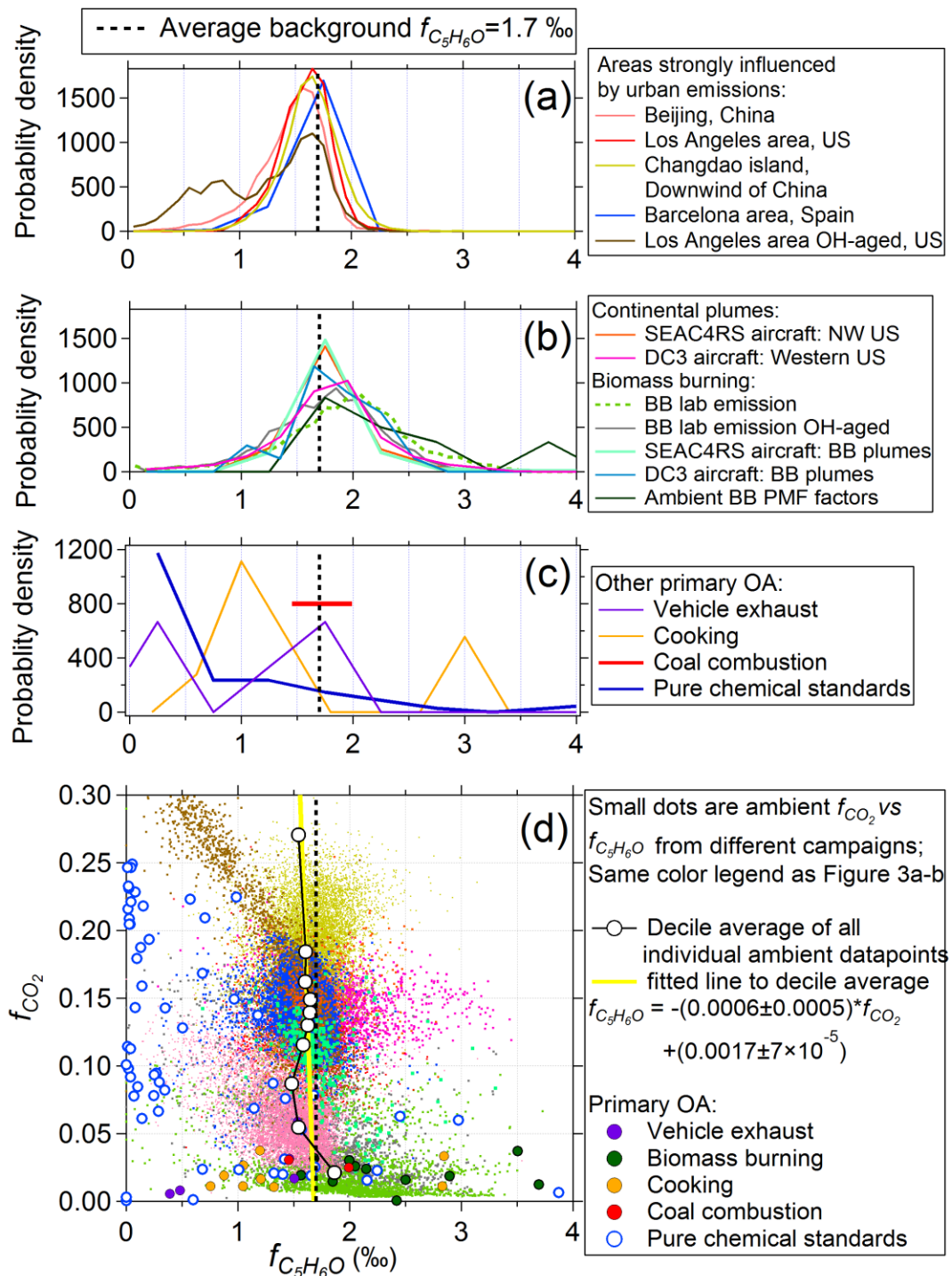
1146

1147



1148

1149 **Figure 2.** Results from the SOAS campaign in a SE US forested site. (a) Time series of IEPOX-
 1150 SOA_{PME}, sulfate and particle-phase 2-methylterols (a key IEPOX uptake product) from on-line
 1151 GC/MS; (b) Scatter plot between particle-phase 2-methylterols and IEPOX-SOA. (c) Mass
 1152 spectrum of IEPOX-SOA; (d) Diurnal cycle of IEPOX-SOA, isoprene and gas-phase IEPOX
 1153 (the latter measured by CF_3O^- CIMS).



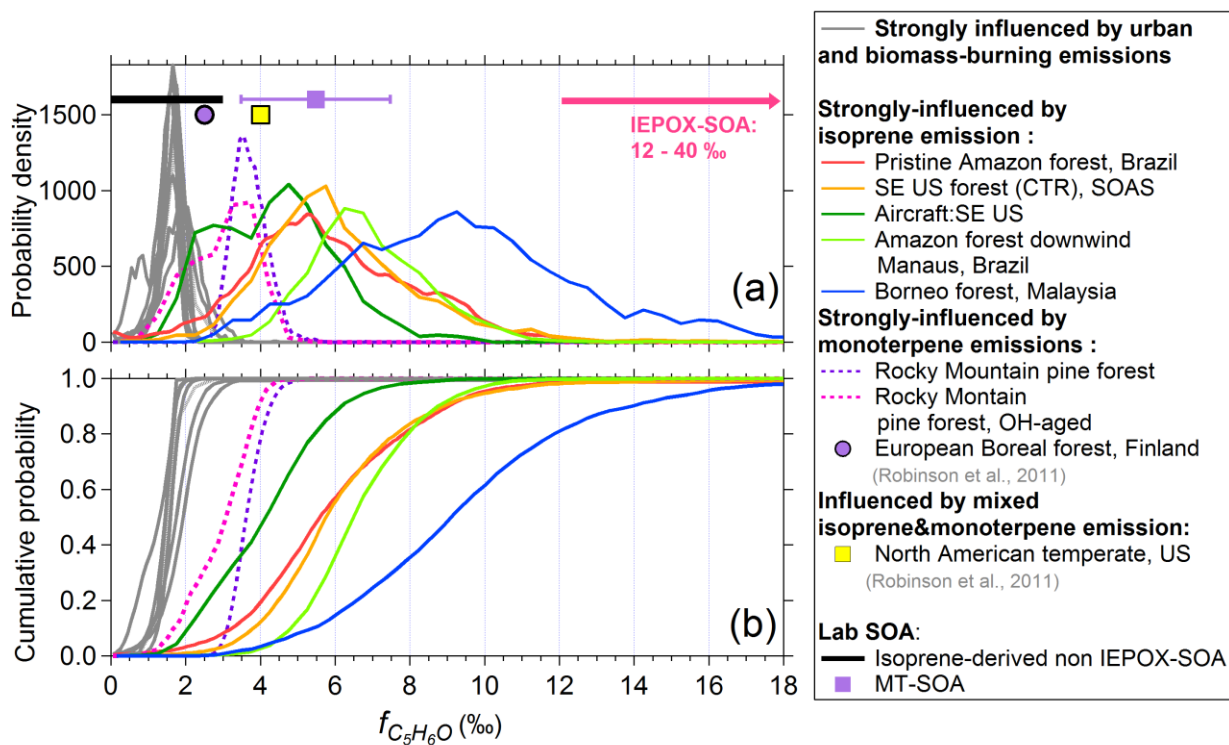
1154

1155 **Figure 3.** Probability density distributions of $f_{C_5H_6O}$ in studies (a) strongly influenced by urban
 1156 emissions; (b) continental air masses sampled from aircraft and biomass-burning emissions; (c)
 1157 other anthropogenic primary OA sources and pure chemical standards. The dashed line (1.7‰) is
 1158 the average $f_{C_5H_6O}$ in studies shown in panels (a) – (b). (d) Scatter plot of f_{CO_2} ($f_{CO_2} = CO_2^+ / OA$)

1159 vs. $f_{C_5H_6O}$ for all studies shown in panels (a) – (c), using the same color scheme. Quantile
1160 averages of $f_{C_5H_6O}$ across all studies sorted by f_{CO_2} are also shown, as is a linear regression line to
1161 the quantile points.

1162

1163

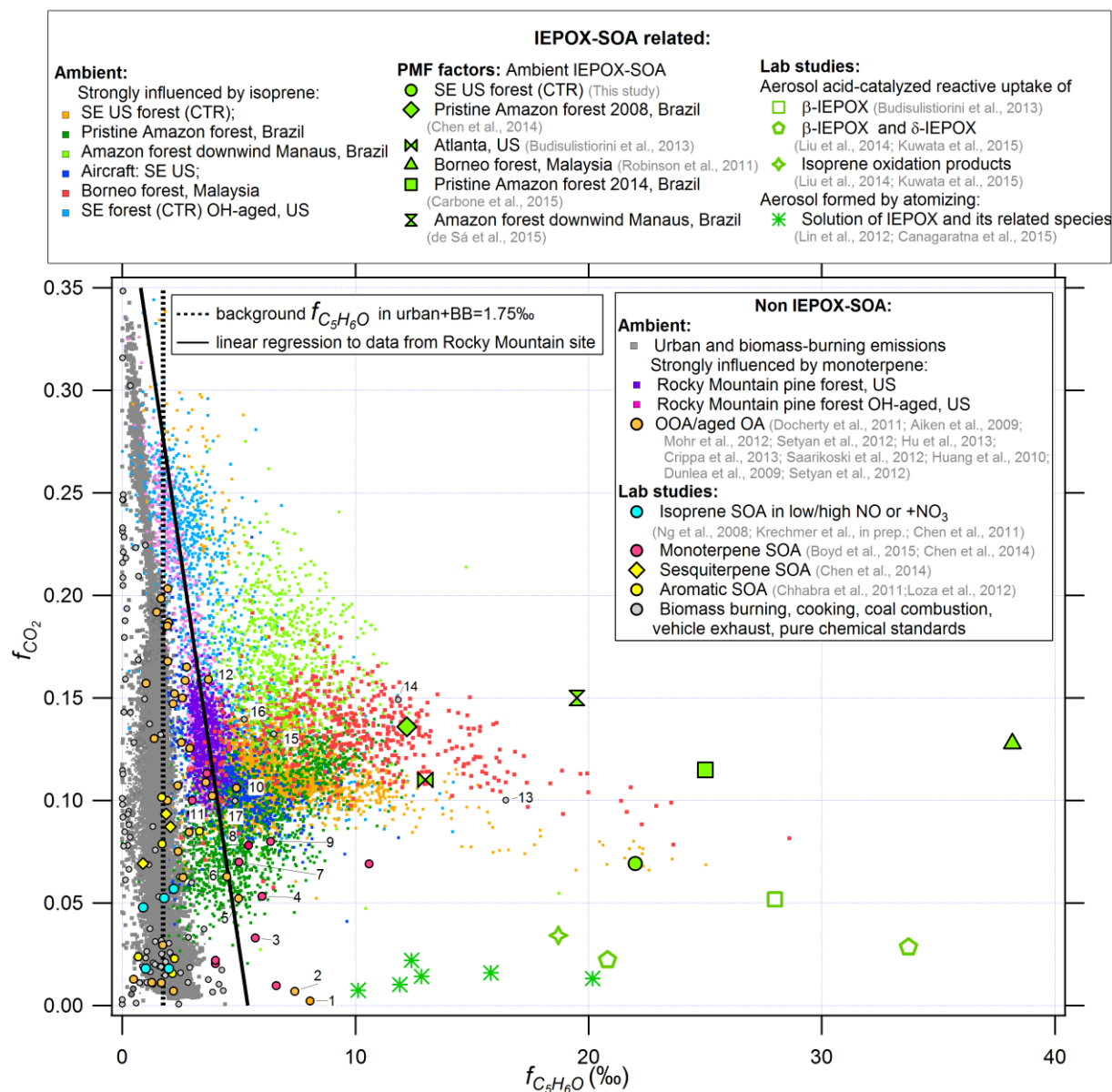


1164

1165

1166 **Figure 4.** (a) Probability density and (b) cumulative probability distributions of $f_{C_5H_6O}^{OA}$ in studies
 1167 strongly influenced by isoprene and/or monoterpene emissions. The ranges of $f_{C_5H_6O}$ from other
 1168 non IEPOX-derived isoprene-SOA and MT-SOA are also shown. The background grey lines are
 1169 from studies strongly influenced by urban and biomass-burning emissions and are the same data
 1170 from Fig. 3a – b. The arrow in Fig. 4a indicates the range of $f_{C_5H_6O}^{IEPOX-SOA}$ between 12‰ (start of
 1171 the arrow) to 40‰ which is beyond the range of x-axis scale.
 1172

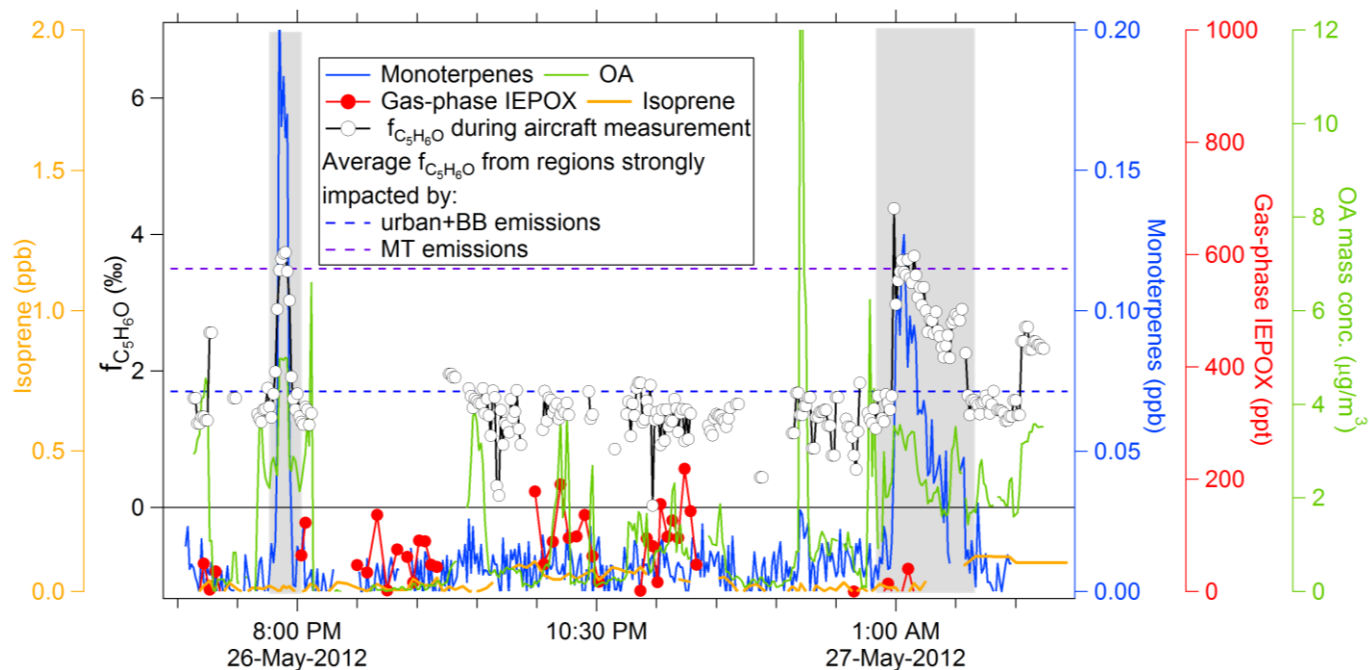
1173
1174
1175



1176
1177

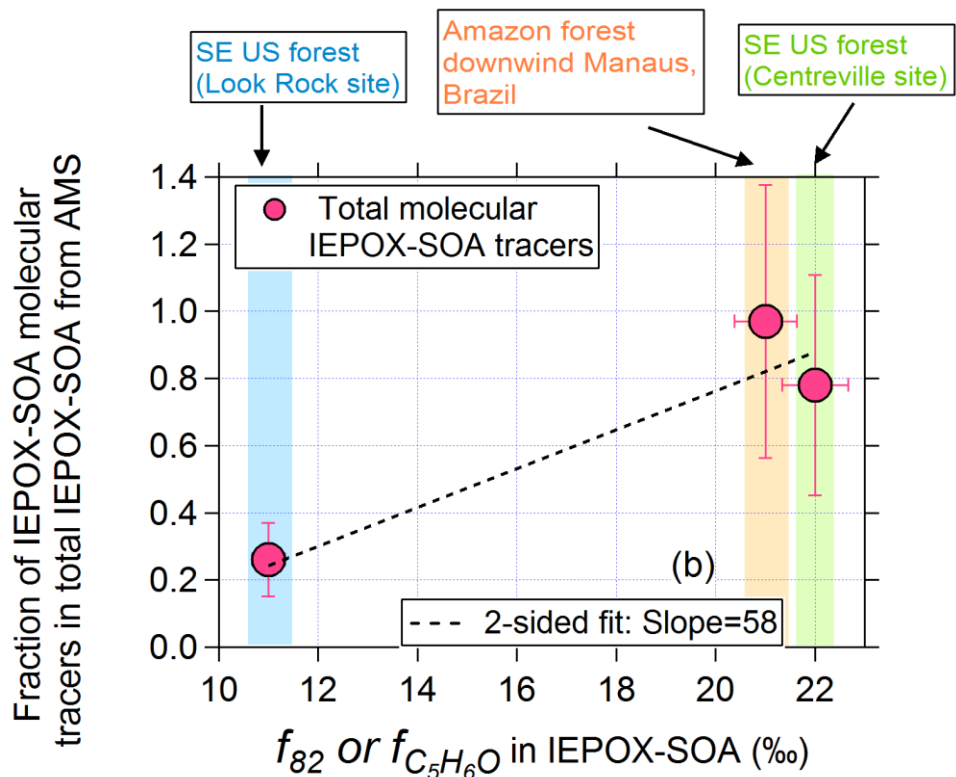
1178 **Figure 5.** Scatter plot of f_{CO_2} and $f_{C_5H_6O}$ in studies strongly by isoprene and monoterpene
 1179 emissions, as well as other OA sources. The grey dots represent background levels from studies
 1180 strongly influenced by urban and biomass-burning emissions in Fig. 3d. f_{CO_2} and $f_{C_5H_6O}$ values
 1181 from multiple sources of OA are also shown, together with IEPOX-SOA from different ambient
 1182 PMF factors and chamber studies. A linear regression line of f_{CO_2} and $f_{C_5H_6O}$ calculated from
 1183 Rocky Mountain pine forest is also displayed. We labeled some symbols with high $f_{C_5H_6O}$ in
 1184 numbers. From number 1 – 12 are all OAs with biogenic influences. Number 13 – 17 are some

1185 pure chemical standards (acids) as discussed above. For detailed information on the meaning of
 1186 the numbered symbols see supporting information Table S2.
 1187



1188
 1189 **Figure 6.** Time series of ambient $f_{C_5H_6O}^{OA}$, gas-phase IEPOX, monoterpenes and isoprene in DC3
 1190 aircraft measurement. Average $f_{C_5H_6O}$ from regions strongly impacted by urban and biomass-
 1191 burning emissions and MT emissions are also shown for reference. Two areas with grey
 1192 background indicate the periods when $f_{C_5H_6O}^{OA}$ increases when monoterpene concentrations
 1193 increase.

1194



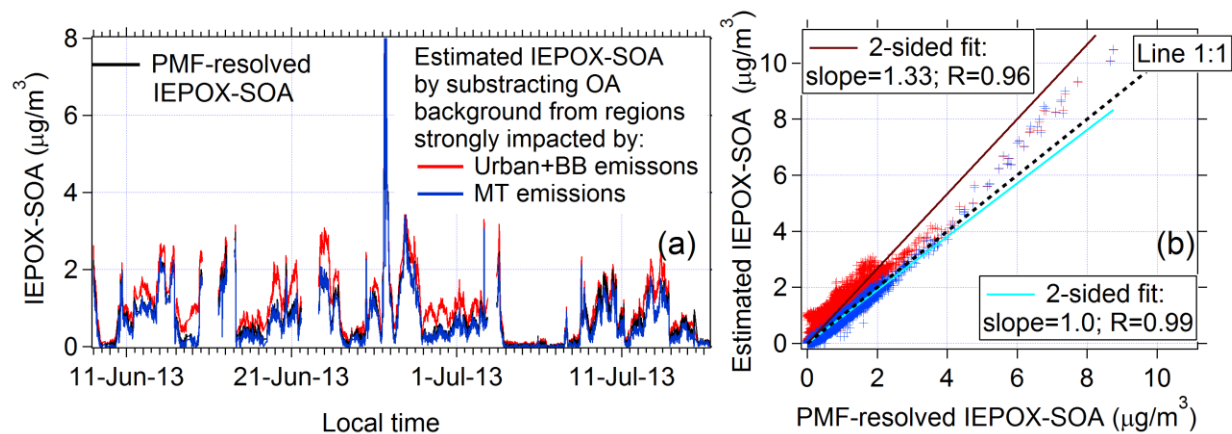
1195

1196 **Figure 7.** Scatter plot between total IEPOX-SOA molecular tracers (=Methyltetrol + C5-alkene
 1197 triols +IEPOX-derived organosulfates and dimers) in IEPOX-SOA_{PMF} and $f_{82}^{IEPOX-SOA}$. Besides
 1198 SOAS, the other two datasets in the graph are from Budisulistiorini et al. (2015) and de Sá et
 1199 al.(2015). The relative uncertainty value estimated for the SOAS study is applied to the other two
 1200 datasets.

1201

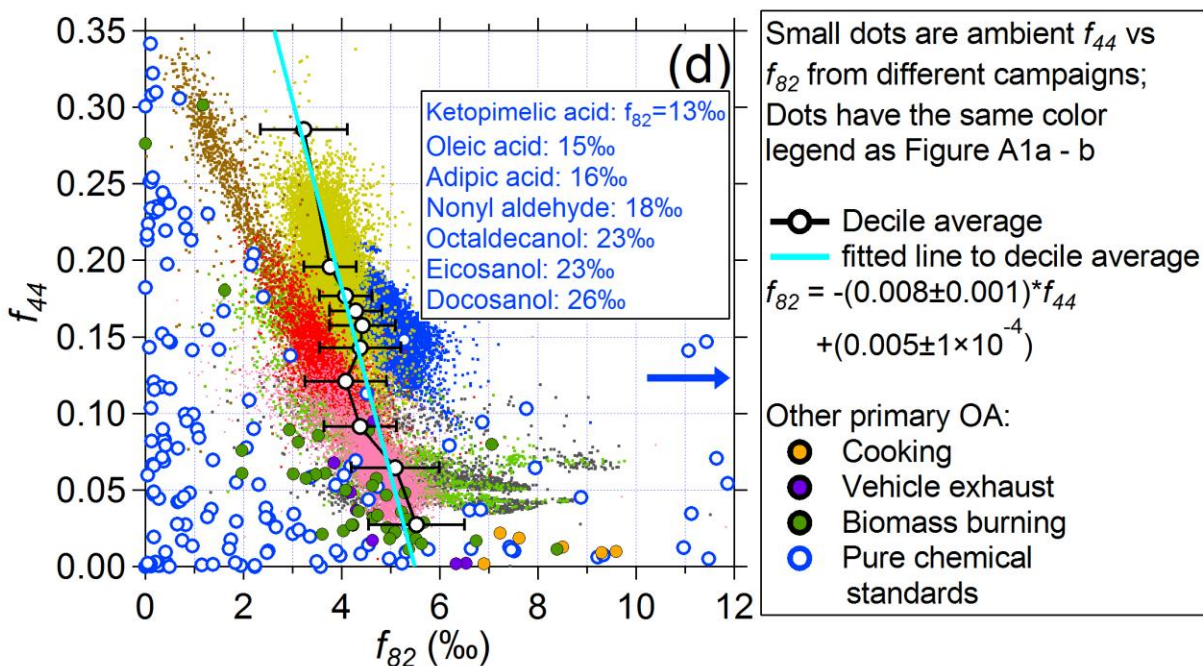
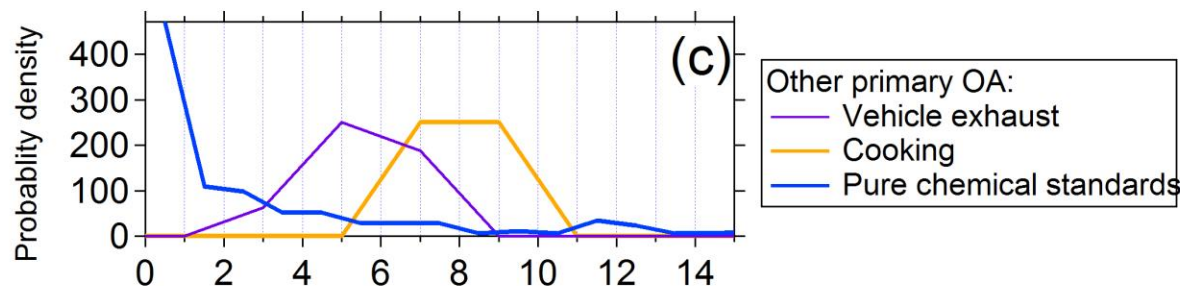
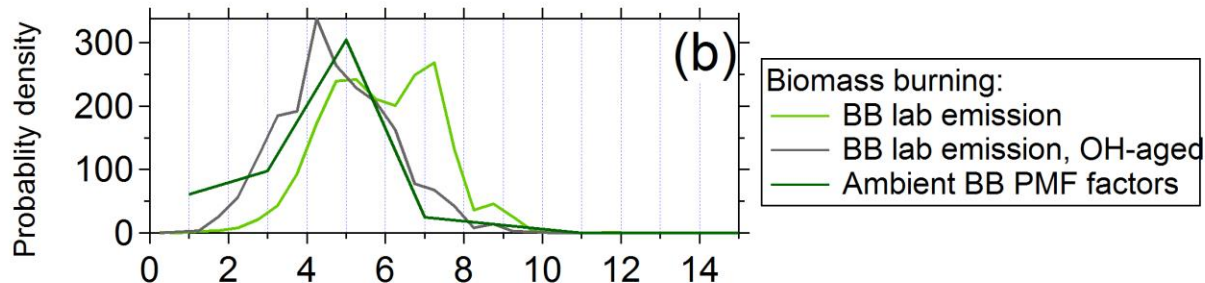
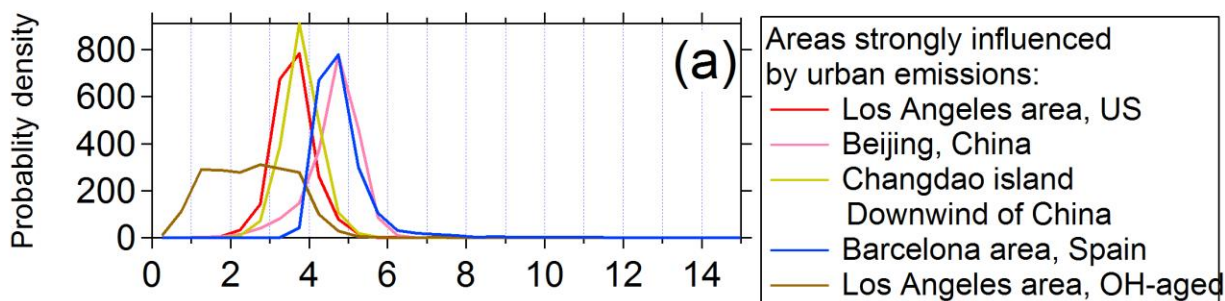
1202

1203



1204

1205 **Figure 8.** (a) Time series of IEPOX-SOA_{PMF} and estimated IEPOX-SOA based on $\text{C}_5\text{H}_6\text{O}^+$ for
1206 the SOAS data in SE US. Two different estimates of background $\text{C}_5\text{H}_6\text{O}^+$ are shown, using
1207 values from regions strongly impacted by urban and biomass-burning emissions vs. regions with
1208 strong monoterpene emissions. (b) Scatter plot of estimated IEPOX-SOA vs. IEPOX-SOA_{PMF}.
1209 Note that the largest IEPOX-SOA plume on 26-Jun-13 had a slightly higher $f_{\text{C}_5\text{H}_6\text{O}}^{\text{OA}}$ of 24%,
1210 resulting in a slight overestimation of IEPOX-SOA for those data points.

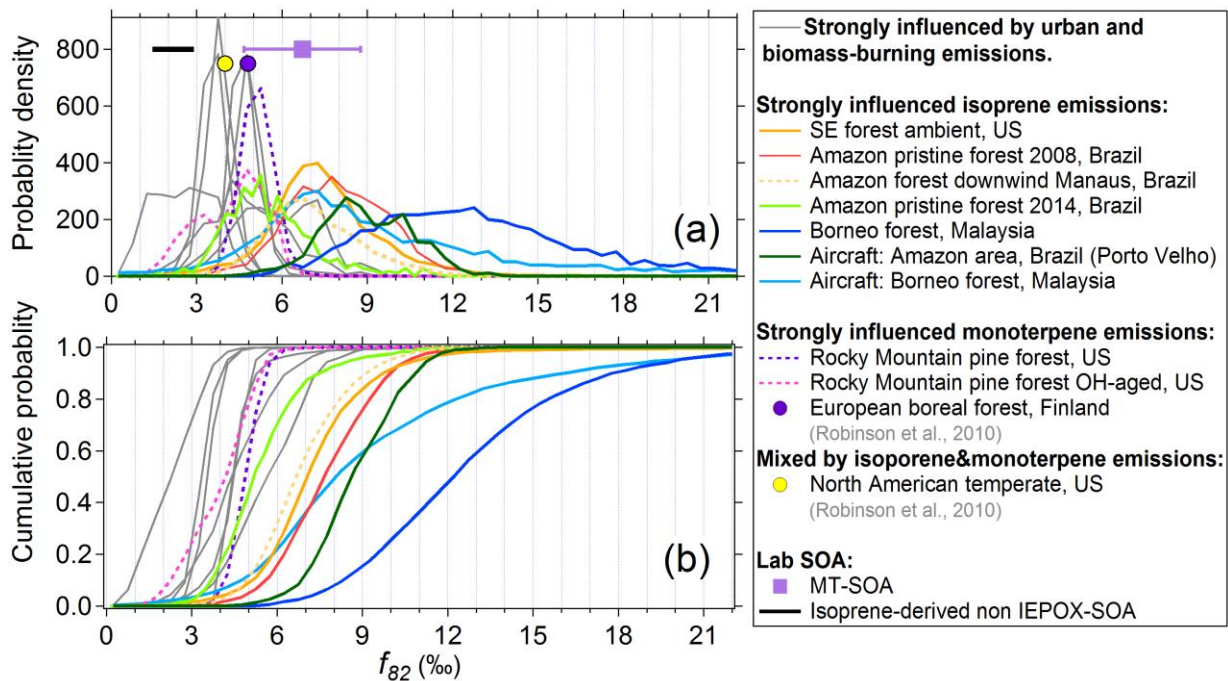


1212 **Figure A1.** Probability density distributions of f_{82} in studies (a) strongly influenced by urban
1213 emissions; (b) biomass-burning emissions; (c) other anthropogenic primary OA sources and pure
1214 chemical standards. Several pure chemical species showing higher f_{82} between 15 – 30‰ are
1215 labeled with arrow. (d) Scatter plot of f_{44} ($f_{44}=m/z\ 44/OA$) vs. f_{82} for all studies shown in panels
1216 (a) – (c), using the same color scheme. Quantile averages of f_{82} across all studies sorted by f_{44}
1217 are also shown, as is a linear regression line to the quantile points.

1218

1219

1220

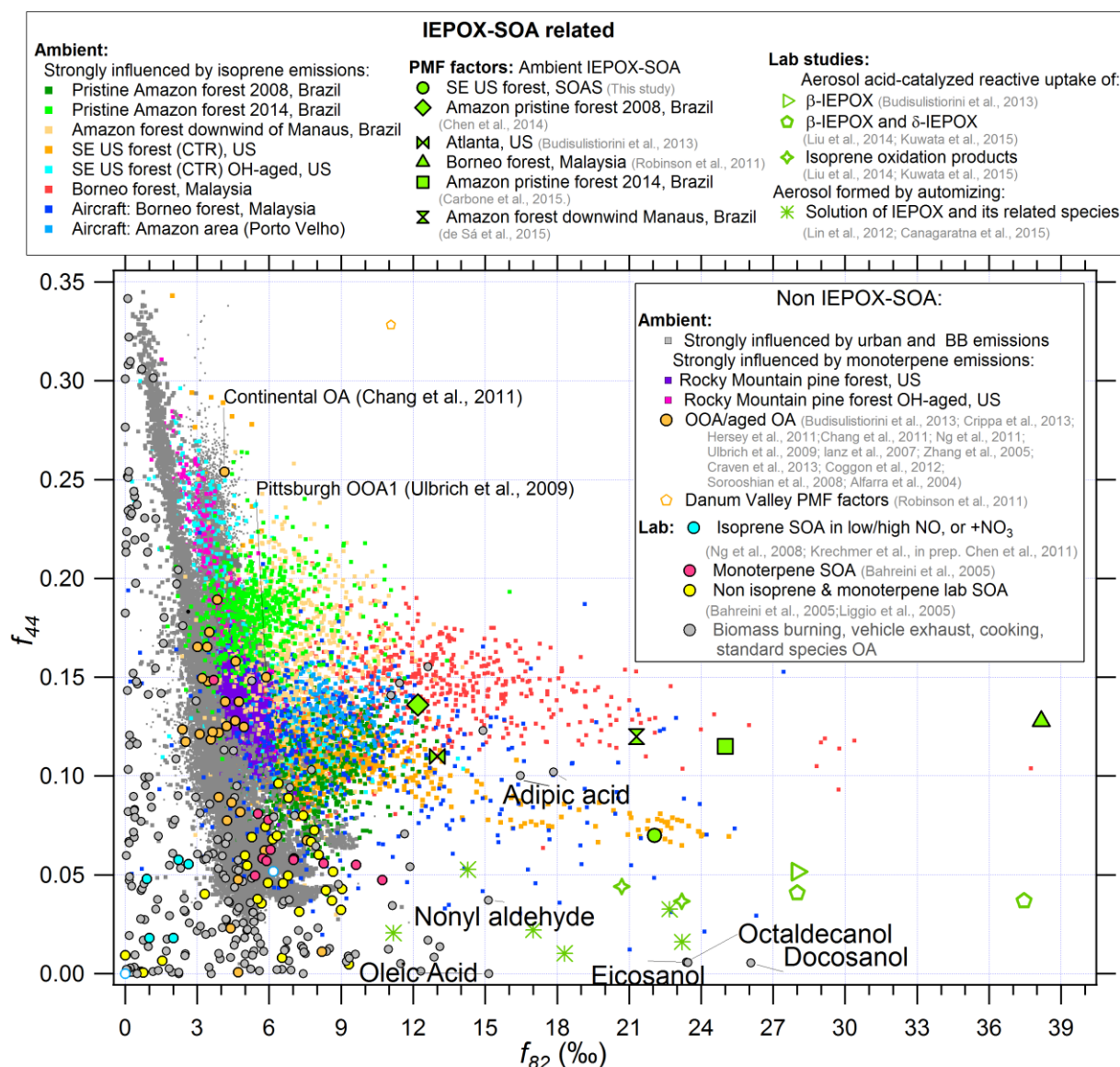


1221

1222 **Figure A2.** (a) Probability density and (b) cumulative probability distributions of f_{82} in studies
 1223 strongly influenced by isoprene and/or monoterpene emissions. The ranges of f_{82} from other non
 1224 IEPOX-derived isoprene-SOA and MT-SOA are also shown. The background grey lines are
 1225 from studies strongly influenced by urban and biomass-burning emissions and are the same data
 1226 from Fig. A1a – b.

1227

1228

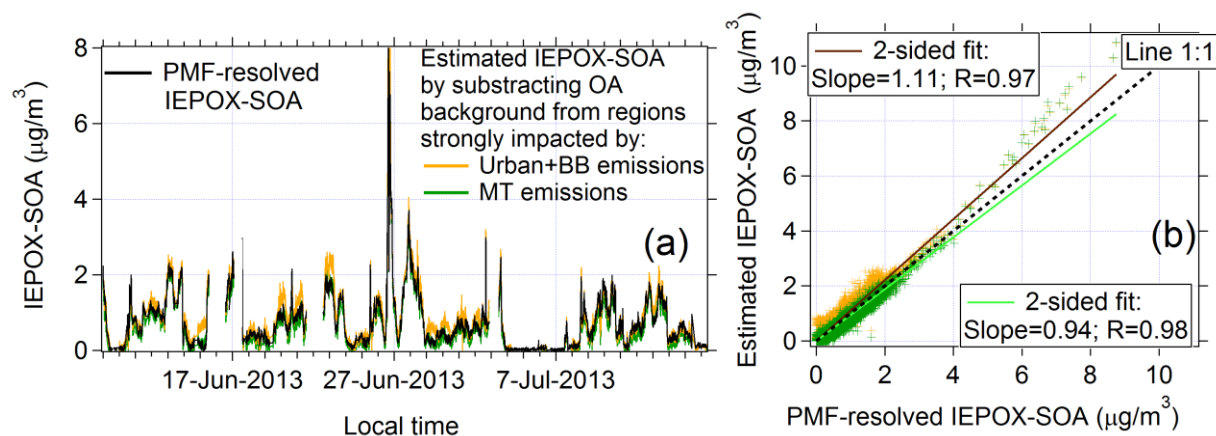


1229
 1230 **Figure A3.** Scatter plot of f_{44} and f_{82} in studies strongly by isoprene and monoterpene
 1231 emissions, as well as other OA sources. The grey dots represent background levels from studies
 1232 strongly influenced by urban and biomass-burning emissions in Fig. A1d. f_{44} and f_{82} values
 1233 from multiple sources of OA (Jimenez-Group, 2015) are also shown, together with IEPOX-SOA
 1234 from different ambient PMF factors and chamber studies.
 1235

1236

1237

1238



1239

1240 **Figure A4.** (a) Time series of IEPOX-SOA_{PMF} and estimated IEPOX-SOA based on m/z 82 for
1241 the SOAS-CTR data in SE US forest. Two different estimates of background m/z 82 are shown,
1242 using values from regions strongly impacted by urban and biomass-burning emissions vs.
1243 regions with strong monoterpene emissions. (b) Scatter plot of estimated IEPOX-SOA vs.
1244 IEPOX-SOA_{PMF}. Note that the largest IEPOX-SOA plume ($> 4 \mu\text{g m}^{-3}$) on 26-Jun-13 had a
1245 slightly higher f_{82}^{OA} of 24%, resulting in a slight overestimation of IEPOX-SOA for those data
1246 points.

1247

1248

1 **The Supporting information of “Characterization of a Real-Time Tracer for Isoprene**
2 **Epoxydiols-Derived Secondary Organic Aerosol (IEPOX-SOA) from Aerosol Mass**
3 **Spectrometer Measurements”**

4 Weiwei Hu^{1,2}, Pedro Campuzano-Jost^{1,2}, Brett B. Palm^{1,2}, Douglas A. Day^{1,2}, Amber M.
5 Ortega^{1,3}, Patrick L. Hayes^{1,2*}, Jordan E. Krechmer^{1,2}, Qi Chen^{4,5}, Mikinori Kuwata^{4,6}, Yingjun
6 Liu⁴, Suzane S. de Sá⁴, Karena McKinney⁴, Scot T. Martin⁴, Min Hu⁶, Sri Hapsari
7 Budisulistiorini⁷, Matthieu Riva⁷, Jason D. Surratt⁷, Jason M. St. Clair^{8**,***}, Gabriel Isaacman-
8 Van Wertz⁹, Lindsay D. Yee⁹, Allen H. Goldstein^{9,10}, Samara Carbone¹¹, Joel F. de Brito¹¹

9 Paulo Artaxo¹¹, Joost de A. Gouw^{1,2,12}, Abigail Koss^{2,12}, Armin Wisthaler^{13,14}, Tomas
10 Mikoviny¹³, Thomas Karl¹⁵, Lisa Kaser^{16,14}, Werner Jud¹⁴, Armin Hansel¹⁴, Kenneth S.
11 Docherty¹⁷, M. Lizabeth Alexander¹⁸, Niall H. Robinson^{19****}, Hugh. Coe¹⁹, James D. Allan^{19,20},
12 Manjula R. Canagaratna²¹, Fabien Paulot^{22,23}, and Jose L. Jimenez^{1,2}.

13 1 Cooperative Institute for Research in Environmental Sciences, University of Colorado,
14 Boulder, CO, USA

15 2 Department of Chemistry and Biochemistry, University of Colorado, Boulder, CO, USA

16 3 Department of Atmospheric and Oceanic Sciences, University of Colorado, Boulder, CO, USA

17 4 School of Engineering and Applied Sciences and Department of Earth and Planetary Sciences,
18 Harvard University, Cambridge, MA, USA

19 5 State Key Joint Laboratory of Environmental Simulation and Pollution Control, College of
20 Environmental Sciences and Engineering, Peking University, Beijing, China

21 6 Earth Observatory of Singapore, Nanyang Technological University, Singapore 7 Department
22 of Environmental Sciences and Engineering, Gillings School of Global Public Health, The
23 University of North Carolina at Chapel Hill, Chapel Hill, NC, USA

24 8 Division of Geological and Planetary Sciences, California Institute of Technology, Pasadena,
25 CA, USA

26 9 Department of Environmental Science, Policy, and Management, University of California,
27 Berkeley, CA, USA

28 10 Department of Civil and Environmental Engineering, University of California, Berkeley, CA,
29 USA

30 11 Department of Applied Physics, University of Sao Paulo, Sao Paulo, Brazil

31 12 NOAA Earth System Research Laboratory, Boulder, CO, USA

32 13 Department of Chemistry, University of Oslo, Oslo, Norway

33 14 Institute for Ion Physics and Applied Physics, University of Innsbruck, Innsbruck, Austria

34 15 Institute of Atmospheric and Cryospheric Sciences, University of Innsbruck, Innsbruck, Austria

35 16 Atmospheric Chemistry Division (ACD), National Center for Atmospheric Research,
36 Boulder, CO, USA

37 17 Alion Science and Technology, Research Triangle Park, NC, USA

38 18 Environmental Molecular Sciences Laboratory, Pacific Northwest National Laboratory,
39 Richland, WA, USA

40 19 School of Earth, Atmospheric and Environmental Sciences, University of Manchester, UK

41 20 National Centre for Atmospheric Science, University of Manchester, UK

42 21 Aerodyne Research, Inc., Billerica, MA, USA

43 22 NOAA Geophysical Fluid Dynamics Laboratory, Princeton, NJ, USA

44 23 Program in Atmospheric and Oceanic Sciences, Princeton University, Princeton, NJ, USA.

45 *Now at: Department of Chemistry, Université de Montréal, Montréal, QC, Canada
46 ** Now at: Atmospheric Chemistry and Dynamics Laboratory, NASA Goddard Space Flight
47 Center, Greenbelt, MD, USA
48 *** Now at: Joint Center for Earth Systems Technology, University of Maryland Baltimore
49 County, Baltimore, MD, USA.
50 **** Now at: Met Office, Exeter, UK

| 51

52

Table S1. Pearson's correlation coefficients (R) between time series of organic ions and the PMF IEPOX-SOA factor for the SOAS study (SE US forest).

Ion Formula	Ion mass	Correlation coefficient (R)
Ions with R > 0.8		
C ₅ H ₆ O ⁺	82.0419	0.97
C ₅ H ₅ O ⁺	81.034	0.95
C ₄ H ₅ ⁺	53.0391	0.90
C ₄ H ₆ O ⁺	70.0419	0.88
C ₃ H ₇ O ₂ ⁺	75.0446	0.87
C ₃ H ₅ O ⁺	57.034	0.84
C ₄ H ₆ ⁺	54.047	0.84
CH ₃ O ⁺	31.0184	0.83
C ₄ H ₇ O ₂ ⁺	87.0446	0.83
C ₃ H ₆ ⁺	42.047	0.82
C ₄ H ₂ ⁺	50.0157	0.82
C ₅ H ₈ O ⁺	84.0575	0.82
C ₄ H ₅ O ⁺	69.034	0.82
C ₄ H ⁺	49.0078	0.82
C ₃ H ₃ ⁺	39.0235	0.82
C ₂ H ₃ ⁺	27.0235	0.81
C ₃ H ⁺	37.0078	0.80
C ₂ H ₅ ⁺	29.0391	0.80
C ₄ H ₃ ⁺	51.0235	0.80
C ₃ H ₂ ⁺	38.0157	0.80
C ₃ H ₅ ⁺	41.0391	0.80
CH ₂ O ⁺	30.0106	0.80
Ions with lowest R		
CHNO ⁺	43.0058	-0.37
CNO ⁺	41.998	-0.12
CN ⁺	26.0031	-0.11
Other common used ions in AMS		
C ₂ H ₃ O ⁺	43.0184	0.72
C ₃ H ₇ ⁺	43.0548	0.57
CO ₂ ⁺	43.9898	0.66
C ₃ H ₃ O ⁺	55.0184	0.72
C ₄ H ₇ ⁺	55.0548	0.68
C ₂ H ₄ O ₂ ⁺	60.0211	0.60

53

54

55

56 **Table S2.** Description of spectra which have higher $f_{C_5H_6O}$ than background $f_{C_5H_6O}$, labeled by
 57 number in Fig. 5.

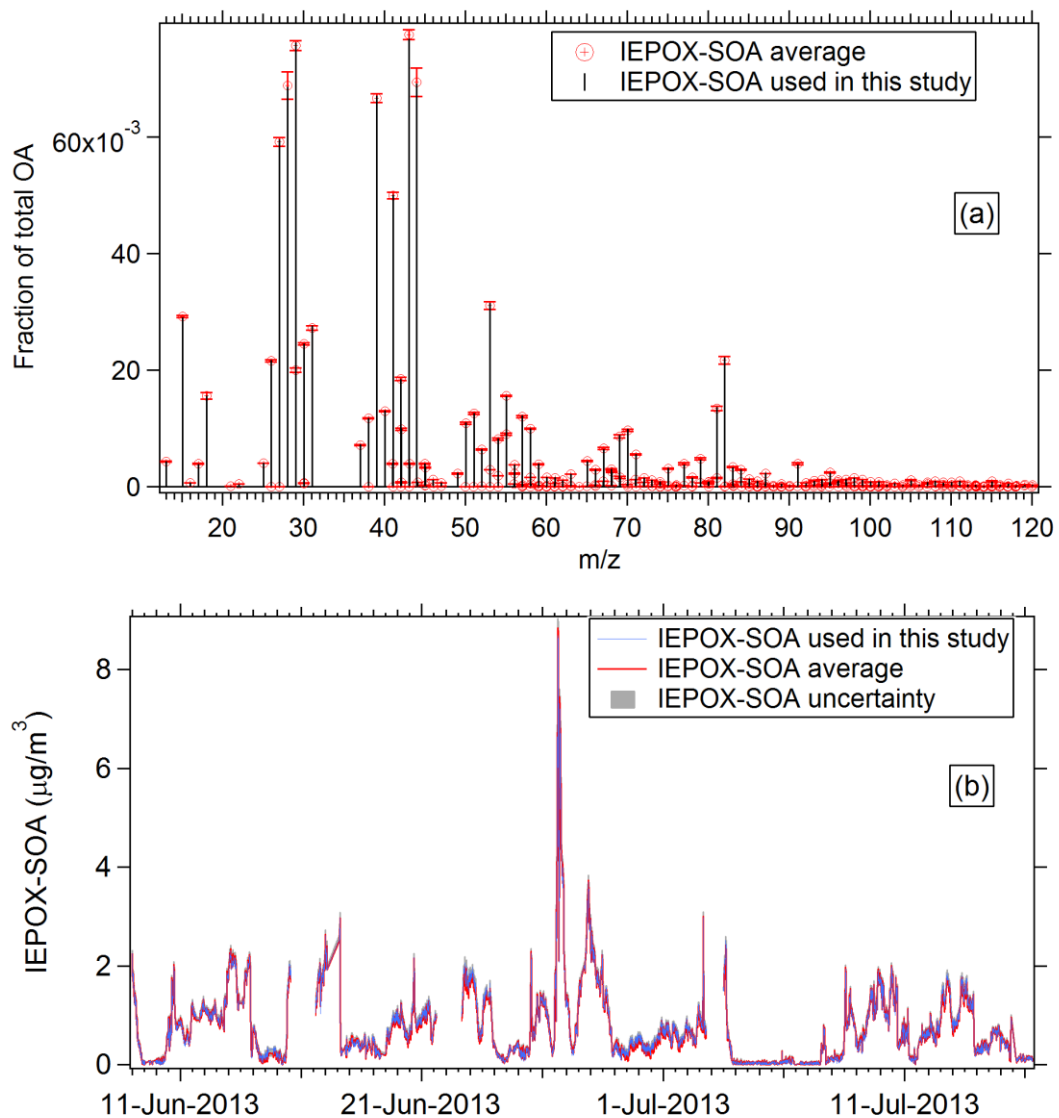
Index	Spectra name	Description of spectra sources	References
1	HOA ^a from CARES campaign	Isoprene emission influenced, aerosol is neutralized	(Setyan et al., 2012)
2	OA from CA Central Valley	Isoprene emission influenced, aerosol is slightly acidic.	(Dunlea et al., 2009)
3	NO ₃ + Δ-Carene reaction in Chamber	Biogenic SOA	Chamber study in CU
4	Ozonolysis α-terpene in Chamber	Biogenic SOA	(Chhabra et al., 2010)
5	SV-OOA ^b from SOAR	Slight biogenic influence	(Docherty et al., 2011)
6	SV-OOA from Paris summer campaign	Not mentioned in study, however, forests around the sampling site.	(Crippa et al., 2013)
7	NO ₃ + Δ-Carene reaction in Chamber	Biogenic SOA	Chamber study in CU
8	SV-OOA from SOAS	Isoprene and monoterpene influenced	This study
	NO ₃ + Δ-Carene reaction in Chamber	Biogenic SOA	Chamber study in CU
10	MO-OOA ^c in CARES campaign	Urban SOA with isoprene emission-influenced	(Setyan et al., 2012)
11	SV-OOA in MILAGRO	Urban SOA	(Aiken et al., 2009; Ulbrich et al., 2009)
12	LV-OOA in Paris summer	Urban-background SOA, forests around the sampling site.	(Crippa et al., 2013)
13	Adipic acid	Pure chemical OA standards	(Canagaratna et al., 2015)
14	3-Hydroxy-3-Methylglutaric Acid	Pure chemical OA standards	(Canagaratna et al., 2015)
15	4-ketopimelic acid	Pure chemical OA standards	(Canagaratna et al., 2015)
16	5-Oxoazelaic acid	Pure chemical OA standards	(Canagaratna et al., 2015)
17	Gamma ketopimelic acid dilactone	Pure chemical OA standards	(Canagaratna et al., 2015)

58 ^aHOA=Hydrocarbon-like OA

59 ^bSV-OOA=Semi-volatile oxygenated OA

60 ^cMO-OOA=More-oxidized oxygenated OA

61



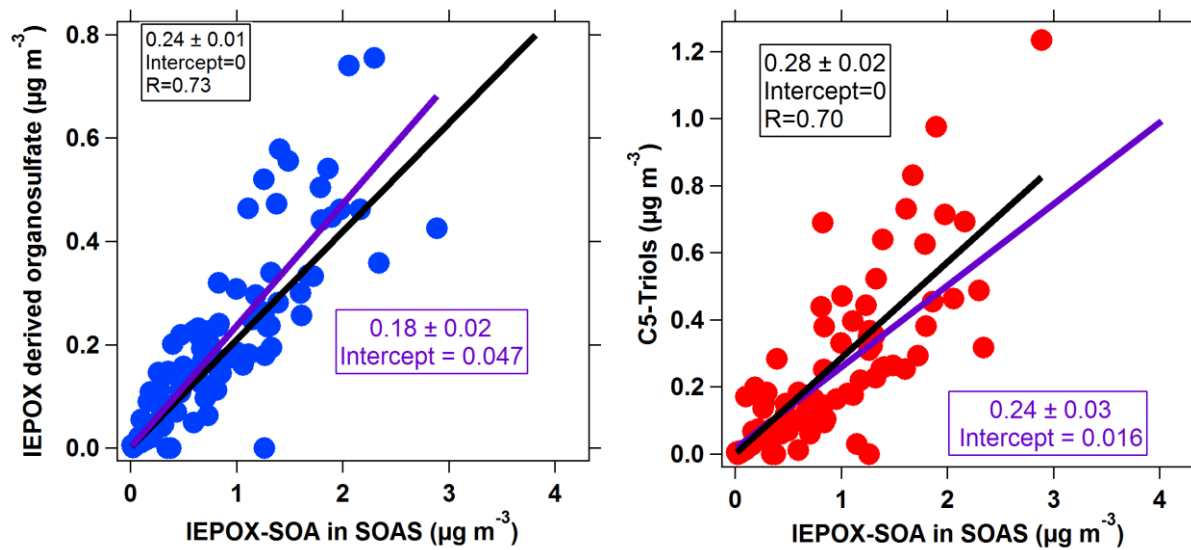
62

63 **Figure S1.** Results from bootstrapping analysis of the 4-factor solution of the SOAS dataset.
 64 Average IEPOX-SOA, with standard deviation, are shown for IEPOX-SOA (a) mass spectrum
 65 and (b) time series.

66

67

68

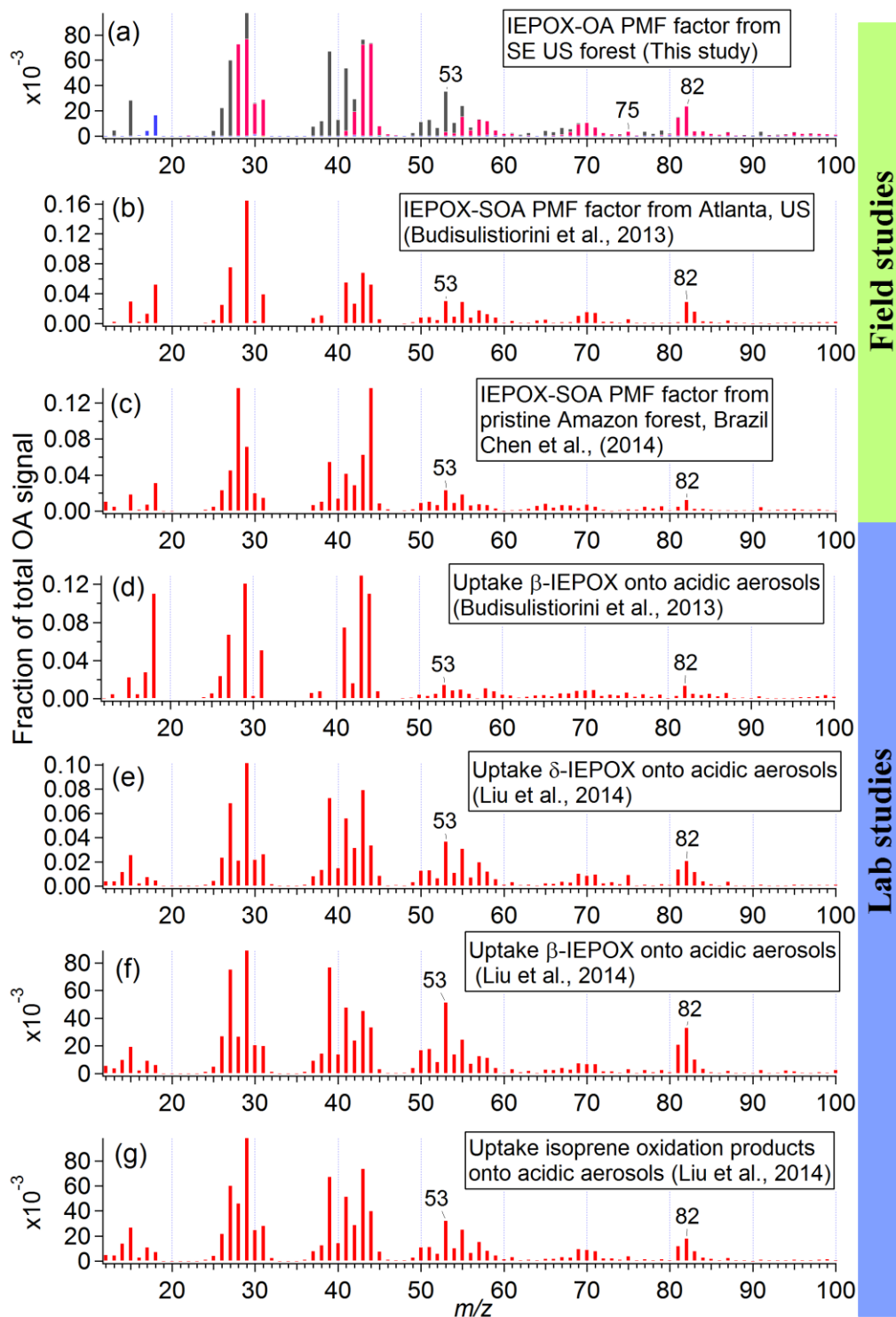


69

70 **Figure S2.** Scatter plots between IEPOX-derived organosulfate and C5-triols vs IEPOX-SOA_{PMF}
 71 in the SOAS study. The IEPOX-derived organosulfate and C5-triols were measured in GC/MS
 72 and LC/MS analysis of filter extracts (Lin et al., 2014; Budisulistiorini et al., 2015).

73

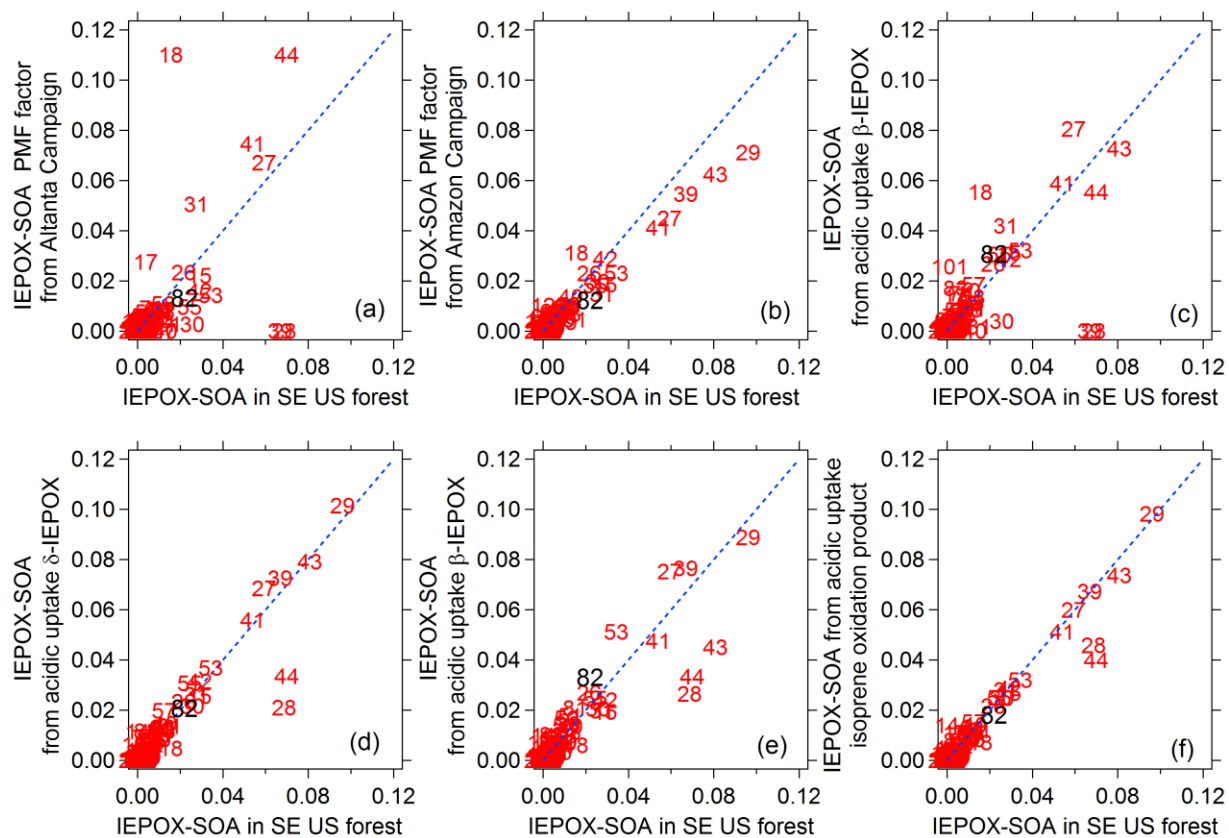
74



75

76 **Figure S3.** Mass spectra of IEPOX-SOA from different studies. Panel (a) – (c) are the results
 77 from field studies. Panel (d) – (g) are the results from lab studies.

78



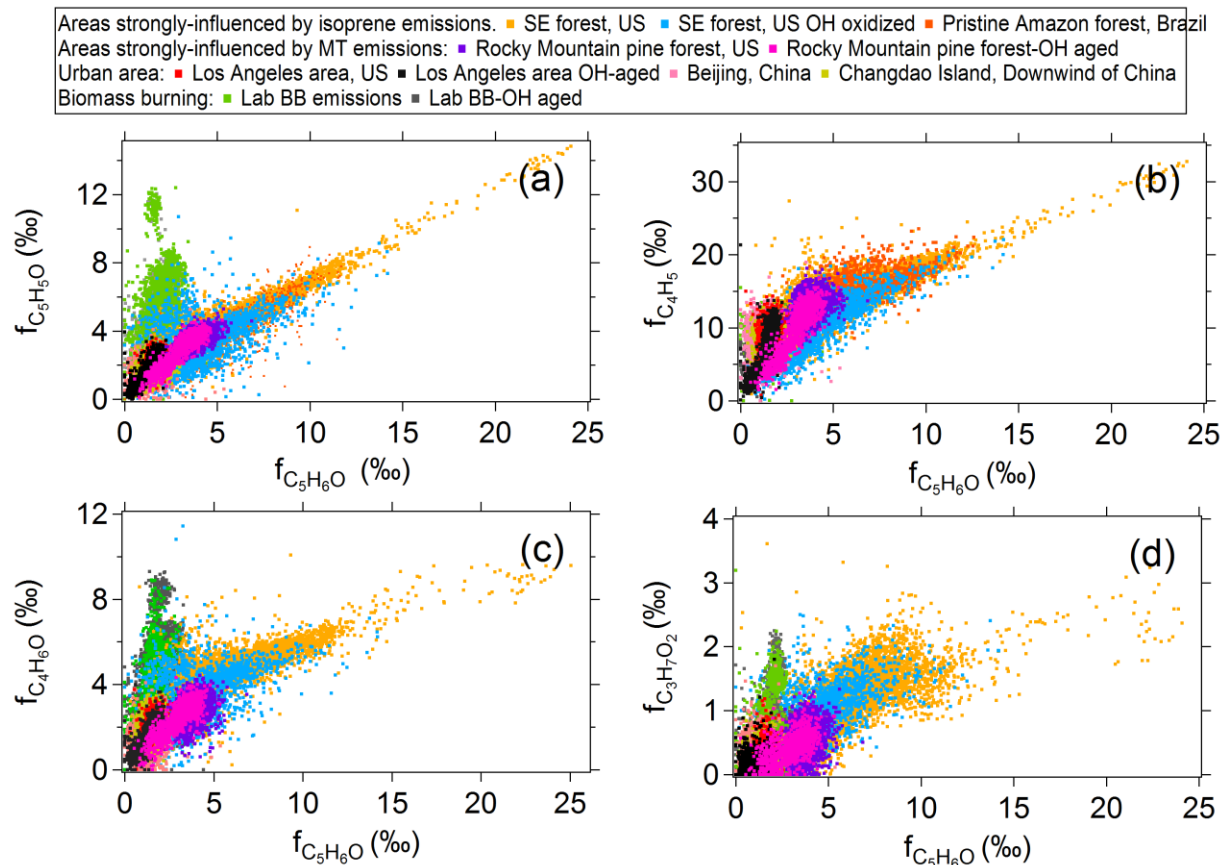
80

81 **Figure S4.** Scatter plots of IEPOX-SOA spectra in other studies vs IEPOX-SOA spectrum from
 82 this study (SOAS, SE US forest). The spectra on the y-axes are in the same order as Figures S1
 83 (b) to (g).

84

85

86



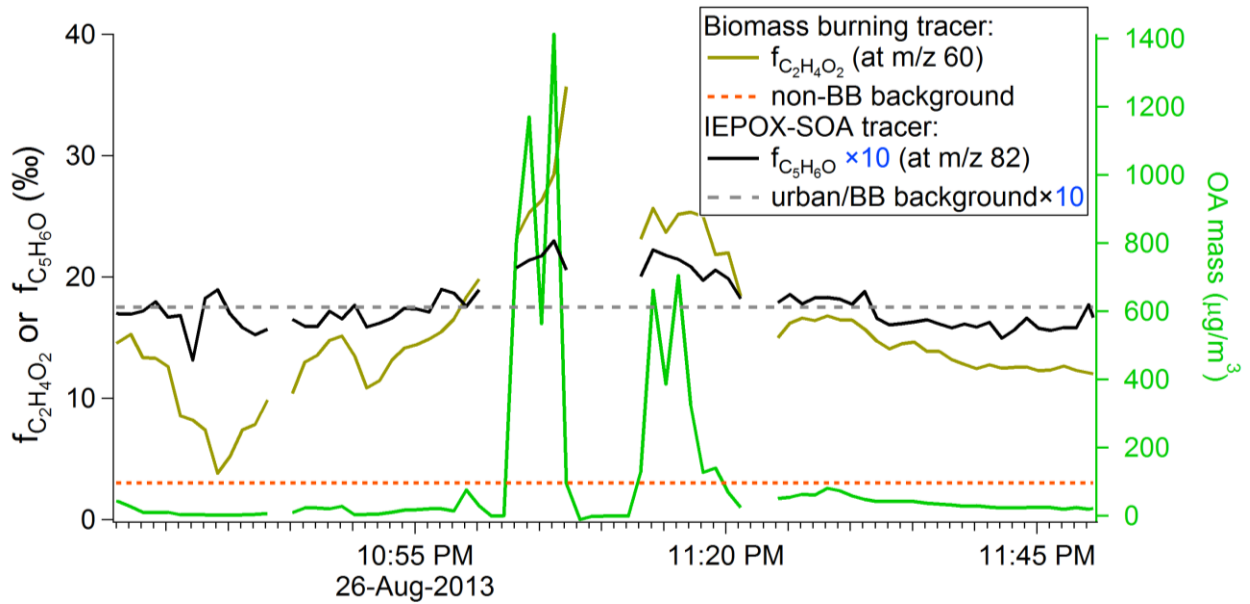
87

88 **Figure S5.** Scatter plots of abundance of ions versus $f_{C_5H_6O}^{OA}$ obtained in different studies: (a)
 89 $f_{C_5H_5O}^{OA}$, (b) $f_{C_4H_5}^{OA}$, (c) $f_{C_4H_6O}^{OA}$, and (d) $f_{C_3H_7O_2}^{OA}$. Compared to $f_{C_5H_6O}^{OA}$, $f_{C_4H_5}^{OA}$, $f_{C_4H_6O}^{OA}$, and $f_{C_5H_5O}^{OA}$ have
 90 high background levels in urban and biomass-burning emissions. The signal to noise of
 91 $f_{C_3H_7O_2}^{OA}$ measured in AMS is very low.

92

93

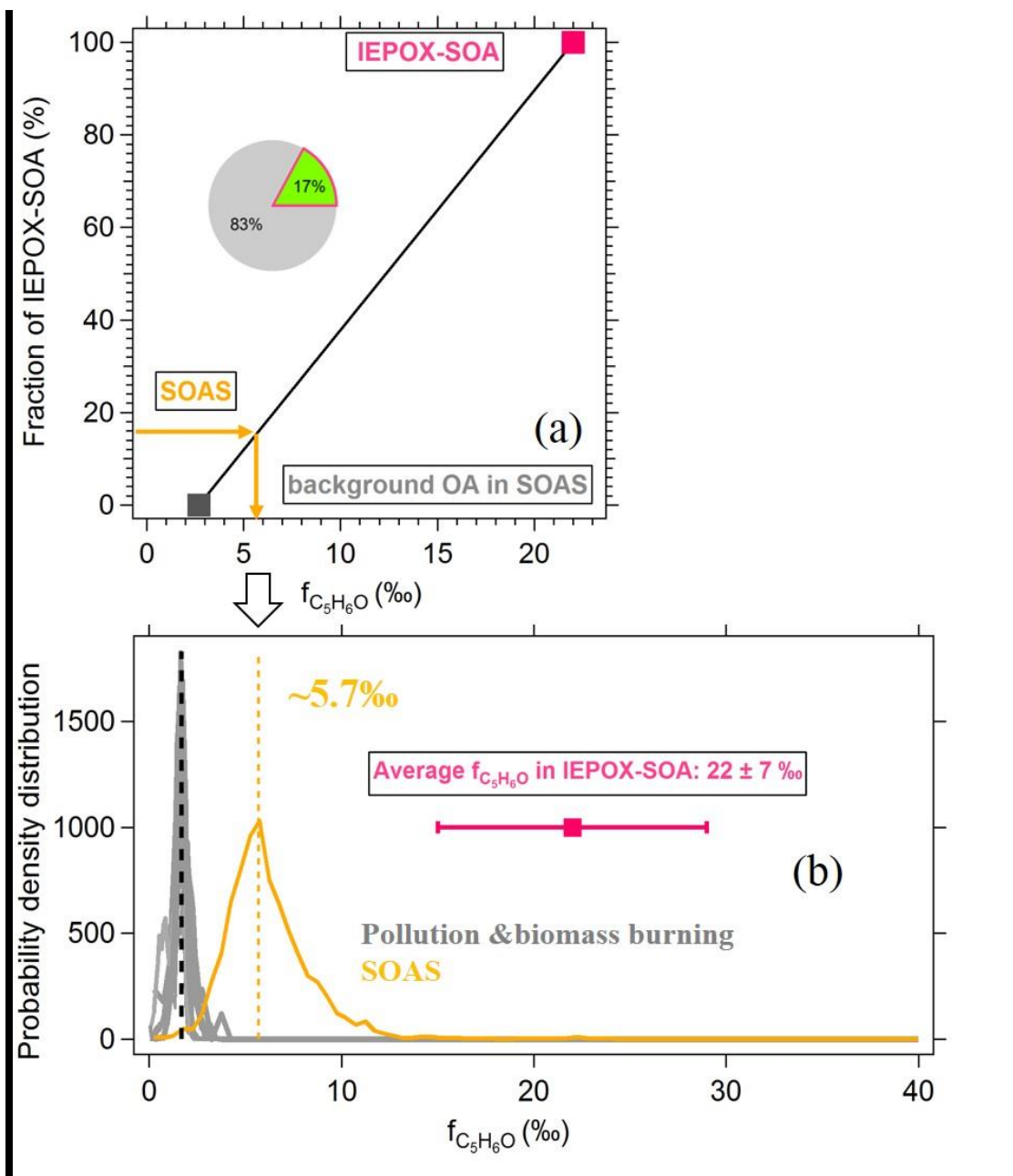
94



95

96 **Figure S6.** Time series of OA mass concentration, and of tracers for IEPOX-SOA ($f_{C_5H_6O}$) and
97 biomass-burning ($f_{C_2H_4O_2}$, m/z 60.0211) compared to their respective backgrounds on the
98 research flight on Aug 26, 2013 during the SEAC4RS campaign. The biomass-burning tracer
99 indicates extensive fire influence during this period, while the IEPOX-SOA tracer stays at
100 background levels across widely varying OA concentrations.

101



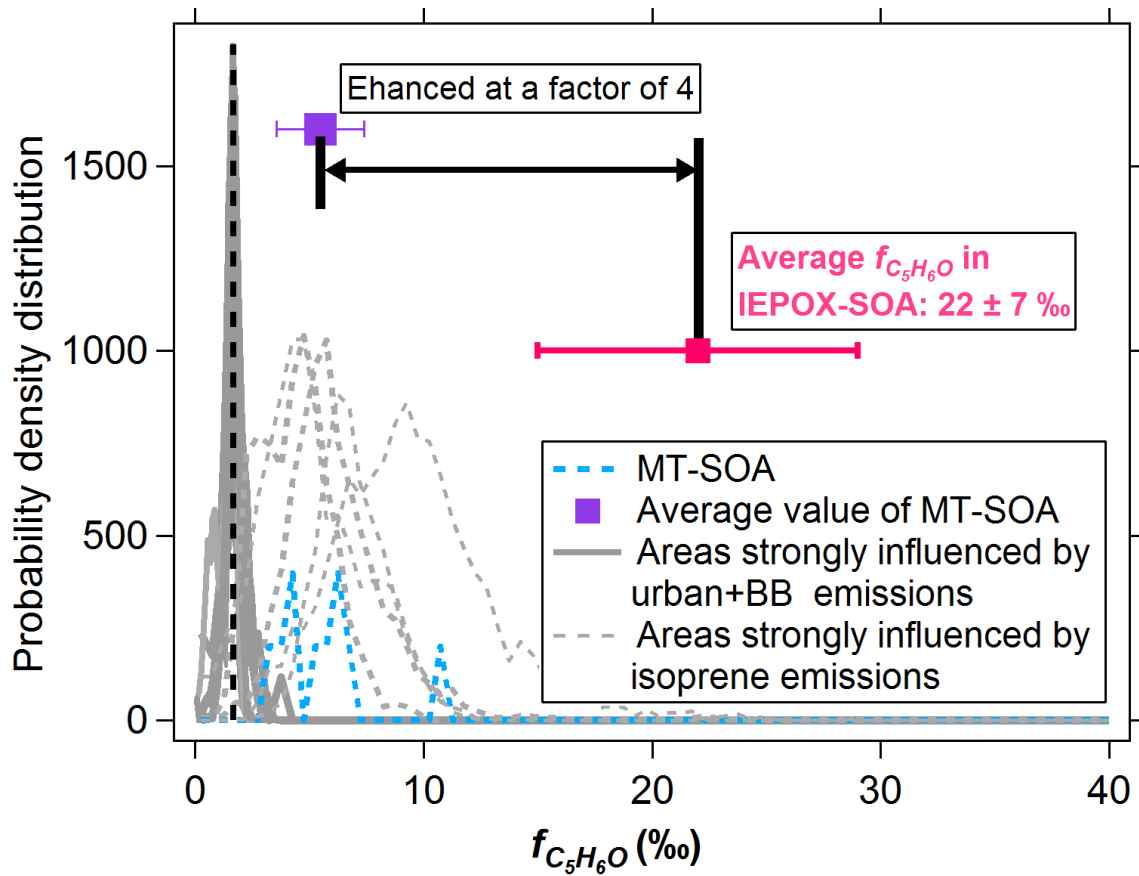
102

103 **Figure S7.** Schematic of the estimation method of IEPOX-SOA based on ambient $f_{C_5H_6O}$. (a)
 104 Fraction of IEPOX-SOA in total OA vs ambient $f_{C_5H_6O}^{OA}$ (b) probability distribution of $f_{C_5H_6O}^{OA}$ in
 105 SOAS and in background studies. The average background of $f_{C_5H_6O}^{OA}$ -from SOAS-CTR should
 106 be between the $f_{C_5H_6O}$ from urban and biomass burning emissions (~ 1.7 ‰) and $f_{C_5H_6O}$ strongly
 107 influenced by monoterpene emissions, which we can use 3.7‰ from Rocky Mountain site as
 108 representative value. An average $f_{C_5H_6O}^{OA}$ value of 2.7‰ was used here for the background $f_{C_5H_6O}^{OA}$
 109 for SOAS-CTR. $f_{C_5H_6O}$ in IEPOX-SOA_{PMF} is 22‰. Two values corresponding to 0% and 100%
 110 IEPOX-SOA in total OA, are shown as two square points shown in Fig. S5a. If we assume the
 111 air containing these two types of OA are mixed with each other, then we can draw a line between

112 these two points in Fig. S5a. Ambient $f_{C_5H_6O}^{OA}$ partially contributed by IEPOX-SOA should vary
113 along this line. Take SOAS as an example, 17% of OA in SOAS was composed by IEPOX-SOA,
114 then it corresponds to an expected average $f_{C_5H_6O}^{OA}$ of ~5.7 %, which is consistent with what was
115 observed (Fig. S5b). The peak of the probability distribution of $f_{C_5H_6O}^{OA}$ in SOAS is around 5.7%.

116

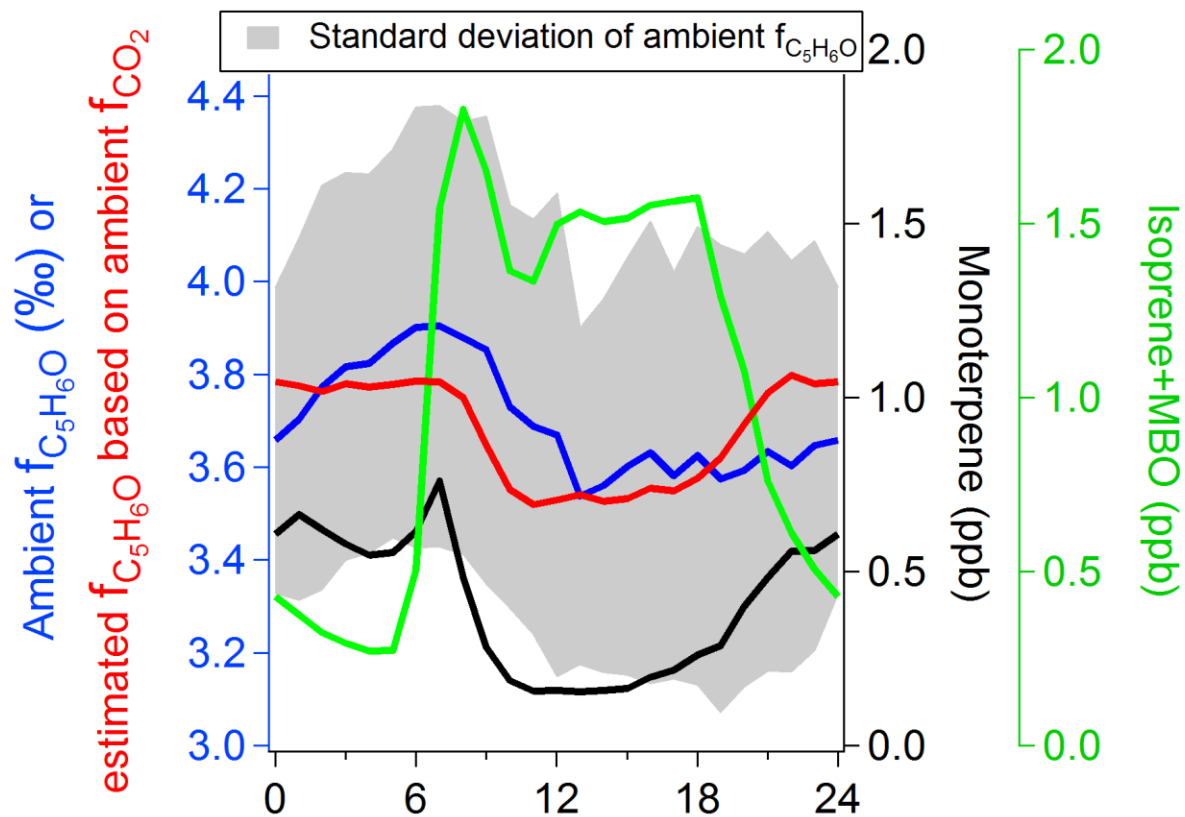
117



118

119 **Figure S8** Comparison between $f_{C_5H_6O}^{MT-SOA}$ and $f_{C_5H_6O}^{IEPOX-SOA}$, $f_{C_5H_6O}^{OA}$ from areas strongly
 120 influenced by urban + biomass burning and isoprene emissions are also shown.

121



122

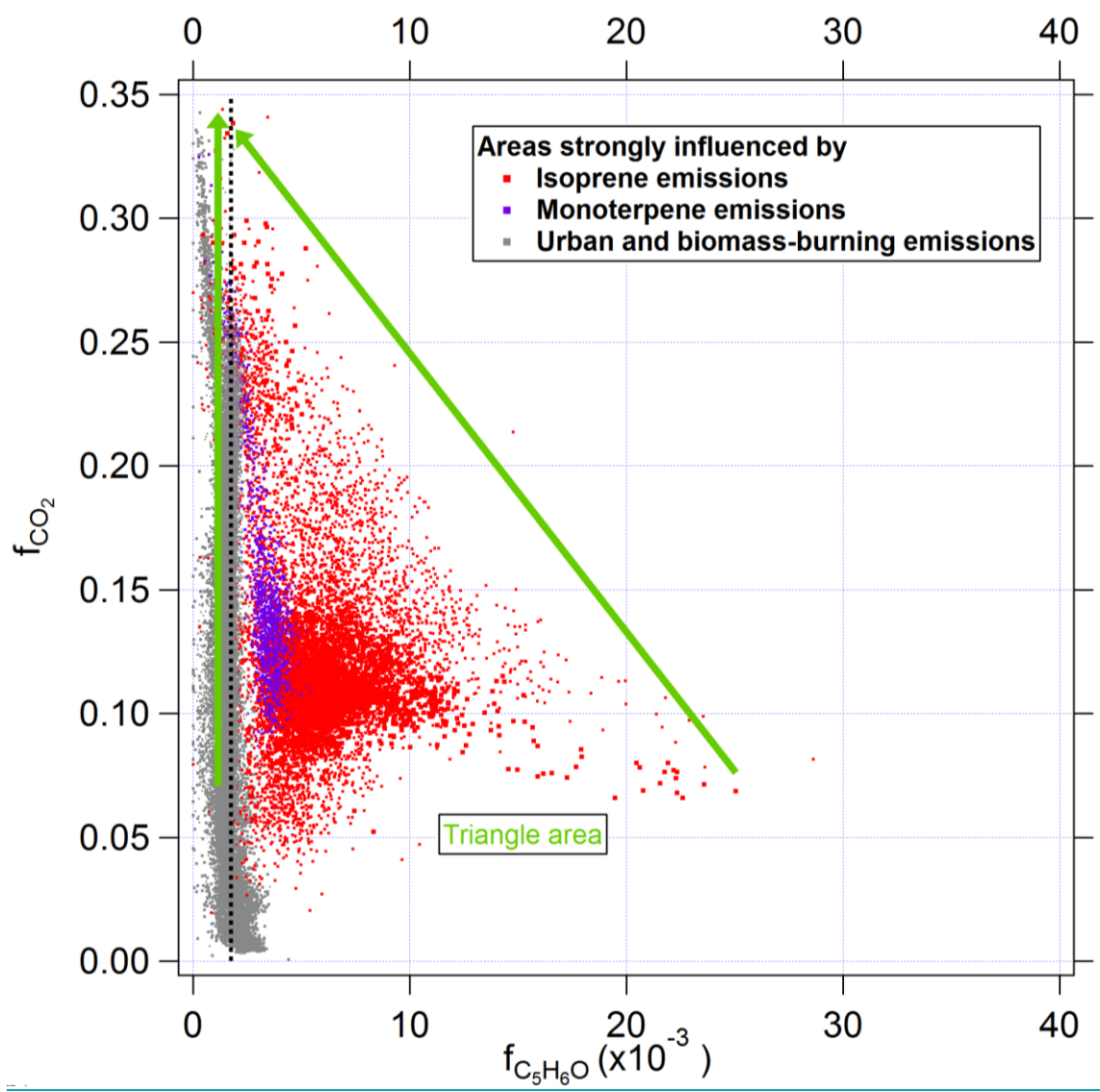
123 **Figure S9.** Diurnal variation of ambient $f_{C_5H_6O}^{OA}$ at the Manitou Forest pine forest site in the
 124 Rocky Mountains during the BEACHON-RoMBAS 2011 field study, together with diurnal
 125 variations of estimated $f_{C_5H_6O}^{OA}$ from $f_{CO_2}^{OA}$ based on regression results between $f_{C_5H_6O}^{OA}$ and $f_{CO_2}^{OA}$
 126 (ambient+Oxidation flow reactor) in this study. The diurnal variation of monoterpene and
 127 isoprene+MBO are also shown.

128

129

130

131



132

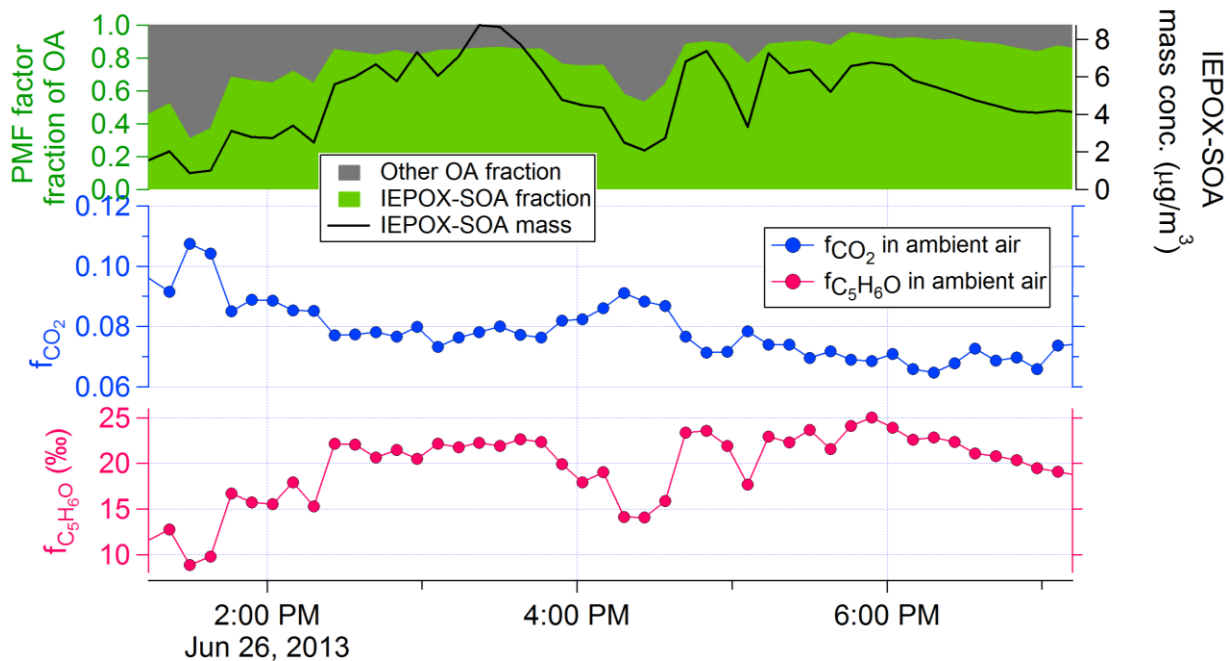
133 Figure S10. Scatter plot between $f_{CO_2}^{OA}$ and $f_{C_5H_6O}^{OA}$ for all the ambient OA dataset. Green arrows
 134 are added to guide the eye.

135

136

137

138

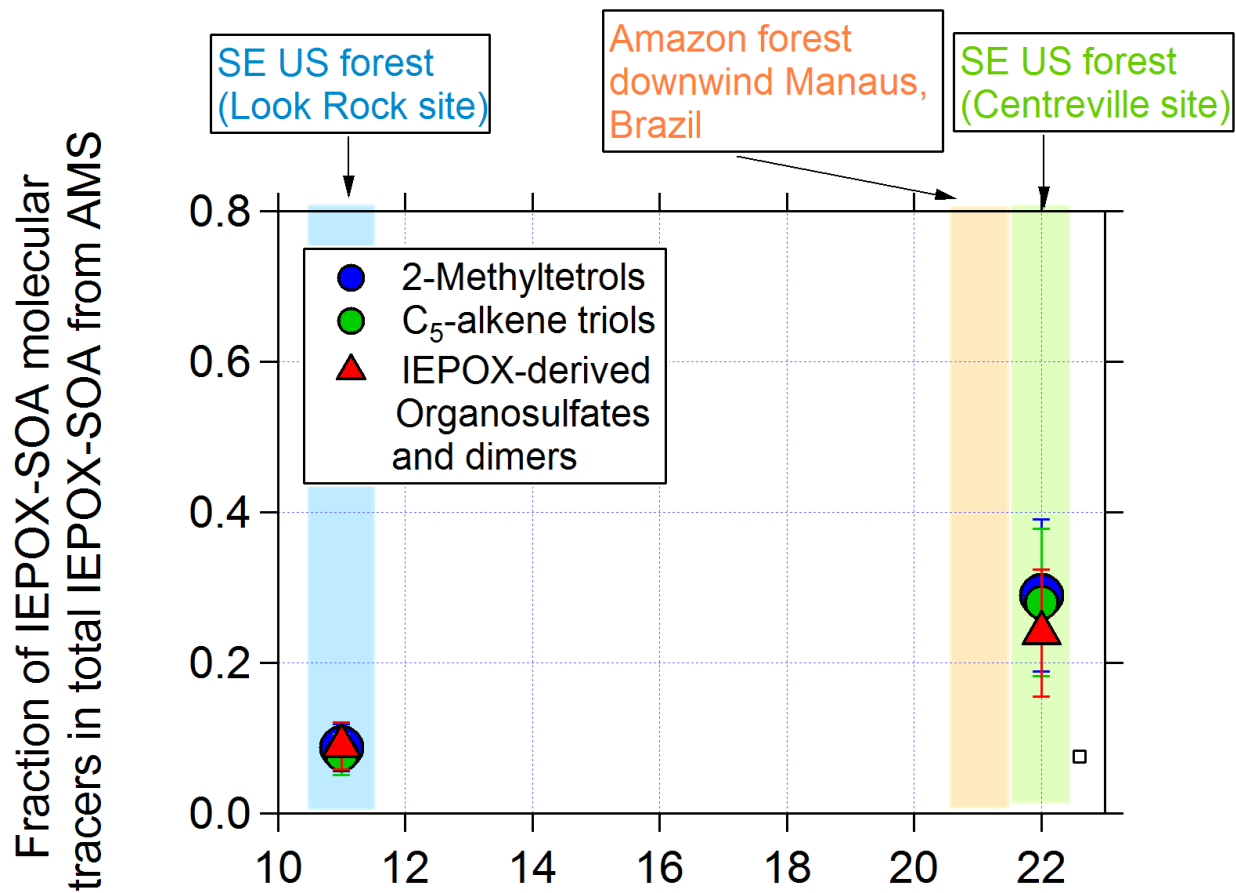


139

140 **Figure S11.** Time series of ambient $f_{C_5H_6O}^{OA}$, $f_{CO_2}^{OA}$, and IEPOX-SOA mass concentrations, together
 141 with the IEPOX-SOA fraction of OA during the SOAS-CTR campaign in a SE US forest. During
 142 this period, high sulfate and IEPOX-SOA mass concentrations and mass fractions are observed.

143

144

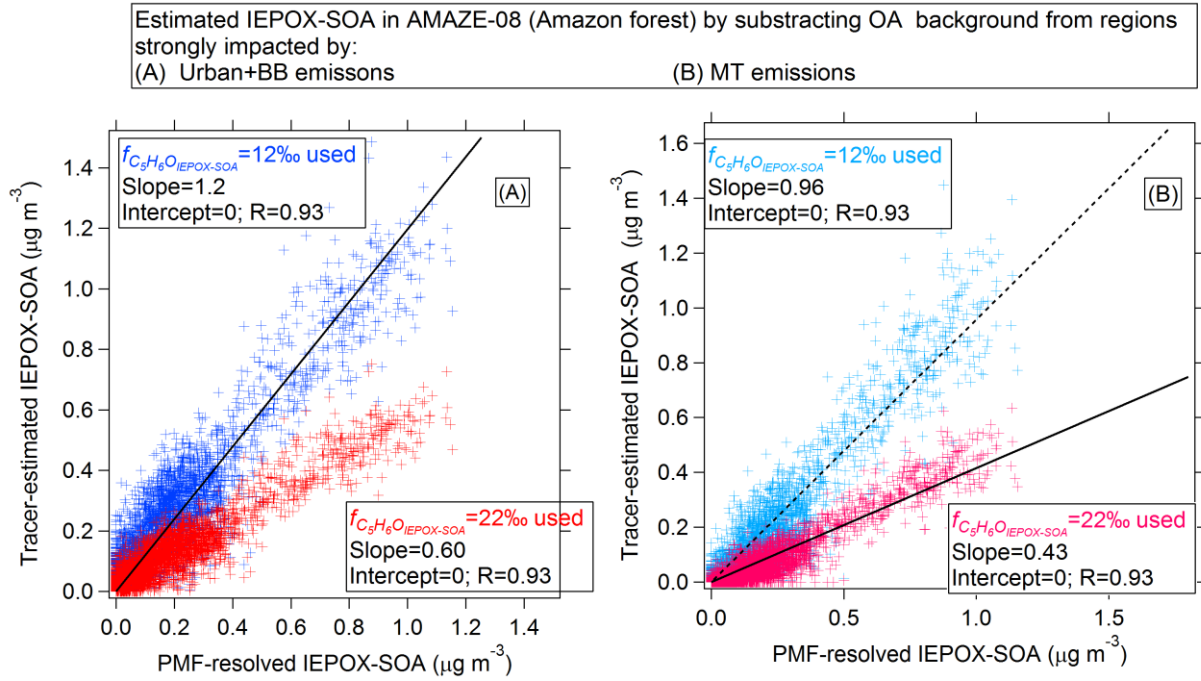


145

146 [Figure S12](#) Scatter plot between different IEPOX-SOA molecular tracers (Methyltetrol, C₅-
 147 alkene triols and IEPOX-derived organosulfates and their dimers) vs IEPOX-SOA_{PMF} and f_{82} in
 148 [IEPOX-SOA](#)

149

150



151

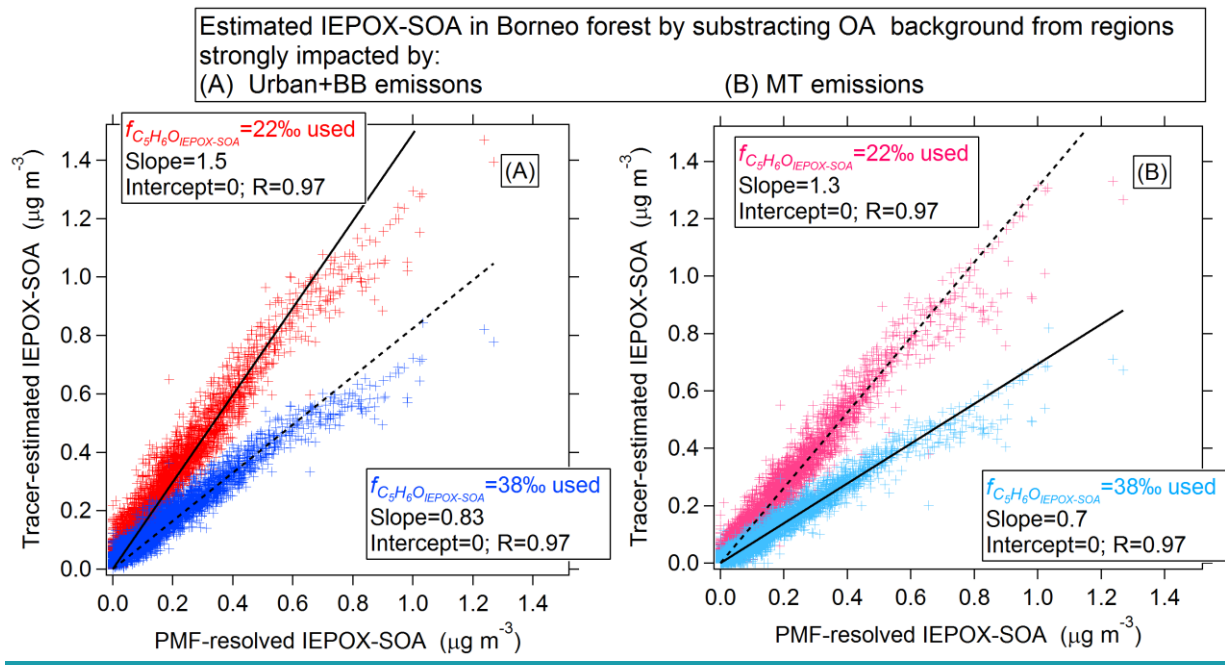
152 **Figure S13.** Scatter plot between tracer-estimated IEPOX-SOA and IEPOX-SOA_{PMF} at a pristine
 153 Amazon forest site (AMAZE-08). The tracer-based IEPOX-SOA was estimated using OA
 154 background from regions strongly influenced by (A) urban and biomass-burning emissions and
 155 (B) monoterpene emissions. In each plot, we used two $f_{C_5H_6O}^{IEPOX-SOA}$, from the average IEPOX-
 156 SOA_{PMF} ($f_{C_5H_6O}^{IEPOX-SOA} = 22\text{‰}$) and from the IEPOX-SOA_{PMF} in Amazon forest study
 157 ($f_{C_5H_6O}^{IEPOX-SOA} = 12\text{‰}$).

158

159

160

161



162

163 **Figure S14** Scatter plot between estimated IEPOX-SOA and IEPOX-SOA_{PMF} at a Borneo forest
 164 site. The tracer-based IEPOX-SOA was estimated using OA background from regions strongly
 165 influenced by (A) urban and biomass-burning emissions and (B) monoterpene emissions. In each
 166 plot, we used two $f_{C_5H_6O}^{IEPOX-SOA}$, from the average IEPOX-SOA_{PMF} ($f_{C_5H_6O}^{IEPOX-SOA}=22\%$) and from
 167 the IEPOX-SOA_{PMF} in Borneo forest study ($f_{C_5H_6O}^{IEPOX-SOA}=38\%$).

168

1.1 Bounds for using the IEPOX-SOA estimation method

In theory, our method can easily produce an estimate of “IEPOX-SOA” from an AMS dataset, but the errors could be substantial in some cases. The guidelines below are meant to limit the errors when applying this method:

- 1) We first recommend making the scatter plot of $f_{CO_2}^{OA}$ and $f_{C_5H_6O}^{OA}$ and then compare it to Fig. 5 in this study to help evaluate the possible presence of IEPOX-SOA.
- 2) For datasets where an important influence of MT-SOA is suspected: if all the $f_{C_5H_6O}^{OA}$ in total OA are $\sim 3.1\%$ or lower within measurement noise, the estimated IEPOX-SOA will show negative and positive values scattered around zero, indicating negligible IEPOX-SOA in the dataset. A similar conclusion can be reached for urban or BB-dominated locations when $f_{C_5H_6O}^{OA} \sim 1.7\%$ or lower for most data points.
- 3) When the scatter plot between $f_{CO_2}^{OA}$ and $f_{C_5H_6O}^{OA}$ shows obvious enhanced $f_{C_5H_6O}^{OA}$ above the most-relevant background value, users can easily use the tracer-based method to estimate the IEPOX-SOA mass concentration. If the source of the background OA is not known, we suggest using both background corrections and reporting the range of results.
- 4) Cases intermediate between No. 2 and 3 above, i.e. when $f_{C_5H_6O}^{OA}$ is only slightly above the relevant background level will have the largest relative uncertainty. In this case we recommend applying the method and evaluating the results carefully, as exemplified for the Rocky Mountain dataset in this paper (section 3.5). E.g. diurnal variations of $f_{C_5H_6O}^{OA}$ and SOA precursors (e.g., isoprene and monoterpene), together with diurnal variation of estimated IEPOX-SOA, provide useful indicators about whether the results are meaningful. For cases in which the fraction of IEPOX-SOA in total OA is relatively low (e.g., $<5\%$) and the fraction of MT-SOA in total OA is high (e.g., $>50\%$), the uncertainty of the IEPOX-SOA estimate will be very high. For this type of situation the full PMF method may be required.

Besides ease of use, another advantage of the tracer-based estimation method is that it can be used to quantify IEPOX-SOA based on brief periods of elevated concentrations, e.g. as often encountered in aircraft studies. In those cases it may be difficult for PMF to resolve an IEPOX-SOA factor, but no such limitation applies to this estimation method.

1.2 Uncertainties of IEPOX-SOA estimation method.

To estimate the accuracy of our IEPOX-SOA tracer-based estimation method, we used this method to estimate IEPOX-SOA from another two ambient datasets with the lowest and highest $f_{C_5H_6O}^{IEPOX-SOA}$ in PMF-resolved IEPOX-SOA ($f_{C_5H_6O}^{IEPOX-SOA}$) among all the studies in this paper. The lowest value is from a dataset in the pristine Amazon forest (AMAZE-08) where $f_{C_5H_6O}^{IEPOX-SOA} = 12\%$ (Chen et al., 2015) and the highest value from a dataset in a Borneo forest with $f_{C_5H_6O}^{IEPOX-SOA} = 38\%$ (Robinson et al., 2011). Since the $f_{C_5H_6O}^{IEPOX-SOA}$ values in these two datasets are the two farthest from the average $f_{C_5H_6O}^{IEPOX-SOA}$ ($22 \pm 7\%$), the estimation method

206 results from these two datasets represent the worst case scenarios for all datasets published so
207 far.

208 _____ The estimation results from both datasets are shown in Fig. S13 and Fig. S14. Both of the
209 background OA corrections for areas strongly influenced by urban+BB emissions and by
210 monoterpene emissions are used.

211 _____ Overall, all variants of the estimated IEPOX-SOA correlate well with IEPOX-SOA_{PMF} (all
212 $R \geq 0.93$). When average $f_{C_5H_6O}^{IEPOX-SOA} = 22\%$ is used, the slope between estimated IEPOX-SOA
213 vs IEPOX-SOA_{PMF} is between 0.43-1.5, i.e. within a factor of 2.2. When the actual $f_{C_5H_6O}^{IEPOX-SOA}$ in
214 each dataset is used, the slope between estimated IEPOX-SOA vs IEPOX-SOA_{PMF} is in a range
215 of 0.7-1.2, i.e. within 30%.

216

217

218

219 **References**

- 220 Aiken, A. C., Salcedo, D., Cubison, M. J., Huffman, J. A., DeCarlo, P. F., Ulbrich, I. M.,
 221 Docherty, K. S., Sueper, D., Kimmel, J. R., Worsnop, D. R., Trimborn, A., Northway,
 222 M., Stone, E. A., Schauer, J. J., Volkamer, R. M., Fortner, E., de Foy, B., Wang, J.,
 223 Laskin, A., Shutthanandan, V., Zheng, J., Zhang, R., Gaffney, J., Marley, N. A., Paredes-
 224 Miranda, G., Arnott, W. P., Molina, L. T., Sosa, G., and Jimenez, J. L.: Mexico City
 225 aerosol analysis during MILAGRO using high resolution aerosol mass spectrometry at
 226 the urban supersite (T0) - Part 1: Fine particle composition and organic source
 227 apportionment, *Atmos Chem Phys*, 9, 6633-6653, 2009.
- 228 Canagaratna, M. R., Jimenez, J. L., Kroll, J. H., Chen, Q., Kessler, S. H., Massoli, P.,
 229 Hildebrandt Ruiz, L., Fortner, E., Williams, L. R., Wilson, K. R., Surratt, J. D., Donahue,
 230 N. M., Jayne, J. T., and Worsnop, D. R.: Elemental ratio measurements of organic
 231 compounds using aerosol mass spectrometry: characterization, improved calibration, and
 232 implications, *Atmos. Chem. Phys.*, 15, 253-272, 10.5194/acp-15-253-2015, 2015.
- 233 Chen, Q., Farmer, D. K., Rizzo, L. V., Pauliquevis, T., Kuwata, M., Karl, T. G., Guenther, A.,
 234 Allan, J. D., Coe, H., Andreae, M. O., Pöschl, U., Jimenez, J. L., Artaxo, P., and Martin,
 235 S. T.: Submicron particle mass concentrations and sources in the Amazonian wet season
 236 (AMAZE-08), *Atmos. Chem. Phys.*, 15, 3687-3701, 10.5194/acp-15-3687-2015, 2015.
- 237 Chhabra, P. S., Flagan, R. C., and Seinfeld, J. H.: Elemental analysis of chamber organic aerosol
 238 using an aerodyne high-resolution aerosol mass spectrometer, *Atmos. Chem. Phys.*, 10,
 239 4111-4131, 10.5194/acp-10-4111-2010, 2010.
- 240 Crippa, M., El Haddad, I., Slowik, J. G., DeCarlo, P. F., Mohr, C., Heringa, M. F., Chirico, R.,
 241 Marchand, N., Sciare, J., Baltensperger, U., and Prévôt, A. S. H.: Identification of marine
 242 and continental aerosol sources in Paris using high resolution aerosol mass spectrometry,
 243 *Journal of Geophysical Research: Atmospheres*, 118, 1950-1963, doi:
 244 10.1002/jgrd.50151, 2013.
- 245 Docherty, K. S., Aiken, A. C., Huffman, J. A., Ulbrich, I. M., DeCarlo, P. F., Sueper, D.,
 246 Worsnop, D. R., Snyder, D. C., Peltier, R. E., Weber, R. J., Grover, B. D., Eatough, D. J.,
 247 Williams, B. J., Goldstein, A. H., Ziemann, P. J., and Jimenez, J. L.: The 2005 Study of
 248 Organic Aerosols at Riverside (SOAR-1): instrumental intercomparisons and fine particle
 249 composition, *Atmos. Chem. Phys.*, 11, 12387-12420, 10.5194/acp-11-12387-2011, 2011.
- 250 Dunlea, E. J., DeCarlo, P. F., Aiken, A. C., Kimmel, J. R., Peltier, R. E., Weber, R. J.,
 251 Tomlinson, J., Collins, D. R., Shinozuka, Y., McNaughton, C. S., Howell, S. G., Clarke,
 252 A. D., Emmons, L. K., Apel, E. C., Pfister, G. G., van Donkelaar, A., Martin, R. V.,
 253 Millet, D. B., Heald, C. L., and Jimenez, J. L.: Evolution of Asian aerosols during
 254 transpacific transport in INTEX-B, *Atmos Chem Phys*, 9, 7257-7287, 2009.
- 255 Robinson, N. H., Hamilton, J. F., Allan, J. D., Langford, B., Oram, D. E., Chen, Q., Docherty,
 256 K., Farmer, D. K., Jimenez, J. L., Ward, M. W., Hewitt, C. N., Barley, M. H., Jenkin, M.
 257 E., Rickard, A. R., Martin, S. T., McFiggans, G., and Coe, H.: Evidence for a significant
 258 proportion of Secondary Organic Aerosol from isoprene above a maritime tropical forest,
 259 *Atmos. Chem. Phys.*, 11, 1039-1050, 10.5194/acp-11-1039-2011, 2011.
- 260 Setyan, A., Zhang, Q., Merkel, M., Knighton, W. B., Sun, Y., Song, C., Shilling, J. E., Onasch,
 261 T. B., Herndon, S. C., Worsnop, D. R., Fast, J. D., Zaveri, R. A., Berg, L. K.,
 262 Wiedensohler, A., Flowers, B. A., Dubey, M. K., and Subramanian, R.: Characterization
 263 of submicron particles influenced by mixed biogenic and anthropogenic emissions using

264 high-resolution aerosol mass spectrometry: results from CARES, *Atmos. Chem. Phys.*,
265 12, 8131-8156, 10.5194/acp-12-8131-2012, 2012.
266 Ulbrich, I. M., Canagaratna, M. R., Zhang, Q., Worsnop, D. R., and Jimenez, J. L.: Interpretation
267 of organic components from Positive Matrix Factorization of aerosol mass spectrometric
268 data, *Atmos Chem Phys*, 9, 2891-2918, 2009.

269

270